NASA Contractor Report 159227

Bifilar Analysis Study — Volume I

W. Miao, T. Mouzakis

SIKORSKY AIRCRAFT
Stratford, Ct 06602

CONTRACT NAS1-15612
AUGUST 1980

National Aeronautics and
Space Administration

Langley Research Center
Hampton, Virginia 23665
AC 804 827-3966

TP

1. Report No.	2. Government Accession No.	3. Recipient's Catalog No.
NASA CR-159227--Volume I		

4. Title and Subtitle	5. Report Date
Bifilar Analysis Study - Volume I	August 1980
	6. Performing Organization Code

7. Author(s)	8. Performing Organization Report No.
W. Miao, T. Mouzakis	SER-510035
	10. Work Unit No.

9. Performing Organization Name and Address	11. Contract or Grant No.
Sikorsky Aircraft Stratford, Connecticut 06602	NAS1-15612
	13. Type of Report and Period Covered

12. Sponsoring Agency Name and Address	14. Sponsoring Agency Code
National Aeronautics and Space Administration Washington, D.C. 20546	Contractor Report

15. Supplementary Notes

Technical Monitor: Dr. William F. White, Jr., The contract research effort which has led to the results in this report was financially supported by the Structures Laboratory, USARTL (AVRADCOM).

16. Abstract

A coupled rotor/bifilar/airframe analysis has been developed and utilized to study the dynamic characteristics of the centrifugally tuned, rotor-hub-mounted, bifilar vibration absorber. The analysis contains the major components that impact the bifilar absorber performance, namely, an elastic rotor (with hover aerodynamics), a flexible fuselage, and non-linear individual degrees of freedom for each bifilar mass.

The analysis has been validated through correlation of average bifilar mass response and hub response of the flight test data of the BLACK HAWK and the S-76. Airspeed, rotor speed, bifilar mass and tuning variations are considered. The correlation results are generally good.

The performance of the bifilar absorber is shown to be a function of its basic parameters: dynamic mass, damping and tuning, as well as the impedance of the rotor hub. The effect of the dissimilar responses of the individual bifilar masses which are caused by tolerance induced mass, damping and tuning variations is also examined.

17. Key Words (Suggested by Author(s))	18. Distribution Statement
Coupled rotor/bifilar/airframe analysis, hub impedance, dynamic mass, bifilar absorber, BLACK HAWK, S-76, tuning, damping, transmissibility	Unclassified - Unlimited

19. Security Classif. (of this report)	20. Security Classif. (of this page)	21. No. of Pages	22. Price*
Unclassified	Unclassified	81	

TABLE OF CONTENTS

Section		Page
	List of Figures	iv
	List of Tables	viii
1.	Summary	1
2.	Introduction	2
3.	Coupled Rotor/Bifilar/Airframe Analysis	6
4.	Parametric Studies	9
	4.1 Modal Fuselage Model of the BLACK HAWK Helicopter	9
	4.2 Hub Impedance Effect on Bifilar Effectiveness	12
	4.3 Rotor Dynamics Effect on Airframe Response and Bifilar Performance	21
	4.4 Bifilar Sensitivity to Design Parameters and Tolerances	25
	4.5 Interaction of 3/rev and 5/rev Bifilars	40
5.	Comparison with Flight Test Data	43
	5.1 Flight Test Configurations	43
	5.2 Comparsion and Discussion of Flight Test Data	44
6.	Conclusions and Recommendations	79
References		81

LIST OF FIGURES

Figure No.	Title	Page
2-1	Schematic of Bifilar Assembly	3
2-2	Bifilar Installed on Aircraft	4
3-1	Block Diagram of Coupled Rotor/Bifilar/ Airframe Analysis	7
4.1-1	Analytical Shake Test Results	11
4.1-2	Shake Test Results	13
4.2-1	Effect of Inplane Hub Impedance on Bifilar Response	14
4.2-2	Hub Impedance Ratios Affect Bifilar Force Phasing	15
4.2-3	Inplane Bifilar Effectiveness as Affected by Hub Impedance	17
4.2-4	Bifilar Performance for Elliptic Hub Motion	18
4.2-5	(N-1)/Rev Inplane Bifilar Effectiveness on (N+1)/ Rev Excitation as Affected by Hub Impedance	20
4.3-1	Effect of Rotor on Airframe Response and Bifilar Performance to 3/Rev Excitation	22
4.3-2	Effect of Flexible Rotor on Coupled Frequencies	23
4.3-3	Effect of Rotor on Airframe Response and Bifilar Performance to 5/Rev Excitation	24
4.4-1	Effect of Dynamic Mass on Bifilar Response Amplitude and Transmissibility	26
4.4-2	Dynamic Mass Effect on Bifilar Response	27
4.4-3	Validity of Linear Bifilar Analysis	28
4.4-4	Effect of Damping on Bifilar Response Amplitude	31

LIST OF FIGURES (CONTINUED)

Figure No.	Title	Page
4.4-5	Bifilar Pattern as Affected by Variation in Damping	32
4.4-6	Bifilar Pattern as Affected by 2/Rev Hub Force	33
4.4-7	Bifilar Performance as Affected by Tolerance on Damping	34
4.4-8	Bifilar Pattern as Affected by Variation in Tuning	36
4.4-9	Bifilar Performance as Affected by Tolerance in Tuning	37
4.4-10	Effect of Combined Over- And Under-Tuning on Bifilar Performance	38
4.4-11	Bifilar Pattern as Affected by Combined Tolerances in Damping and Tuning	39
4.5-1	Interaction of (N-1)/Rev and (N+1)/Rev Bifilars	41
4.5-2	Residual Hub Force as Affected by Interaction of 3/Rev and 5/Rev Bifilars	42
5.2-1	Prototype BLACK HAWK 3/Rev Bifilar Response Pattern as Affected by Airspeed	45
5.2-2	Difference in Tuning and Damping Affects Bifilar Response	46
5.2-3	Prototype BLACK HAWK 3/Rev Bifilar Response Pattern as Affected by Rotor Speed	48
5.2-4	Rotor Speed Effect on Prototype BLACK HAWK 3/Rev Bifilar Response	49
5.2-5	3/Rev Inplane Hub Force, Configuration 1	51
5.2-6	Correlation of 3/Rev Bifilar Mass Motion, Configuration 1	52

LIST OF FIGURES (CONTINUED)

Figure No.	Title	Page
5.2-7	Correlation of 3/Rev Inplane Hub Motion, Configuration 1	53
5.2-8	Configuration 2, 3/Rev Bifilar Mass Response - Effect of Airspeed	54
5.2-9	Configuration 2, 5/Rev Bifilar Mass Response - Effect of Airspeed	56
5.2-10	Configuration 2, 3/Rev Bifilar Mass Response - Effect of Rotor Speed	58
5.2-11	Configuration 2, 5/Rev Bifilar Mass Response - Effect of Rotor Speed	59
5.2-12	3/Rev Inplane Hub Force, Configuration 2	61
5.2-13	5/Rev Inplane Hub Force, Configuration 2	62
5.2-14	Correlation of 3/Rev Bifilar Mass Motion, Configuration 2	63
5.2-15	Correlation of 3/Rev Hub Motion, Configuration 2	64
5.2-16	Correlation of 5/Rev Bifilar Mass Motion, Configuration 2	65
5.2-17	Correlation of 5/Rev Hub Motion, Configuration 2	66
5.2-18	Configuration 2, 3/Rev Bifilar Mass Response With Combined Tuning and Mass Variation From Baseline - Effect of Airspeed	67
5.2-19	Configuration 2, 3/Rev Bifilar Mass Response With Combined Tuning and Mass Variation from Baseline - Effect of Rotor Speed	69
5.2-20	Correlation of 3/Rev Bifilar Mass Motion With Combined Tuning and Mass Variation From Baseline, Configuration 2	70
5.2-21	Correlation of 3/Rev Hub Motion With Combined Tuning and Mass Variation from Baseline, Configuration 2	71
5.2-22	Correlation of 3/Rev Hub and Bifilar Mass Motion With Tuning Variation from Baseline, Configuration 2	73

LIST OF FIGURES (CONTINUED)

Figure No.	Title	Page
5.2-23	Configuration 3, 3/Rev Bifilar Mass Response - Effect of Airspeed	74
5.2-24	Correlation of 3/Rev Bifilar Mass Motion, Configuration 3	76
5.2-25	Correlation of 3/Rev Hub Motion, Configuration 3	77
5.2-26	Correlation of 5/Rev Hub Motion, Configuration 3	78

LIST OF TABLES

Table No.	Title	Page
4.1-1	Modal Fuselage Representation of BLACK HAWK	10
4.4-1	Bifilar Performance as Affected by Tolerance on Dynamic Mass	30

SECTION 1

SUMMARY

A coupled rotor/bifilar/airframe analysis has been developed and utilized to study the dynamic characteristics of the centrifugally tuned, rotor-hub-mounted, bifilar vibration absorber. The analysis contains the major components that impact the bifilar absorber performance, namely, an elastic rotor (with hover aerodynamics), a flexible fuselage and non-linear individual degrees of freedom for each bifilar mass. Multiple bifilar absorbers are modelled each of which can function in either in the plane of rotation of the rotor or normal to it. A linear mathematical representation of the absorber is also available to save computer CPU time when the situation warrants.

The performance of the bifilar absorber is shown to be a function of its basic design parameters: dynamic mass, damping and tuning. Since the absorber acts to reduce the motion of its attachment point to the main rotor hub, hub impedance is of equal importance. For the case of a bifilar absorber which reacts cyclic response (e.g. 3/rev rotating response on a 4-bladed rotor) the degree of symmetry of hub impedance in the two orthogonal directions also influences absorber effectivity.

Because of manufacturing tolerances, every individual bifilar mass can be slightly different from the others in terms of its basic parameters. Bifilar mass motion is greatly affected by the tolerances and, in general, the set of mass motions of the bifilar absorber will form a response pattern short of ideal. As a result, there is the potential that the bifilar will introduce non-N/rev excitation of the fuselage.

The coupled rotor/bifilar/airframe analysis is validated by correlation with BLACK HAWK and S-76 flight test data. Airspeed, rpm and bifilar mass and tuning variations are considered. The correlation results are generally good for the average bifilar mass response and hub response. The analysis also predicts the dissimilar responses of the individual bifilar masses which are caused by tolerance induced mass, damping and tuning variations.

The analysis in its present form should prove very useful in evolving new bifilar designs, establishing tolerance design criteria and analyzing bifilar anomalies that may be observed in flight tests.

SECTION 2

INTRODUCTION

The bifilar rotor hub absorber is a centrifugally tuned vibration suppression device mounted to the main rotor hub of a helicopter. Figure 2-1 shows schematically the components of the bifilar system. The primary components are a support frame arm and sets of bifilar masses each of which is comprised of a dynamic mass, and two cylindrical tuning pins. These pins constrain the mass radially and, together with the circular tracking holes in the support arm and mass define the pendular radius of the mass. The installation of the system on a helicopter is shown in Figure 2-2.

The bifilar absorber has been applied to helicopters for the control of N/rev vibration resulting from main rotor excitation. It is particularly effective because it suppresses airframe vibration through a reduction in a principal system excitation nearly at its source, thus reducing the response of the entire airframe. The original development of the bifilar was performed by Sikorsky Aircraft, Reference 1. The subsequent application to numerous Sikorsky helicopters: the S-58T, the S-61 series, the S-67, the S-70 (BLACK HAWK), the S-72 (RSRA), and the S-76 has yielded an understanding of the fundamental characteristics governing bifilar effectiveness such as damping, absorber tuning, and the ratio of bifilar weight to uncoupled airframe impedance requirements. However, this experience also indicated that the capability of predicting the magnitude of vibration attenuation achievable with bifilars, or characteristics such as dissimilar bifilar response amplitudes requires strengthening.

The development of the second generation rotor hub absorbers will require a more thorough understanding of the dynamic characteristics of the coupled rotor/bifilar/airframe system. The rotor/bifilar/airframe system is dynamically coupled and significant airframe participation occurs in what are typically called blade modes. The proximity of these modes to N/rev, coupled with the established sensitivity of the bifilar to its attachment point impedance characteristics makes the inclusion of the coupled rotor/ bifilar/airframe dynamics necessary in any reasonable attempt to fully understand the bifilar absorber.

The purpose of the study reported herein is to gain a more complete understanding of the capabilities and limitations of the bifilar absorber system as a helicopter vibration control device. A coupled rotor/bifilar/airframe analysis has been developed and used as a tool for parametric study. The validity of the analysis is established by comparing calculated results with flight test data. This work provides a technical base for the development of second generation rotor hub absorbers with the goal of more weight efficient control of airframe N/rev vibration.

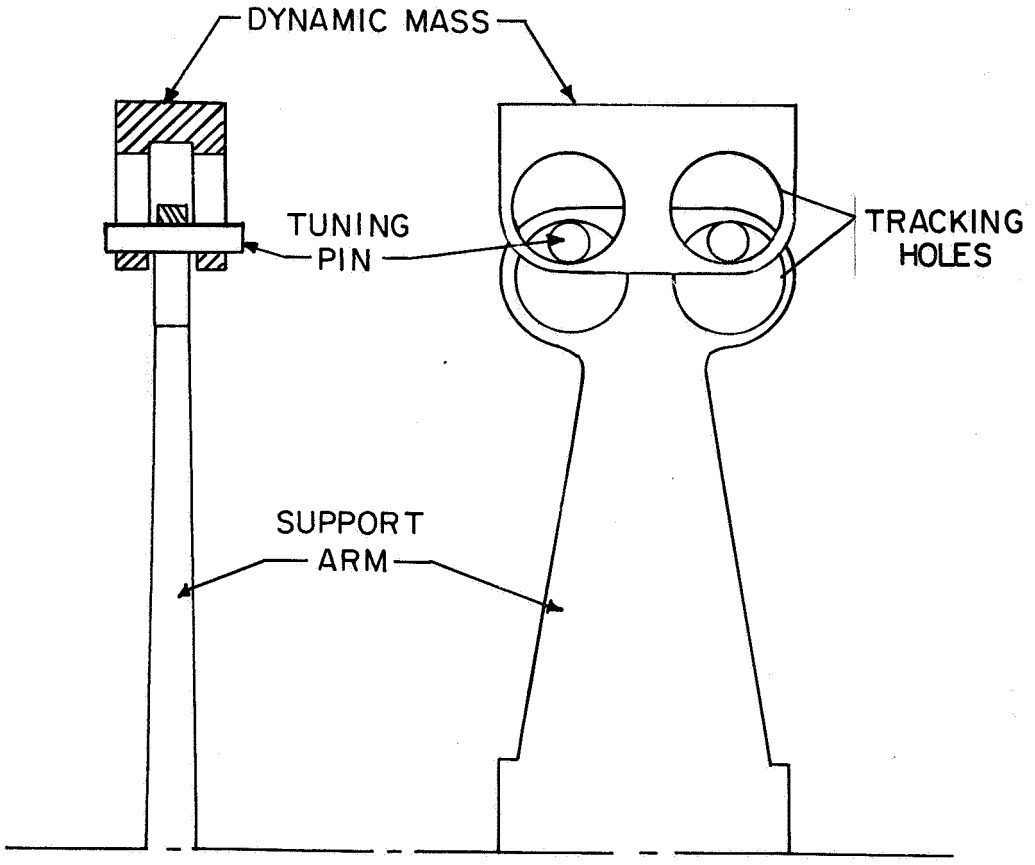

Figure 2-1. Schematic of Bifilar Assembly

FIGURE 2-2.

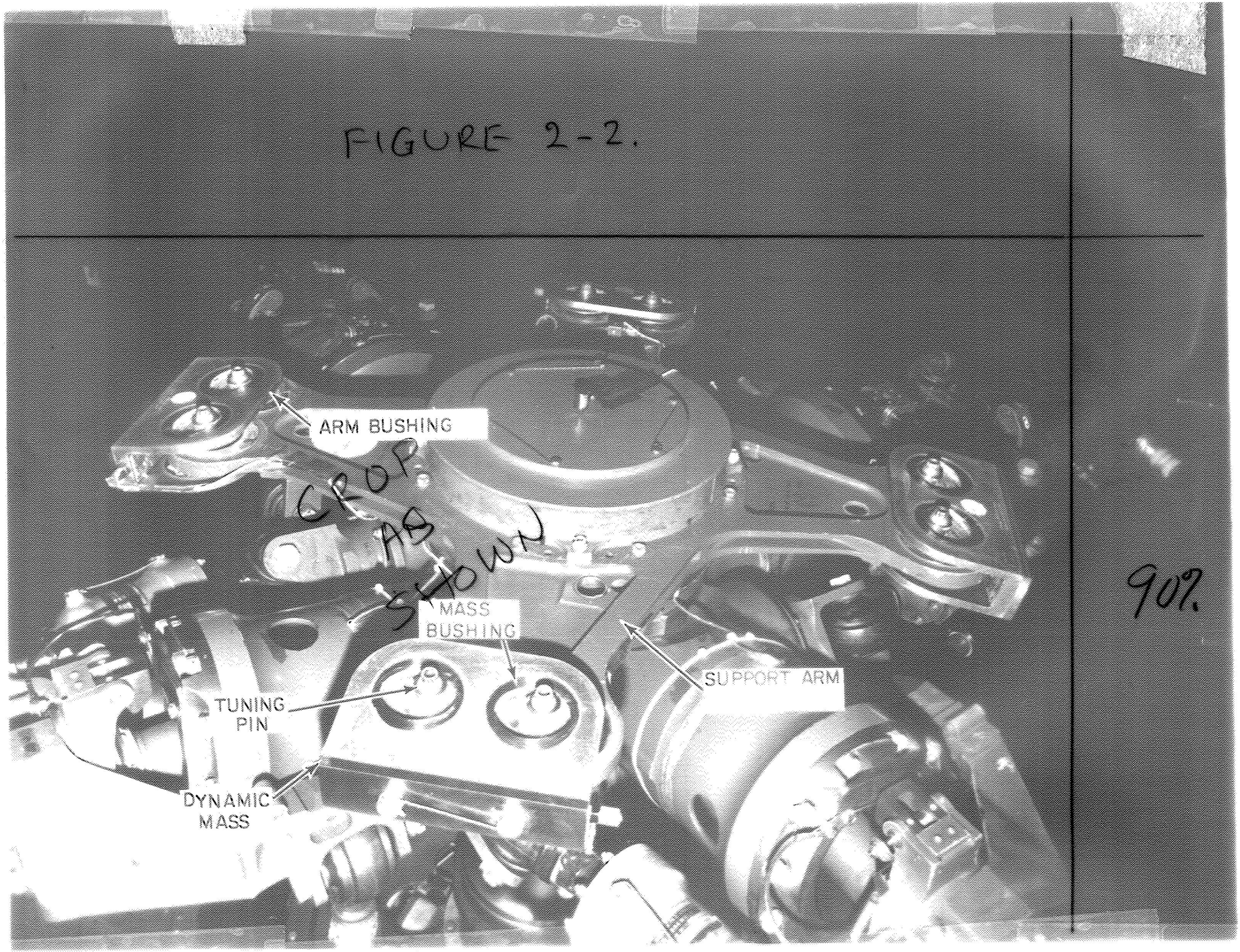

907.

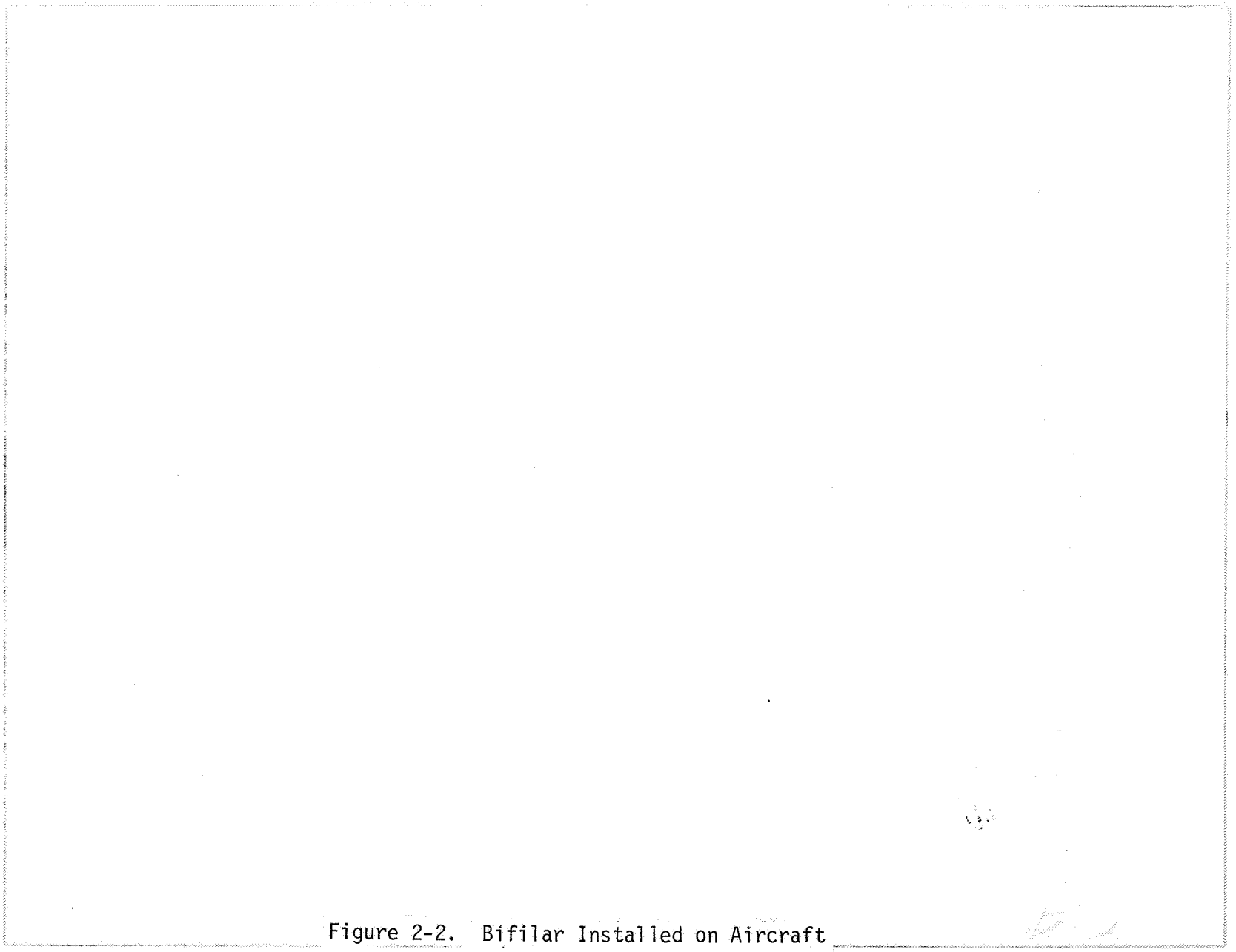

Figure 2-2. Bifilar Installed on Aircraft

The report briefly describes the coupled analysis with the detailed mathematical formulation presented in Reference 2, a companion report prepared under the same contract. Results of the parametric studies using the analysis are presented next, followed by the comparison with flight test data.

SECTION 3

COUPLED ROTOR/BIFILAR/AIRFRAME ANALYSIS

The rotor/bifilar/airframe analysis has been developed to provide the engineer with an analytical tool capable of rapid parametric evaluation of bifilar absorber configurations. A conceptual block diagram of the analysis is shown in Figure 3-1. A brief description of the analytical model, with primary components of fuselage, rotor, rotating and fixed-system absorbers, is given below.

Rotor - The rotor system is represented by a modal approach which utilizes the equations of motion shown in Reference 2. The rotor blade degrees-of-freedoms which can be incorporated in the analysis are: up to four blade elastic modes (coupled flatwise/edgewise), up to 2 blade torsional blade modes (first mode represents a rigid blade while the second one is an elastic mode) and rigid blade flapping and lead-lag motions - a total of 8 blade modes which correspond to 24 degrees-of-freedom (d.o.f.) (each mode has one symmetric and two cyclic components). The rotor/airframe coupling terms are incorporated in the analysis using 5 airframe modes corresponding to uncoupled fuselage longitudinal (x), lateral (y), vertical (z), roll (θ_x) and pitch (θ_y) motions - yaw motion (θ_z) is not included.

The major assumptions made in the development of the rotor system model are listed below:

1. Dynamic and aerodynamic effects assume small perturbations about steady initial values of the system generalized coordinates.

2. Aerodynamic forces are developed using strip theory in hover.

3. The number of rotor blades must be greater than two due to the polar symmetry assumption made in the rotating system generalized coordinate transformations.

Fuselage - The fuselage dynamic model is a set of linear modal equations which are discussed in Reference 2. The computer program accepts inputs of system modal properties of up to 16 airframe modes.

Rotating-System Absorbers - The bifilar absorber analysis includes linear and non-linear inplane rotor head absorbers and linear vertical absorbers. Detail derivation of the equations of motion are discussed in Reference 2. The forced response analysis can use up to 5 types of linear absorbers (inplane plus vertical). A maximum of 12 non-linear inplane pendulums can be employed in the time history analysis. Viscous damping of the absorbers is assumed. Provision for inclusion of a two-plane, vertical and inplane, bifilar absorber mounted on the hub is provided through the modular structure of the computer program.

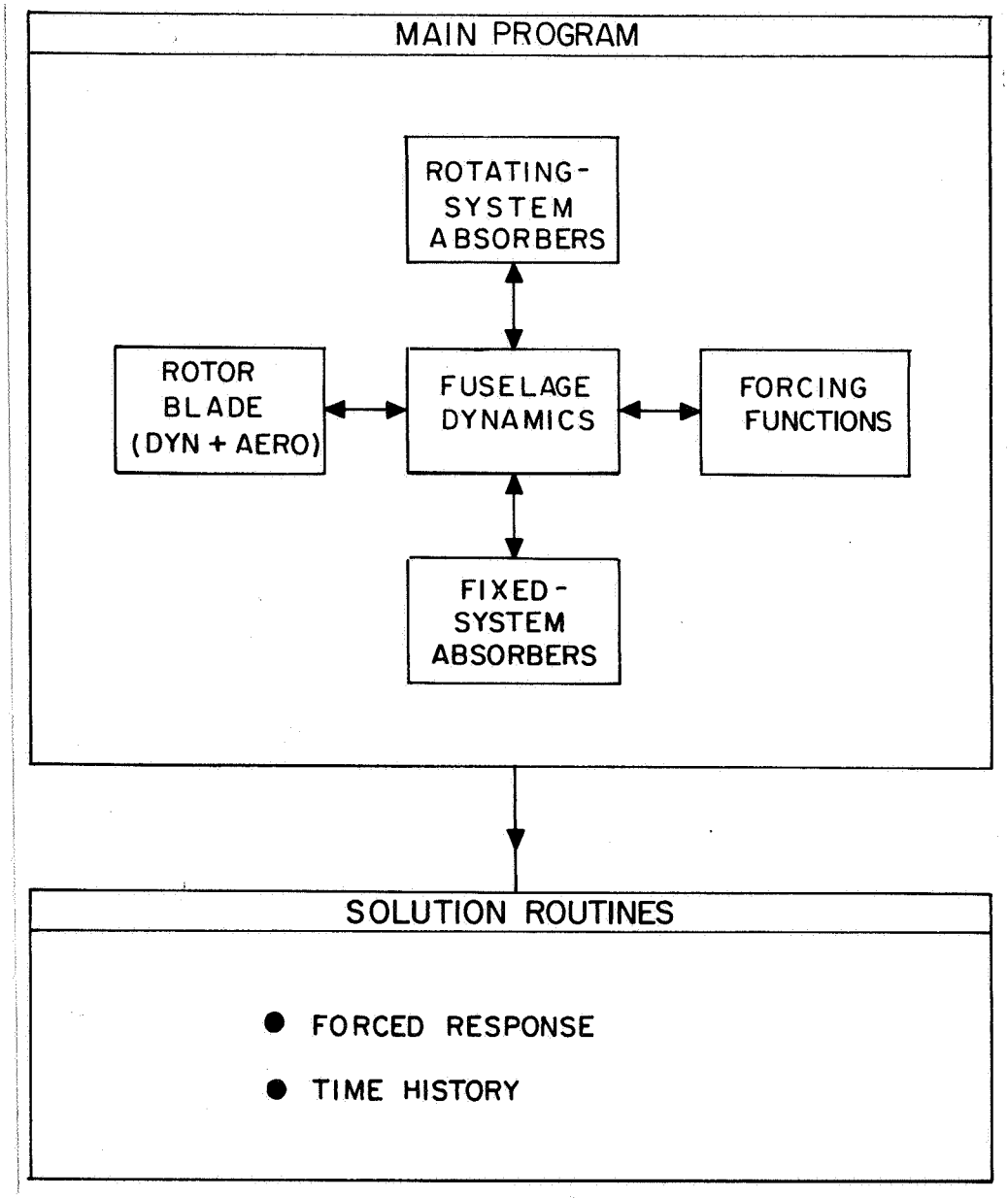

Figure 3-1. Block Diagram of Coupled Rotor/Bifilar/Airframe Analysis

Fixed-System Absorbers - Fixed system absorbers are modelled in the analysis as simple unidirectional spring-mass-damper system. Detail derivation of the equations of motion is given in Reference 2. The absorbers attachment point must be at a defined modal vector point. Provisions for up to 5 absorbers are provided for in the analysis.

It can be seen from Figure 3-1 that a modular approach has been adopted to form this mathematical model. Modularization is achieved when each component block outputs the mass, damping and stiffness matrices or force vectors with the pertinent degrees-of-freedom (d.o.f.) including the 6 d.o.f. of the attachment point, i.e. 6 d.o.f. at the hub for rotor or absorber attachment. Where two blocks merge together, the degrees-of-freedom of the attachment point are eliminated and replaced by fuselage modal degrees-of-freedom. Details of this procedure are discussed in Reference 2.

In general, the computer program initially develops the mass, damping and stiffness matrices for the fixed system (fuselage), rotor, fixed absorbers and linear rotating absorbers (both inplane and vertical). Coupling of associated matrices, using the technique previously discussed, is accomplished during this development.

At this point, a decision is made on the type of solution to be calculated: forced response or time-history. If the forced response solution is requested, then the generalized forces are calculated followed by the evaluation of the forced response solution. If the time-history solution is required, then the program proceeds to calculate the dynamic matrices of the non-linear inplane bifilars, adds them to the matrices from the linear analysis, solves for the acceleration vector and integrates it to obtain the velocity and displacement vectors. The final results are harmonically analyzed (up to 10 harmonics) and printed out.

SECTION 4

PARAMETRIC STUDIES

In order to examine the effects of various parameters on the bifilar performance leading to an understanding of the fundamental characteristics governing the effectiveness of the bifilar absorbers, the analysis described in Section 3 was applied. A representative modal fuselage model was set up to provide a realistic impedance at the main rotor hub. The effect of hub impedance and rotor dynamics on bifilar response was then examined. The bifilar performance as affected by design parameters such as dynamic mass, damping, tuning, together with sensitivity to tolerances, was investigated. Finally, the interaction of 3/rev and 5/rev bifilar absorbers on a four-bladed rotor system was studied. The non-linear bifilar absorber model with time history solution was used for these studies. Although these studies were conducted for inplane absorbers, the results should apply to vertical absorbers, used to reduce hub moment excitations, as well.

4.1 Modal Fuselage Model of BLACK HAWK Helicopter

The BLACK HAWK fuselage was selected as a representative fuselage modal model for the parametric studies. Shake test results were reviewed and nine relevant flexible modes were selected. The criterion for the selection of the modes was to include all flexible fuselage modes with frequencies up to 20% beyond the primary 4/rev excitation frequency (17.2 Hz) of the BLACK HAWK main rotor. These modes are listed below. All modes are fully coupled with the descriptions indicative of the primary motions only.

Frequency Hz	Mode Description
5.1	First lateral
6.4	First vertical
11.6	Second lateral
12.1	Tail vertical
13.8	Transmission vertical/pitch
14.3	Transmission roll
15.3	Second vertical
17.4	Transmission pitch
21.1	Cabin torsion

The corresponding generalized masses and the modal vectors at the main rotor hub are listed in Table 4.1-1. Also shown in the table are the six rigid body modes, which were also included in the parametric studies.

An analytical shake test was performed by applying a constant vibratory force at the hub with varying excitation frequencies, simulating the procedure used during actual shake test. Shown in Figure 4.1-1 are the calcu-

TABLE 4.1-1 Modal Fuselage Representation of BLACK HAWK

Mode No.	Freq. Hz.	Generalized Mass kg	Generalized Mass $\frac{lb\text{-}s^2}{in}$	x	y	z	Modal Vector at Hub θ_x rad/m	Modal Vector at Hub θ_x (rad/in)	Modal Vector at Hub θ_y rad/m	Modal Vector at Hub θ_y (rad/in)	Modal Vector at Hub θ_z rad/m	Modal Vector at Hub θ_z (rad/in)
1	5.1	2.2	(1.808)	.001	.15	.001	-.2016	(-.0051)	.0187	(.000476)	.0617	(.001568)
2	6.4	3.72	(3.061)	-.34	.001	.11	-.0047	(-.00012)	-.204	(-.005183)	.011	(.00028)
3	11.6	2.36	(1.941)	.05	-.065	.022	-.049	(-.001244)	-.0186	(-.000473)	-.236	(-.006)
4	12.1	2.43	(2)	.24	-.15	.022	-.049	(-.001244)	-.0186	(-.000473)	-.236	(-.006)
5	13.8	3.34	(2.747)	-.402	.15	-.11	-.315	(-.008)	-.126	(-.0032)	-.0173	(-.00044)
6	14.3	2.76	(2.268)	.001	.54	-.001	.478	(.01214)	.0031	(.00008)	.0157	(.0004)
7	15.3	6.24	(5.13)	1.	.001	-.31	.5126	(.01302)	-.2126	(-.0054)	.006	(.00015)
8	17.4	5.77	(4.75)	.7	.52	.125	-.0027	(-.00007)	.91	(.0231)	.006	(.00015)
9	21.1	7.65	(6.291)	-.05	.22	.001	.25	(.00635)	.0086	(.00022)	-.05	(-.00127)
10	0.	52.9	(43.5)	1.	0.	0.	0.		0.		0.	
11	0.	52.9	(43.5)	0.	1.	0.	0.		0.		0.	
12	0.	52.9	(43.5)	0.	0.	1.	0.		0.		0.	
13	0.	12.96	(10.66)	0.	1.	0.	-.5433	(-.0138)	0.		0.	
14	0.	107.26	(88.2)	1.	0.	.257	0.		.5433	(.0138)	0.	
15	0.	1552.	(1276)	0.	1.	0.	0.		0.		-2.126	(-.054)

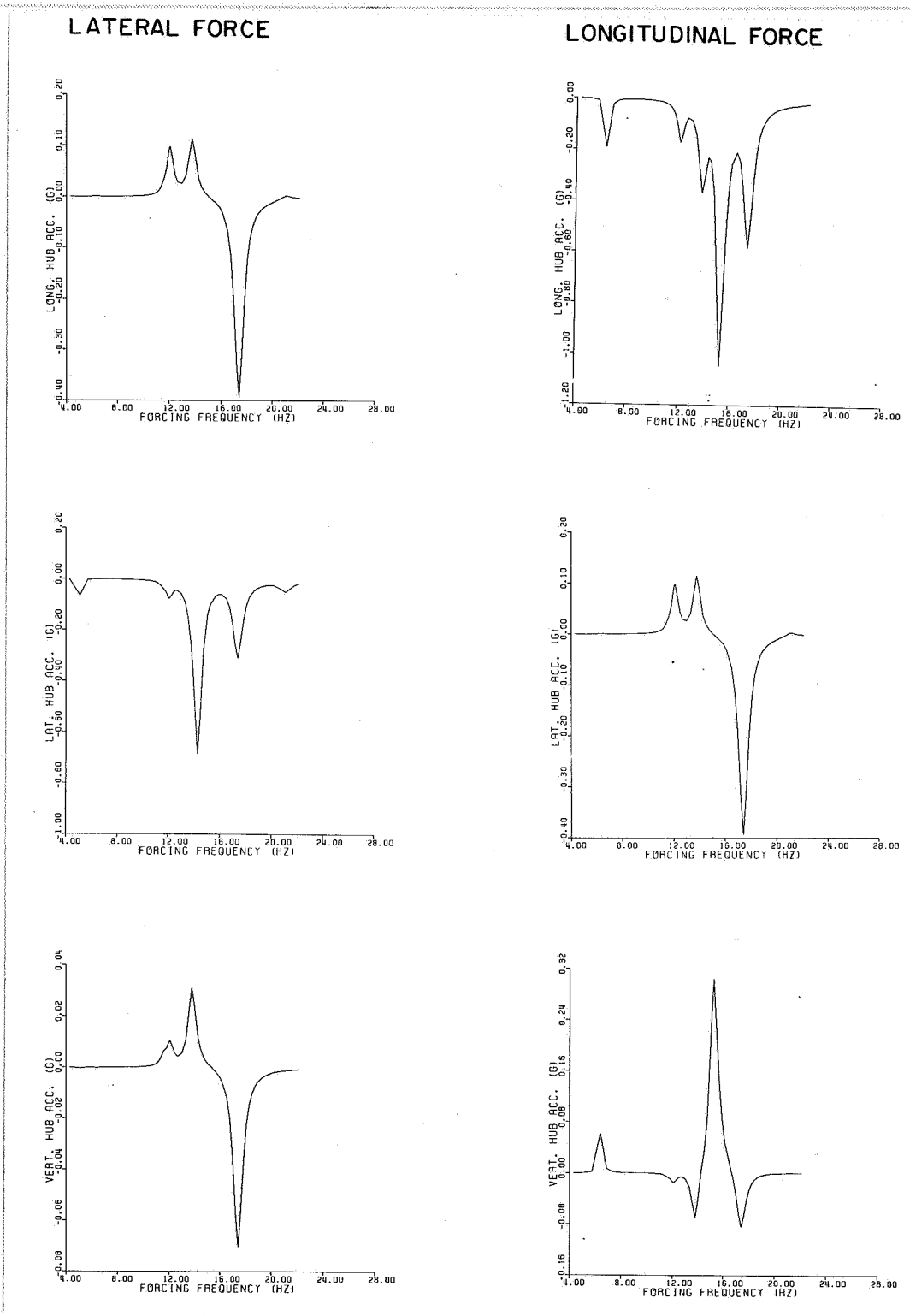

Figure 4.1-1. Analytical Shake Test Results

lated hub responses in longitudinal, lateral and vertical directions produced by a lateral force at hub and by a longitudinal force. These results compare quite well with the shake test results, shown in Figure 4.1-2. The correlation could be further improved with minor adjustments to the mode shapes but was deemed unnecessary since the modal model has provided a realistic fuselage representation.

4.2 Hub Impedance Effect on Bifilar Effectiveness

The response of four bifilar masses to a 2224 N (500 lb) rotating hub force at a frequency of 3/rev is shown in Figure 4.2-1. The figure shows the magnitude of the individual bifilar mass response and the corresponding phase angle. For bifilar with four identical masses in terms of weight, damping and tuning, the response pattern is of a square shape as shown in the figure. Also shown on the same polar plot are the bifilar response patterns for three sets of hub impedance variation in addition to the baseline. Note that the amplitudes for the bifilar response for all four sets of hub impedance studied remain essentially the same. Tabulated on the bottom of Figure 4.2-1 are the residual, or transmitted, forces in the longitudinal and lateral directions up to nine harmonics in the non-rotating system. The small discrepency between the longitudinal force transmitted and the lateral one is partly due to the unequal hub impedance and partly due to the time history solution of the coupled fuselage and non-linear inplane bifilars where the time history has not been carried out sufficiently long to reach a true steady-state forced response.

For the baseline case, square symbol in Figure 4.2-1, with the bifilar mass to longitudinal hub impedance ratio of .559 and the lateral ratio of .159, the transmitted 4/rev hub force is only 6% of the applied 3/rev rotating force. Reducing the mass ratios to .28 and .08 in the longitudinal and the lateral directions respectively, triangle symbol in Figure 4.2-1, the transmitted hub force rose to 13% of the applied force. Further reduction of the mass ratios to .056 in both the longitudinal and the lateral directions increased the transmissibility to 40%.

As noted earlier, the bifilar amplitudes remain essentially the same for these hub impedance combinations, although the transmissibility has varied through a relatively large range. The higher transmissibility is due to the fact that the phase of the bifilar response pattern has rotated from the baseline configuration. For ideal bifilar response, i.e., absorbing 100% hub excitation force, the two vectors, hub excitation force and bifilar output force, should coincide leaving zero residual force. As shown in Figure 4.2-2, the phase of the resultant bifilar output force with respect to the input hub excitation force is a function of the hub impedance. As the bifilar output force is rotated away from the input excitation force, a residual force is generated and becomes the source of excitation. The residual force is perpendicular to the bifilar force and increases its magnitude with increasing bifilar output force rotation as shown in Figure 4.2-2.

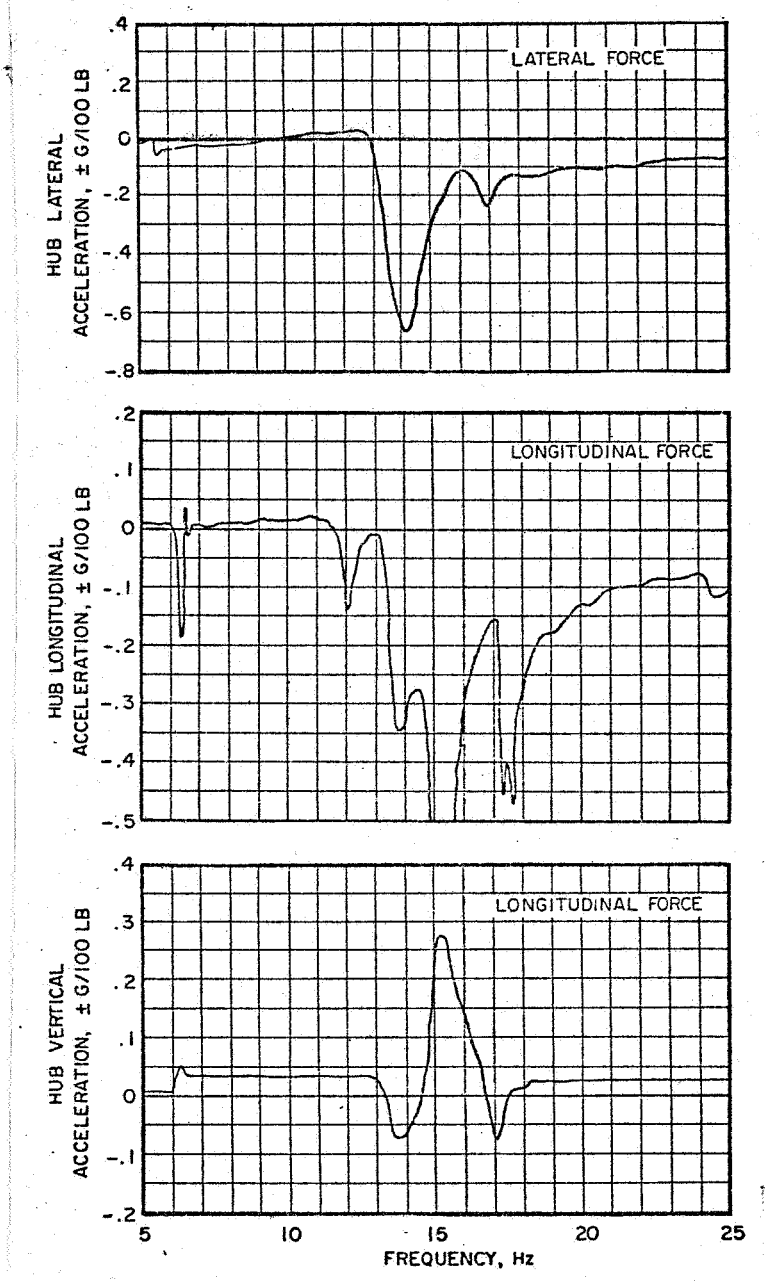

Figure 4.1-2 Shake Test Results

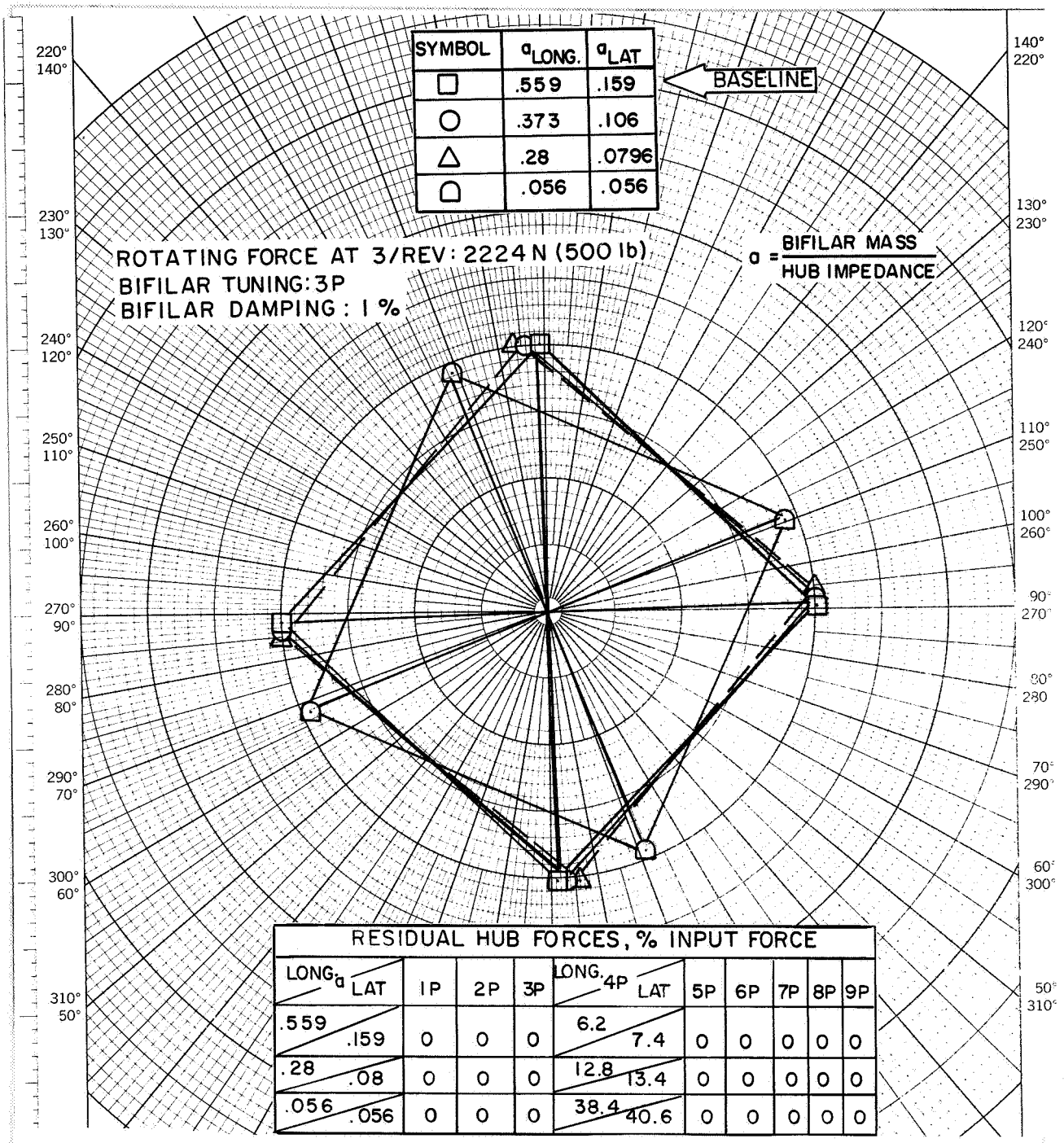

RESIDUAL HUB FORCES, % INPUT FORCE

$LONG._a$ / LAT	1P	2P	3P	$LONG._{4P}$ / LAT	5P	6P	7P	8P	9P
.559 / .159	0	0	0	6.2 / 7.4	0	0	0	0	0
.28 / .08	0	0	0	12.8 / 13.4	0	0	0	0	0
.056 / .056	0	0	0	38.4 / 40.6	0	0	0	0	0

Figure 4.2-1. Effect of Inplane Hub Impedance on Bifilar Response

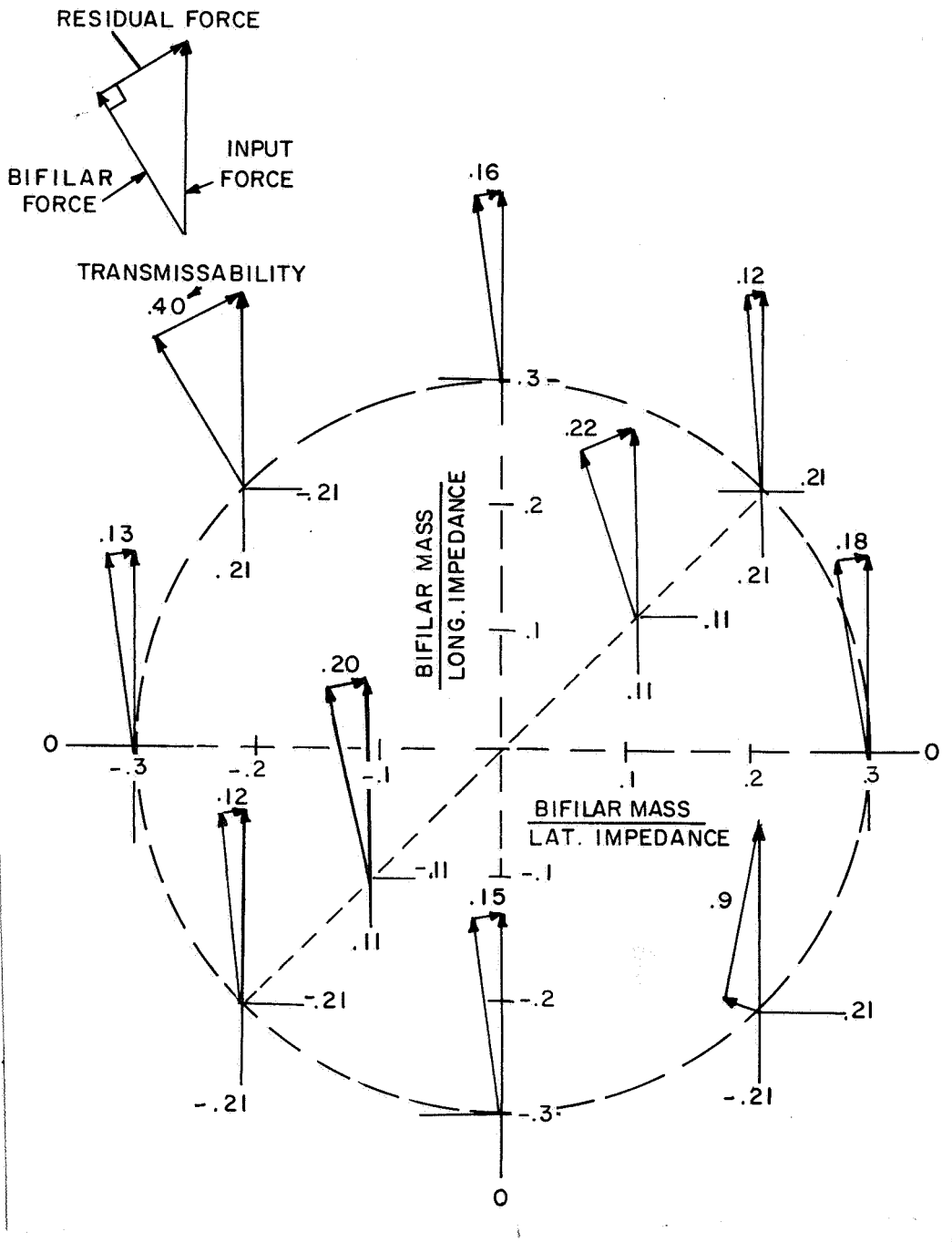

Figure 4.2-2. Hub Impedance Ratios Affect Bifilar Force Phasing

For bifilars with small amount of damping, say 1% to 3%, there are two prime factors that determine the phase angle of the bifilar response pattern. One is the ratio of the hub longitudinal impedance to the lateral. The other is the ratio of the bifilar mass to the inplane hub impedance. The former ratio dictates the hub response pattern therefore controls the bifilar effectivenss, consequently the transmitted residual force. The latter ratio is intuitively obvious. When the mass ratio approaches zero, either through the use of a bifilar absorber with insignificant dynamic mass or hub with virtually infinite impedance, the bifilar will have zero output force and permit transmission of the excitation force as the residual force.

Since the excitation force was held constant, 2224 N, for all cases, the bifilar force is therefore equal to the amplitude of the hub excitation force times the cosine of the phase angle between the bifilar force and hub excitation force. This is substantiated by the slight decrease in the bifilar mass motion together with small phase shift, Figure 4.2-1, when the ratio of the longitudinal to the lateral hub impedance was kept constant while varying the magnitude of both, and for the case with equal impedance ratio of .056, the rotation, or the phase angle, is more evident.

Using the transmissibility as a measure of bifilar effectiveness, a comprehensive map can be charted using the ratios of the bifilar mass to the longitudinal and the lateral hub impedance as coordinates. This is shown in Figure 4.2-3. The constant transmissibility lines are almost symmetrical to an imaginary line drawn diagonally from the second quadrant to the fourth quadrant. If the hub impedances had been defined as the total impedance including bifilar mass contributions, the map shown should be exactly symmetrical to that imaginary line. To understand these lines of constant transmissibility, it is instructive to consider the bifilar arm motion as a result of the hub motion.

For a helicopter hub with independent orthogonal impedance in two directions and two rotating, non-cancelling, vibratory inplane loads in the rotating system, the resulting hub motion in fixed coordinates can be described by an ellipse. Elliptic hub motion at N/rev will produce (N-1)/rev and (N+1)/rev motions on the rotating bifilar arm. As shown in Figure 4.2-4, with hub whirling in an elliptical pattern, either backward or forward relative to the rotating bifilars, the bifilar arms experience a mixture of (N-1)/rev and (N+1)/rev excitation. Only the forward circular whirl motion of the hub at N/rev will produce a pure (N+1)/rev motion of the bifilar arm at one extreme, and the backward whirl will produce pure (N-1)/rev motion at the other extreme. The mix of (N-1)/rev and (N+1)/rev excitation seen by the bifilar arms is highly dependent on the elliptic hub response pattern. In general, N/rev backward whirl results in more (N-1)/rev than (N+1)/rev arm motion and N/rev forward whirl produces more (N+1)/rev arm motion until at the extreme, forward circular whirl, there is no motion other than the (N+1)/rev of the arm.

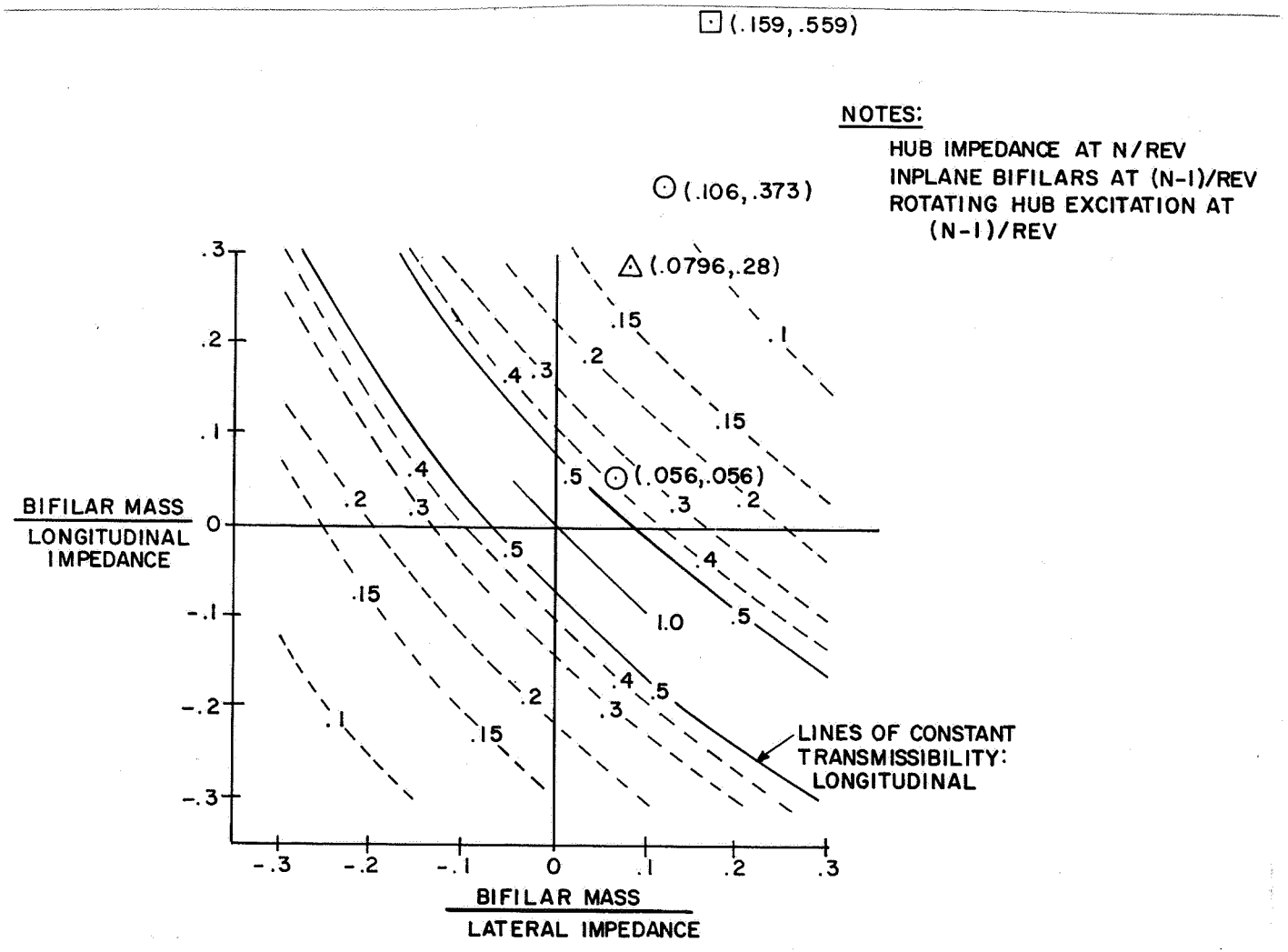

Figure 4.2-3. Inplane Bifilar Effectiveness as Affected by Hub Impedance

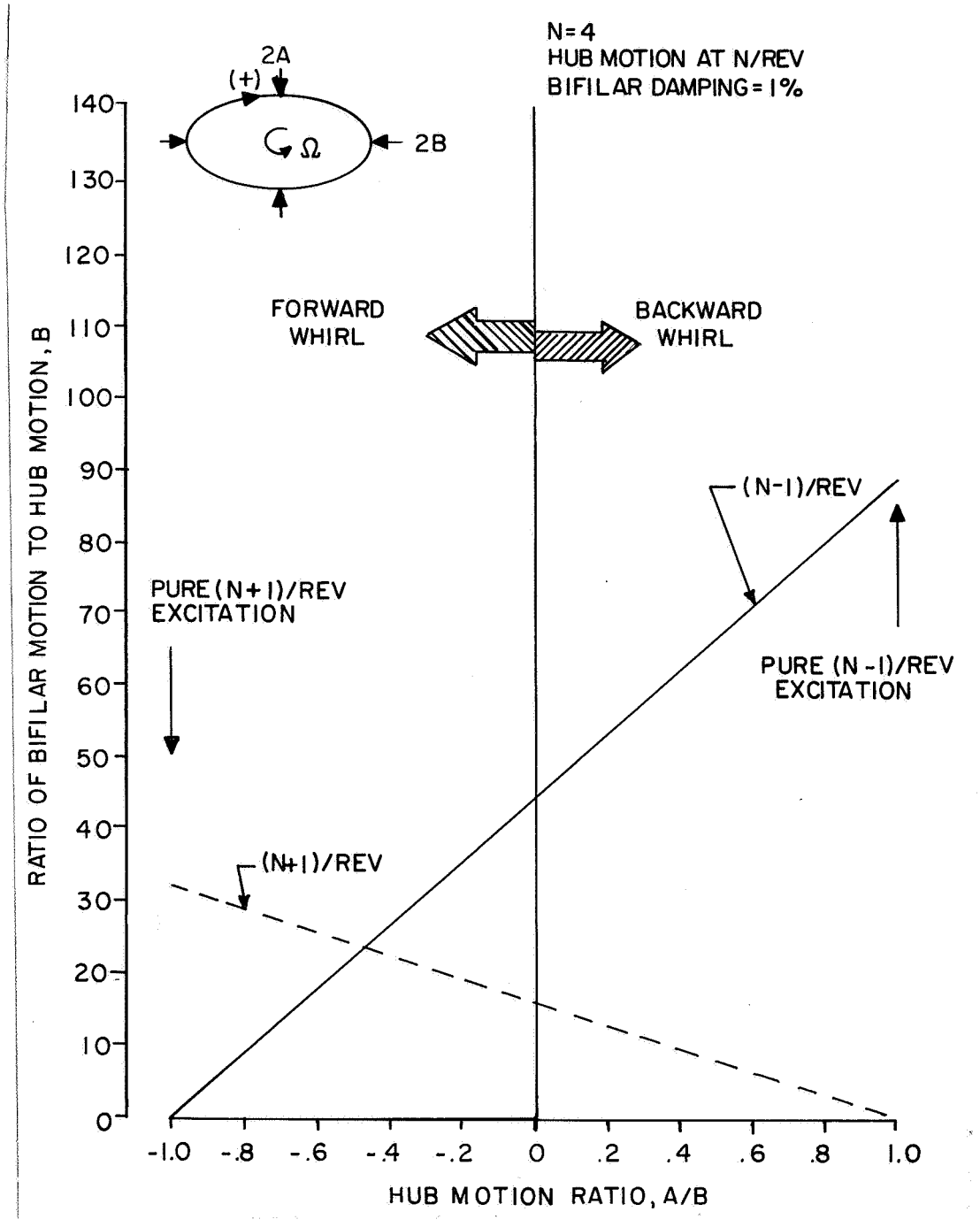

Figure 4.2-4. Bifilar Performance for Elliptic Hub Motion

When the longitudinal and the lateral hub impedances are of the same sign, they result in a backward whirl response at N/rev when forced by an (N-1)/rev rotating force. The (N-1)/rev bifilars are most effective for this combination of impedance since the resultant arm motions are mostly of (N-1)/rev. The opposite is true when the longitudinal and the lateral impedances are of the opposite sign. Forward whirl results, which generates a large amount of (N+1)/rev arm motion and relatively small (N-1)/rev motion. Although the (N-1)/rev bifilars are still effective against the (N-1)/rev motion, a large portion of the force is transmitted due to bifilar's ineffectiveness against the (N+1)/rev motion. In the limit, when the lateral and the longitudinal impedances are equal but of opposite sign, a circular forward whirl will result and will produce pure (N+1)/rev arm motion. The (N-1)/rev bifilars are not effective at all, consequently an unity transmissibility results along a diagonal line drawn from the second quadrant to the fourth quadrant as shown in Figure 4.2-3. In contrast, when the impedance ratio is positive (first and third quadrants of Figure 4.2-3), the (N-1)/rev bifilar is effective and marching out diagonally from the origin rapidly improves the transmissibility. This is merely due to the increase in the mass ratio of the bifilar mass to the hub impedance, the higher the ratio, the more effective the bifilars, consequently the smaller the transmissibility.

Figure 4.2-3 shows the effectiveness of the (N-1)/rev bifilars on the (N-1)/rev hub excitation with variation of N/rev hub impedances. A similar chart showing (N-1)/rev bifilar effectiveness on the (N+1)/rev excitation with hub impedance variation is shown in Figure 4.2-5. As is intuitively obvious, the transmissibility remains relatively high throughout. Even for a combination of bifilar mass/impedance ratio of .275 and .025, longitudinal and lateral respectively, while the longitudinal transmissibility is reasonable, less than .3, the lateral transmissibility becomes close to 2.0. (Note that the lateral transmissibility map is identical to Figure 4.2-5 once the labels for the coordinates are interchanged, and is therefore not shown here).

The results of the study of the effect of hub impedance on bifilar transmissibility show that if the rotor is generating a pure (N-1)/rev force in the rotating system, an (N-1)/rev bifilar absorber will be very effective (provided the bifilar mass/hub impedance ratio is reasonable and provided the hub lateral and longitudinal impedance are of the same sign). If the hub lateral to longitudinal impedance ratio departs from the ideal case of pure isotropy (ratio = +1), the response of the hub to the original (N-1)/rev force will become more and more elliptical and will eventually change from a backward whirl to a forward whirl. This only leads to reduced (N-1)/rev bifilar effectiveness. Low transmissibility can only be achieved, in this situation, by introducing a (N+1)/rev bifilar.

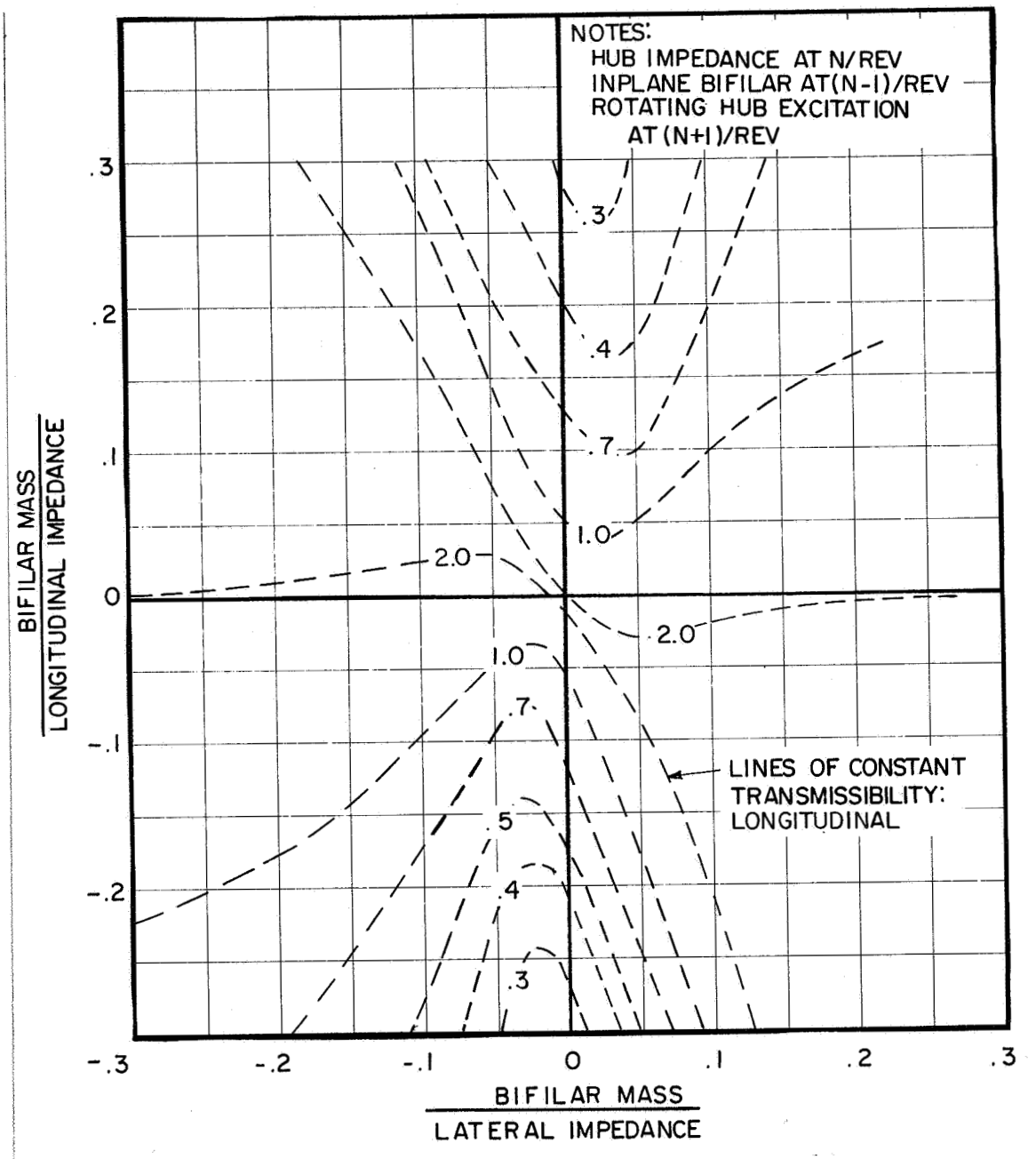

Figure 4.2-5. (N-1)/Rev Inplane Bifilar Effectiveness on (N+1)/Rev Excitation as Affected by Hub Impedance

4.3 Rotor Dynamics Effect on Airframe Response and Bifilar Performance

The impedance that the bifilar sees is not that of the uncoupled airframe. It is, rather, the impedance of the coupled airframe and rotor system. A comparison has been made using the coupled rotor/non-linear bifilar/airframe analysis for a baseline case with and without the rotor. The rotor has been modelled by using one rigid body mode each in blade flap and lag directions, and two flexible, coupled blade flatwise and edgewise bending modes with frequencies of 12.3 Hz and 20.2 Hz, which cover adequately the 3/rev rotating frequency of interest. In addition to the nine flexible airframe modes described in Table 4.1-1, modes No. 1 through 9, the six rigid body modes (No. 10 through 15) have also been utilized to examine the necessity of including airframe rigid body degrees-of-freedom in assessing the bifilar performance.

Shown in Figure 4.3-1 are the hub longitudinal and lateral accelerations and the companion bifilar response to a 3/rev rotating excitation force. With airframe represented by nine flexible modes, inclusion of rotor dynamics reduces the longitudinal acceleration and increases the lateral slightly while the bifilar motion sees no change. Adding the rotor to the coupled system has evidently lowered the frequencies of the modes, with those contributing to the hub longitudinal response move away from the excitation frequency while those for the lateral response move closer to the excitation. This is substantiated by comparing Figure 4.3-2 which shows analytical shake test results with the rotor turning, to Figure 4.1-1.

Also shown in Figure 4.3-1 are the responses calculated using six airframe rigid body modes in addition to and in place of the nine flexible modes, with and without the rotor. Comparing to the results obtained with only nine flexible modes, addition of the six rigid body modes has practically no effect on the responses due to a 3/rev rotating force at hub, except for the hub lateral acceleration without rotor case, including rigid body modes reduces that particular response slightly. It is of interest to note that the hub vibration calculated with the airframe rigid body modes only is totally unrealistic.

Rotor effect on airframe response and bifilar performance to a 5/rev rotating hub force is shown in Figure 4.3-3. Including the rotor, in general, reduces the response. Note that the 3/rev bifilars are still responsive to the 5/rev excitation. This is due to the elliptic hub response at 4/rev that creates some 3/rev bifilar arm motion, as discussed earlier in Section 4.2, which causes the bifilar motion.

It is clear from the comparison of hub accelerations in two inplane directions obtained using analysis with and without the rotor that the coupled rotor/airframe dynamics must be included in the analysis to obtain the correct impedance for evaluation of bifilar performance. In addition,

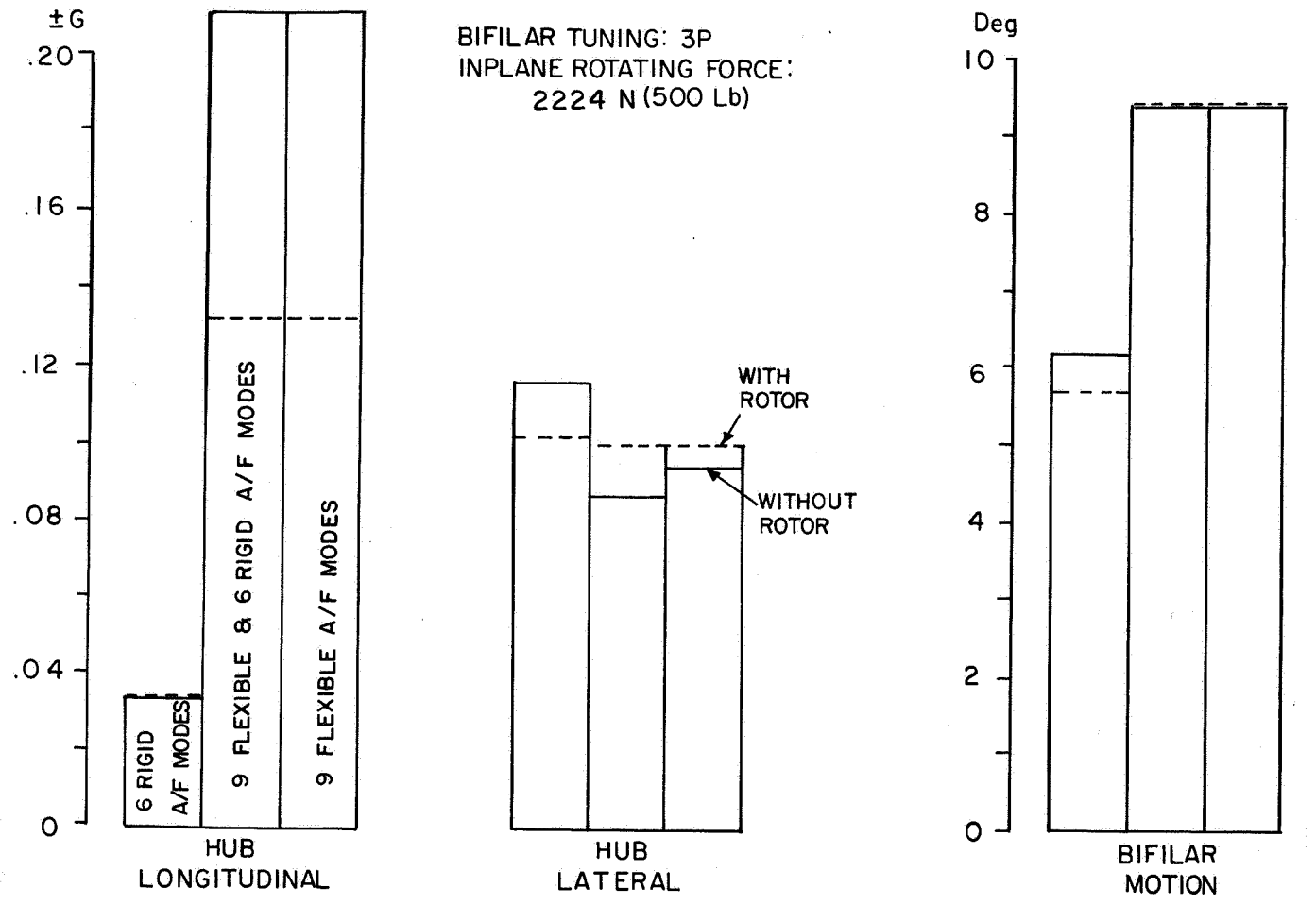

Figure 4.3-1. Effect of Rotor on Airframe Response and Bifilar Performance to 3/Rev Excitation

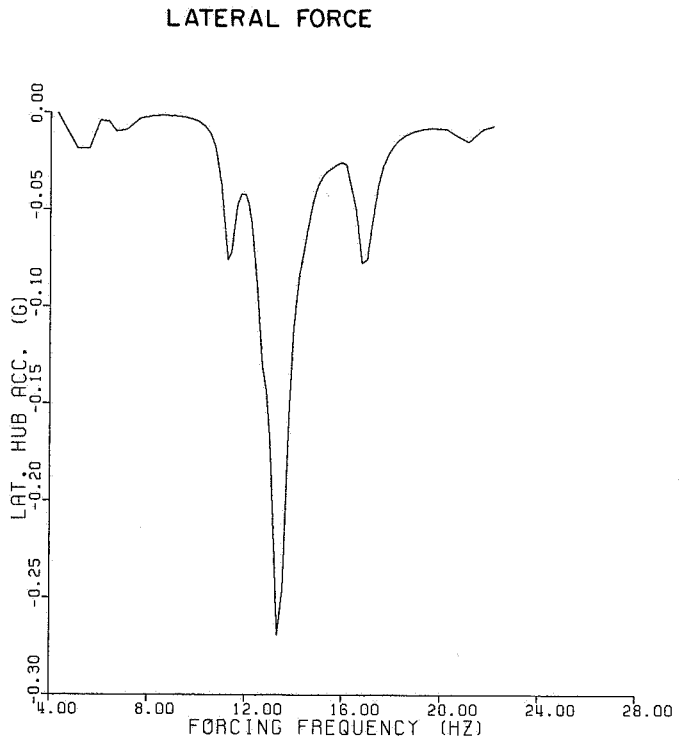

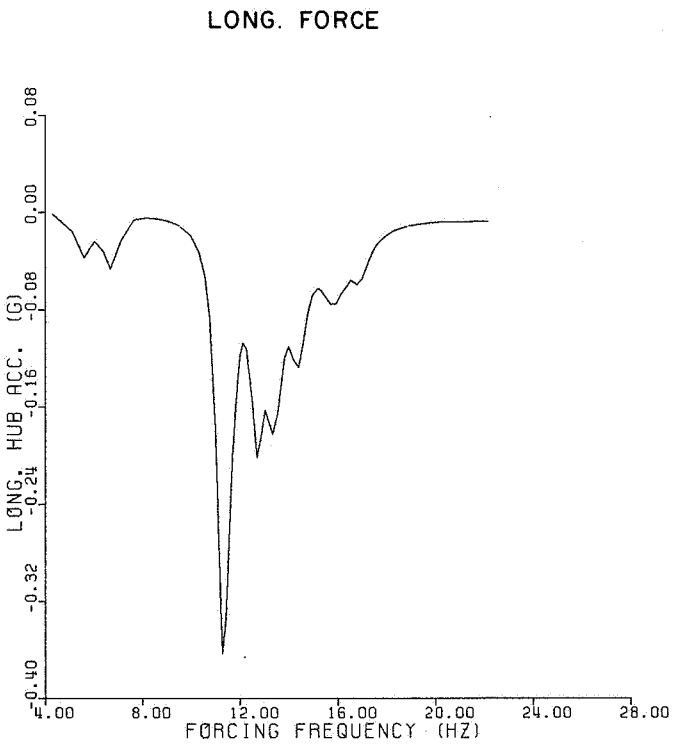

Figure 4.3-2. Effect of Flexible Rotor on Coupled Frequencies

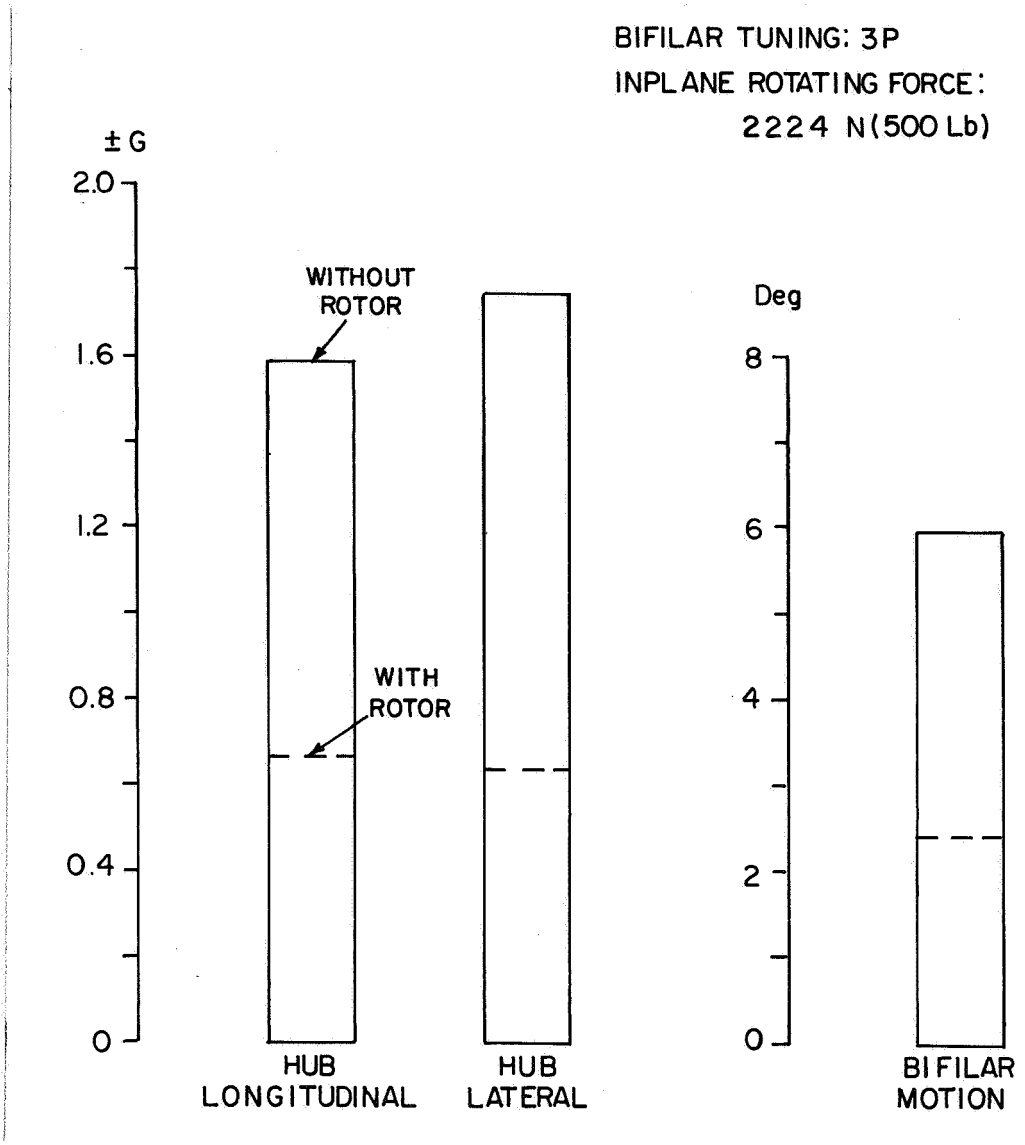

Figure 4.3-3. Effect of Rotor on Airframe Response and Bifilar Performance to 5/Rev Excitation

the so-called cyclic rotor modes, in general, have significant participation of hub, or airframe, motion. Variation of the frequencies of the flexible blade modes should have profound effect on the hub impedance in terms of amplification and phase and deserves further study.

4.4 Bifilar Sensitivity to Design Parameters and Tolerances

The performace of the bifilar is, of course, a function of its basic design parameters, namely, dynamic mass, damping and tuning. Since it is used to reduce the motion of its attachment point, the impedance of the hub is of equal importance. The previous two sections focused on the effect of hub impedance. This section will discuss the effects of the basic design parameters and their tolerances on bifilar performance. The non-linear bifilar absorber model with time history solution was used for these studies.

Dynamic Mass - Figure 4.4-1 shows the bifilar response patterns to a constant rotating force of 2224 N (500 lb) with various dynamic masses. For baseline configuration, with bifilar mass weighing 8.87 kg, the ratios of bifilar mass to longitudinal and lateral impedance are .559 and .159 respectively. As expected, the amplitude of the response increases with decreasing mass. Tabulated at the bottom of Figure 4.4-1 are the residual force transmitted as percentage of applied force. For a dynamic mass of 15.42 kg (34 lb) and 13.61 kg (30 lb), the transmissibilities in longitudinal and lateral directions remain essentially the same, however as the dynamic mass decreases, the transmissibility increases quite rapidly. This is primarily due to the fact that at lower dynamic mass, the ratio of the bifilar mass to the hub impedance becomes smaller, consequently less effective in attenuating excitation as discussed in Section 4.2 relative to Figure 4.2-3. In addition, at large amplitude, the tuning of the bifilar based on the small angle assumption no longer holds true. The bifilar becomes de-tuned, hence the even higher transmissibility.

This is substantiated by comparing Figure 4.4-2, where the bifilar mass amplitude is seen to vary non-linearly with decreasing dynamic mass from 12 kg on down, with Figure 4.4-3, where both linear and non-linear bifilar representations have been used to obtain the forced responses of bifilar and hub with bifilar mass being held constant at 9.07 kg (20 lb). Although for dynamic mass of 9.07 kg, the bifilar amplitude falls on the non-linear portion of the curve in Figure 4.4-2, the linear analysis is seen to yield identical results as the non-linear one until the bifilar mass amplitude exceeds 13 degrees.

For bifilar masses responding with an amplitude where the linear analysis is valid, a small deviation of dynamic mass on one arm, say 3%, should not affect the bifilar absorber performance. Although the discrepant bifilar mass will have a higher or lower amplitude depending on whether the

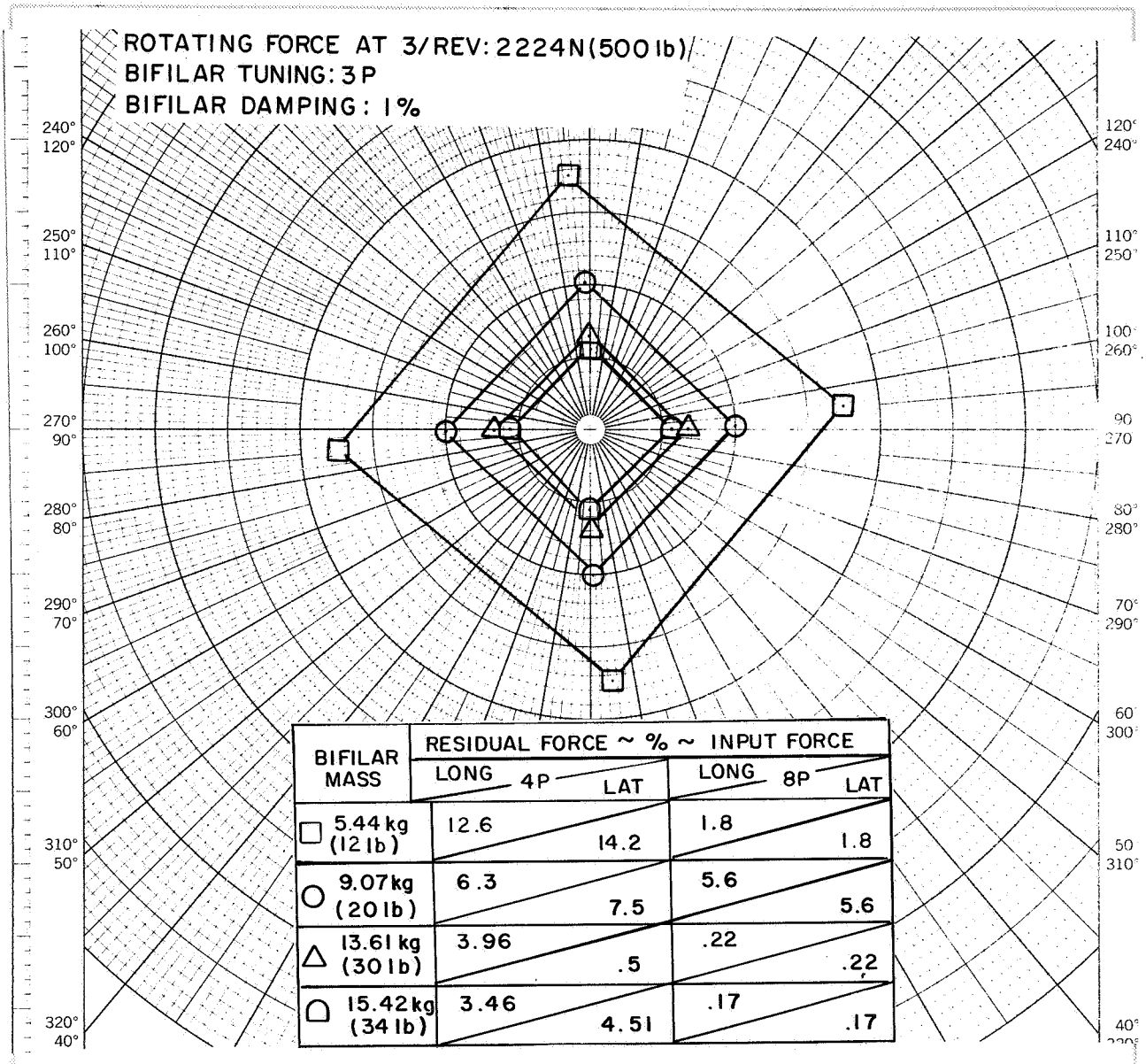

BIFILAR MASS	RESIDUAL FORCE ~ % ~ INPUT FORCE			
	LONG 4P	LAT	LONG 8P	LAT
□ 5.44 kg (12 lb)	12.6	14.2	1.8	1.8
○ 9.07 kg (20 lb)	6.3	7.5	5.6	5.6
△ 13.61 kg (30 lb)	3.96	.5	.22	.22
⌂ 15.42 kg (34 lb)	3.46	4.51	.17	.17

Figure 4.4-1. Effect of Dynamic Mass on Bifilar Response Amplitude and Transmissibility

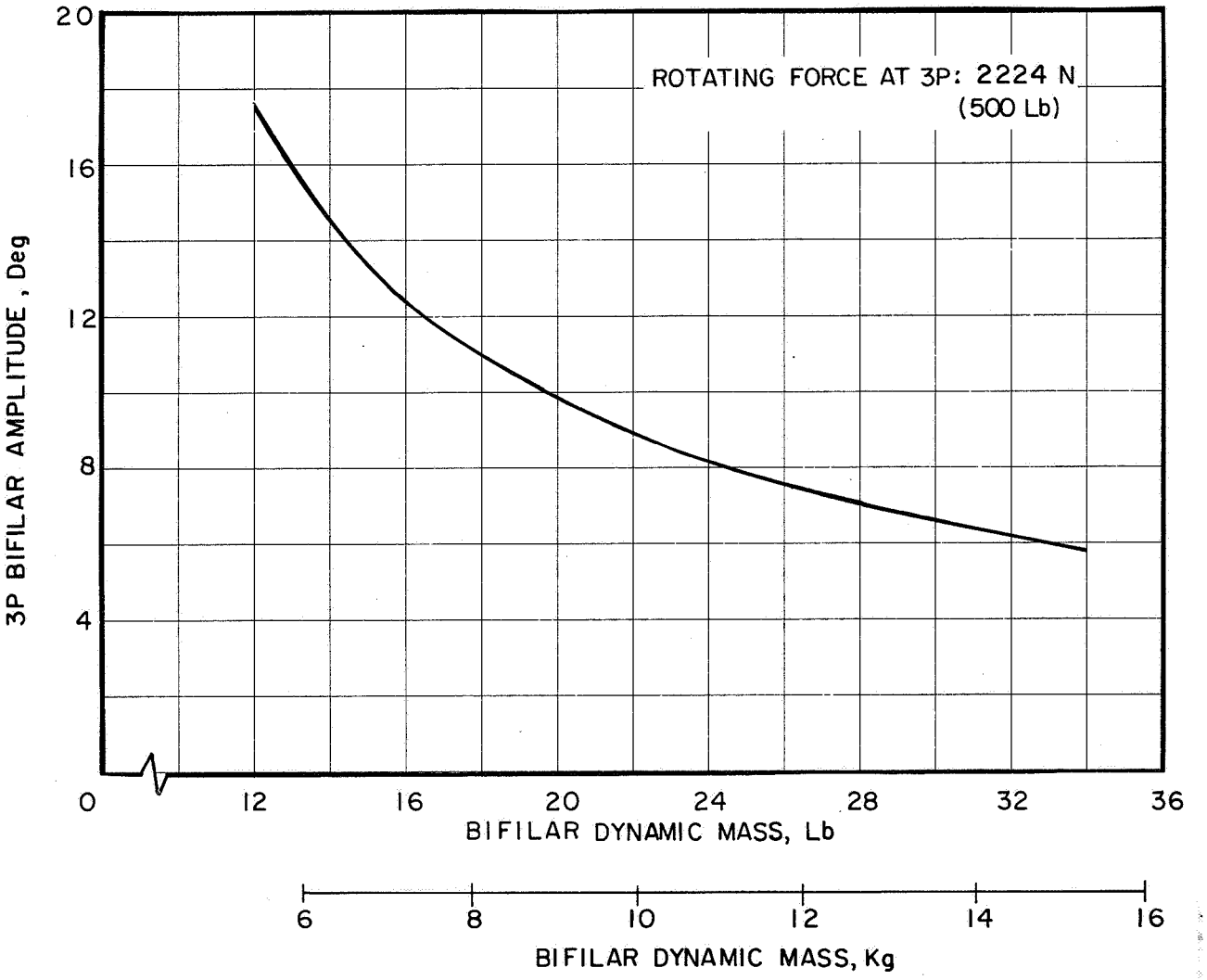

Figure 4.4-2. Dynamic Mass Effect on Bifilar Response

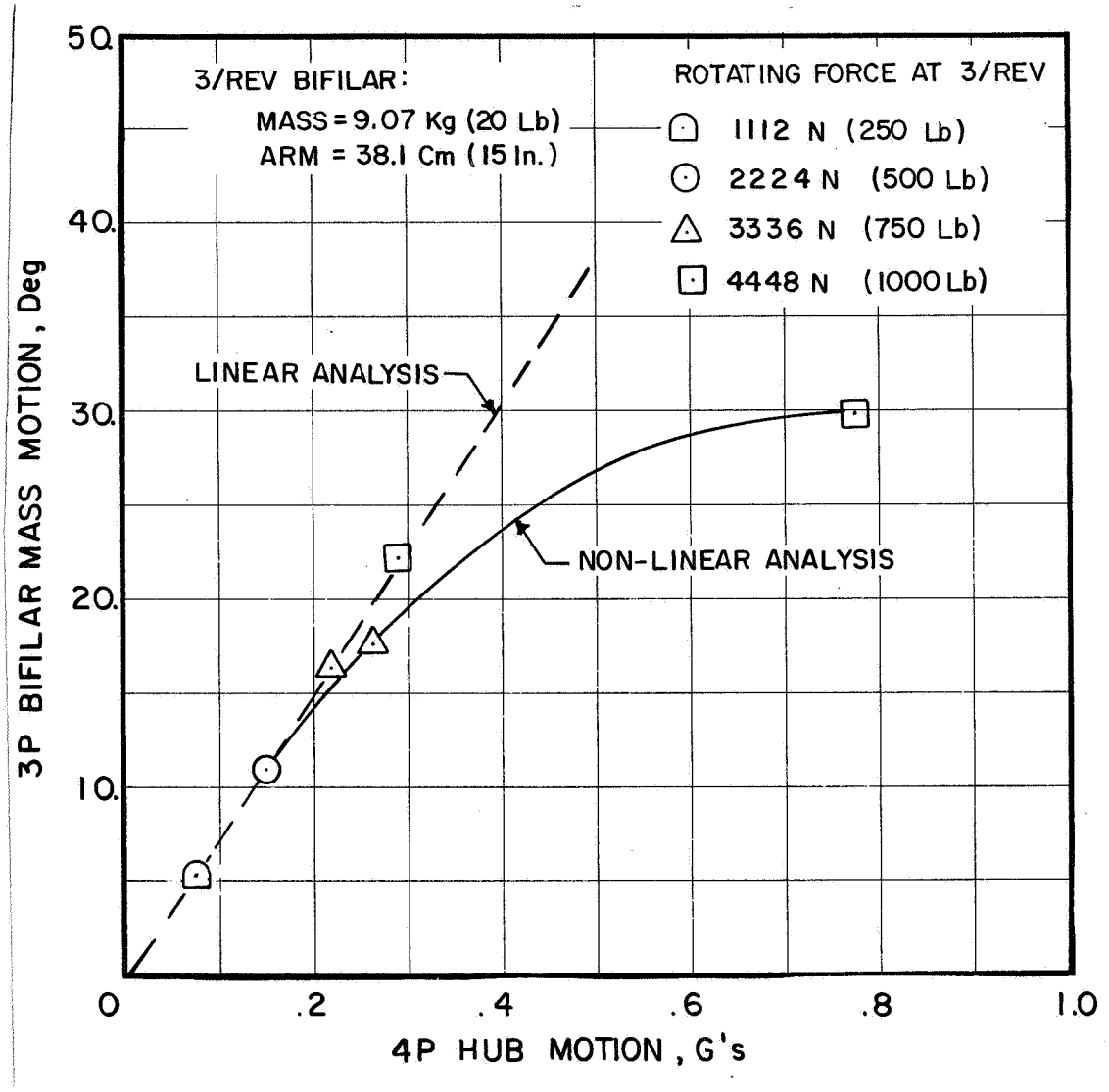

Figure 4.4-3. Validity of Linear Bifilar Analysis

mass is less or more, its total force output remains the same. Since bifilar tuning is independent of its mass, there is no phase shift in the discrepant bifilar mass response, therefore, the bifilar absorber response pattern in terms of output G's will remain the same. This is validated by performing calculation using the non-linear bifilar analysis with variation of one bifilar mass by ±3%, and two adjacent and two opposite masses by -3% and comparing the resultant transmissibility to the baseline case of identical masses. As shown in Table 4.4-1, with the excitation set at 2224 N and at 3336 N, there is no change in transmissibility. Note that with the excitation force at 3336 N, the bifilar response is already slightly beyond the linear range as shown in Figure 4.4-3. Although the bifilars are quite insensitive to deviation in the weight, the resultant 1/rev imbalance force, shown in Table 4.4-1 should not be overlooked.

Damping - The effect of damping on bifilar mass response amplitude, shown in Figure 4.4-4, is as expected, namely, the amplitude is inversely proportional to the amount of damping. Note as the bifilars become less responsive due to higher damping, the resultant response pattern also rotates away from the original set to generate higher residual, or transmitted, force as discussed earlier in Section 4.2. When two opposite bifilar masses have their damping increased from 1% to 2%, their amplitude will decrease as discussed earlier, however, the remaining pair, having 1% damping, will have their amplitudes increased. The resultant diamond-shaped response pattern, illustrated in Figure 4.4-5 against the baseline square pattern, also has the major and minor axes rotated from the baseline square in the opposite directions.

The amplitude for the pair of bifilar masses with 1% damping grows to compensate for the reduction in force output from the pair with 2% damping since their amplitudes have been reduced. However, the rotation of the diamond pattern relative to the square pattern is entirely a different matter than those discussed previously. In general, when the response pattern is not square, non-N/rev residual forces are generated. When the response is of a diamond pattern, 2/rev force results. Phase shift of the axes towards each other is a result of the bifilar masses responding to the 2/rev excitation. This is illustrated in Figure 4.4-6. In addition to the inplane rotating force of 2224 N at 3/rev (which causes the bifilar masses to respond in a square pattern when the 3/rev force is the only excitation and all the bifilar masses are identical), 2/rev forces are added at 445 N and then at 889.4 N. The results are the diamond pattern with skewed axes. It is of interest to note that almost the entire 2/rev excitation has been transmitted to the hub although the 3/rev bifilars do attenuate a very minute amount of the force.

The effect of one bifilar mass having higher damping than the rest is explored in Figure 4.4-7. As the amplitude of the discrepant bifilar mass decreases with increasing damping, the two adjacent masses see an increase in amplitudes compensating for the reduced force output from the discrepant bifilar mass. The transmitted residual hub force at 3/rev changes moderately (from 6.2 and 7.4%, longitudinal and lateral respectively, to 8.0 and

TABLE 4.4-1 Bifilar Performance as Affected by Tolerance on Dynamic Mass

Bifilar Mass Configuration	Rotating Force @ 3P					
	2224 N (500 lb)			3336 N (750 lb)		
	4P Trans.		1P	4P Trans.		1P
	Long	Lat	Force	Long	Lat	Force
Baseline: Identical Mass	6.2%	7.4%	0	7%	8.5%	0
One Odd Mass: -3%	6.2%	7.4%	115.7 N (26 lb)	7%	8.5%	115.7 N (26 lb)
One Odd Mass: +3%	6.2%	7.4%	155.7 N (35 lb)	7%	8.5%	155.7 N (35 lb)
Two Adjacent Mass: -3%	6.2%	7.4%	164.6 N (37 lb)	7%	8.5%	164.6 N (37 lb)
Two Opposite Mass: -3%	6.2%	7.4%	0	7%	8.5%	0

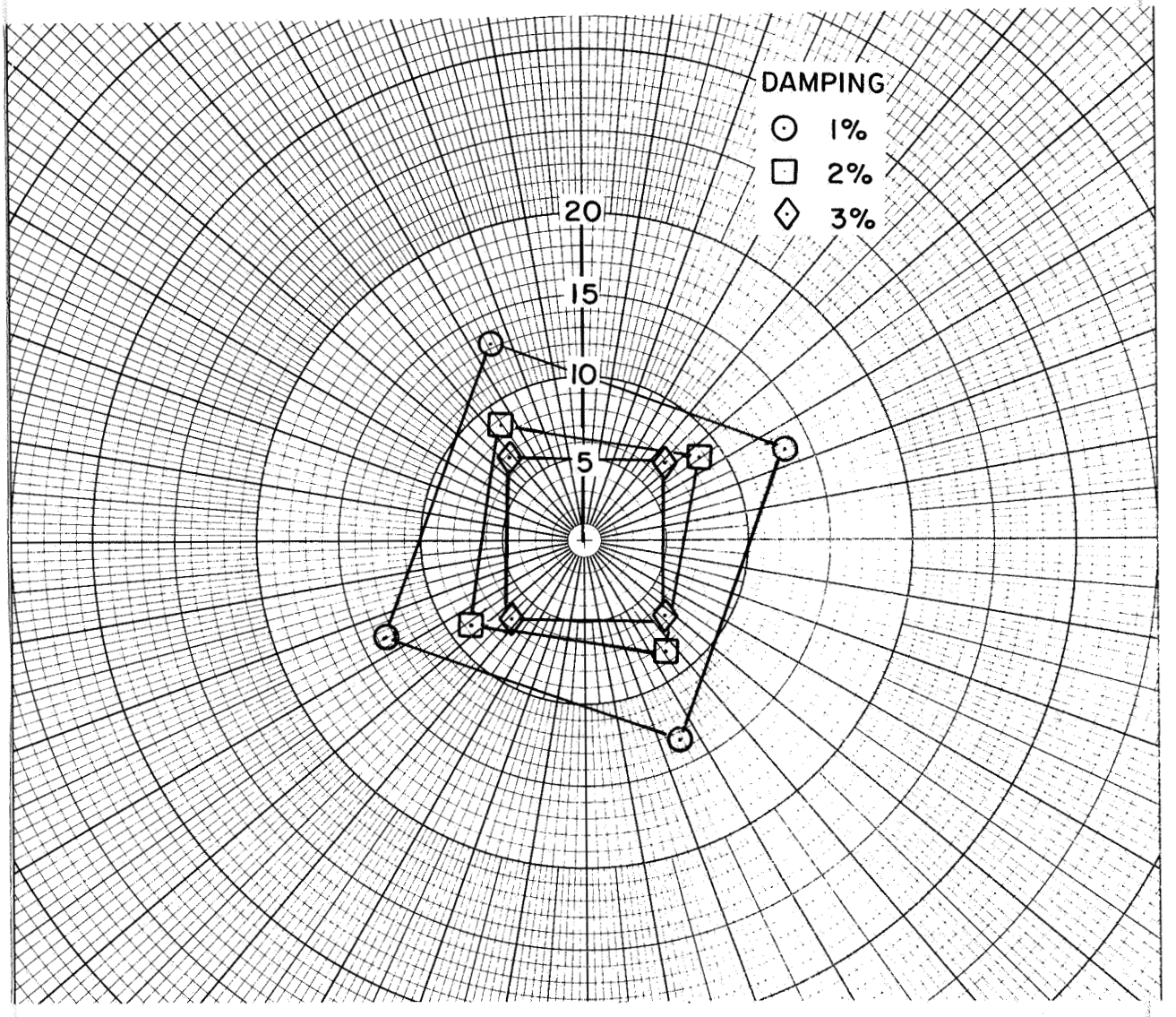

Figure 4.4-4. Effect of Damping on Bifilar Response Amplitude

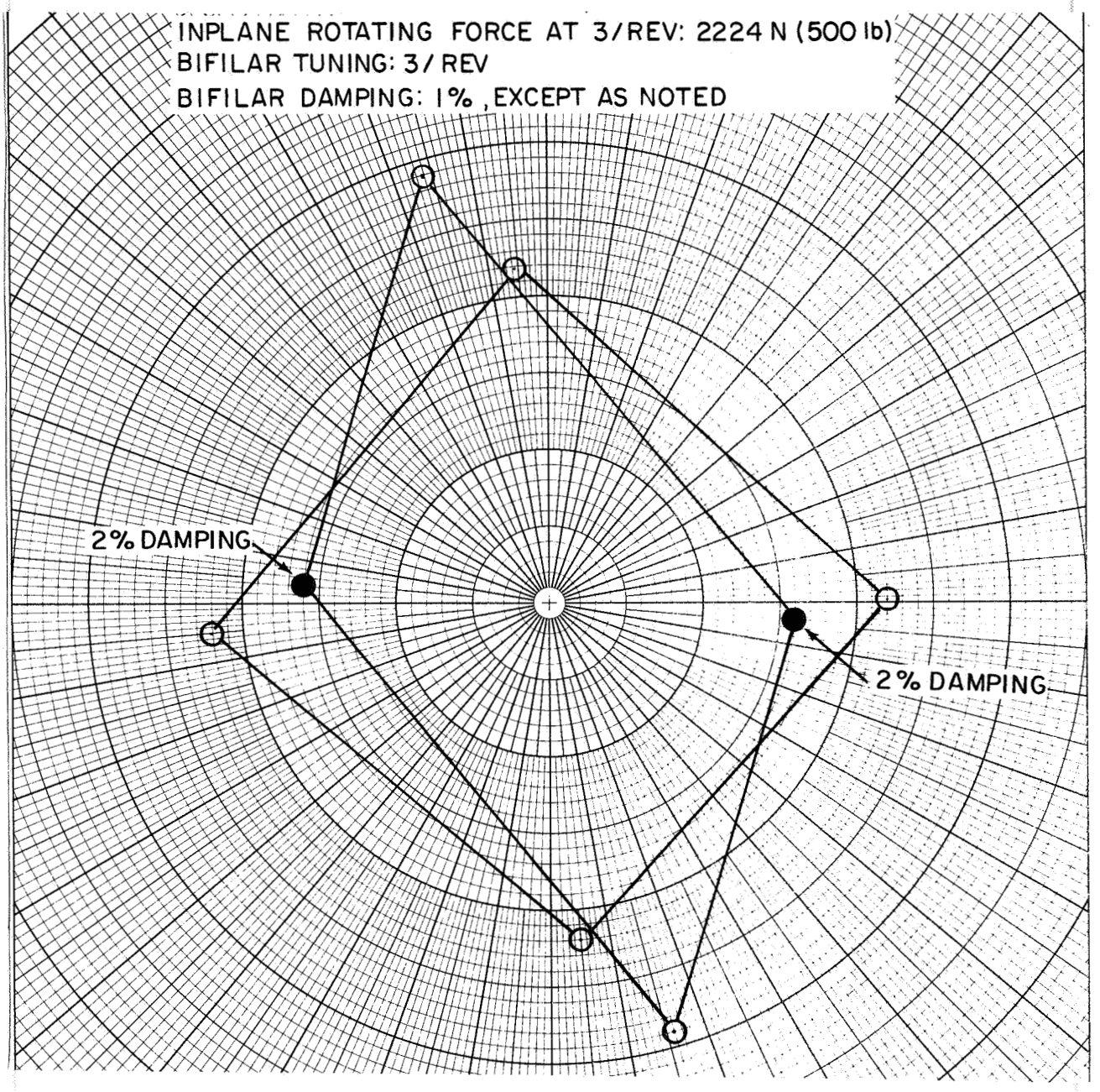

Figure 4.4-5. Bifilar Pattern as Affected by Variation in Damping

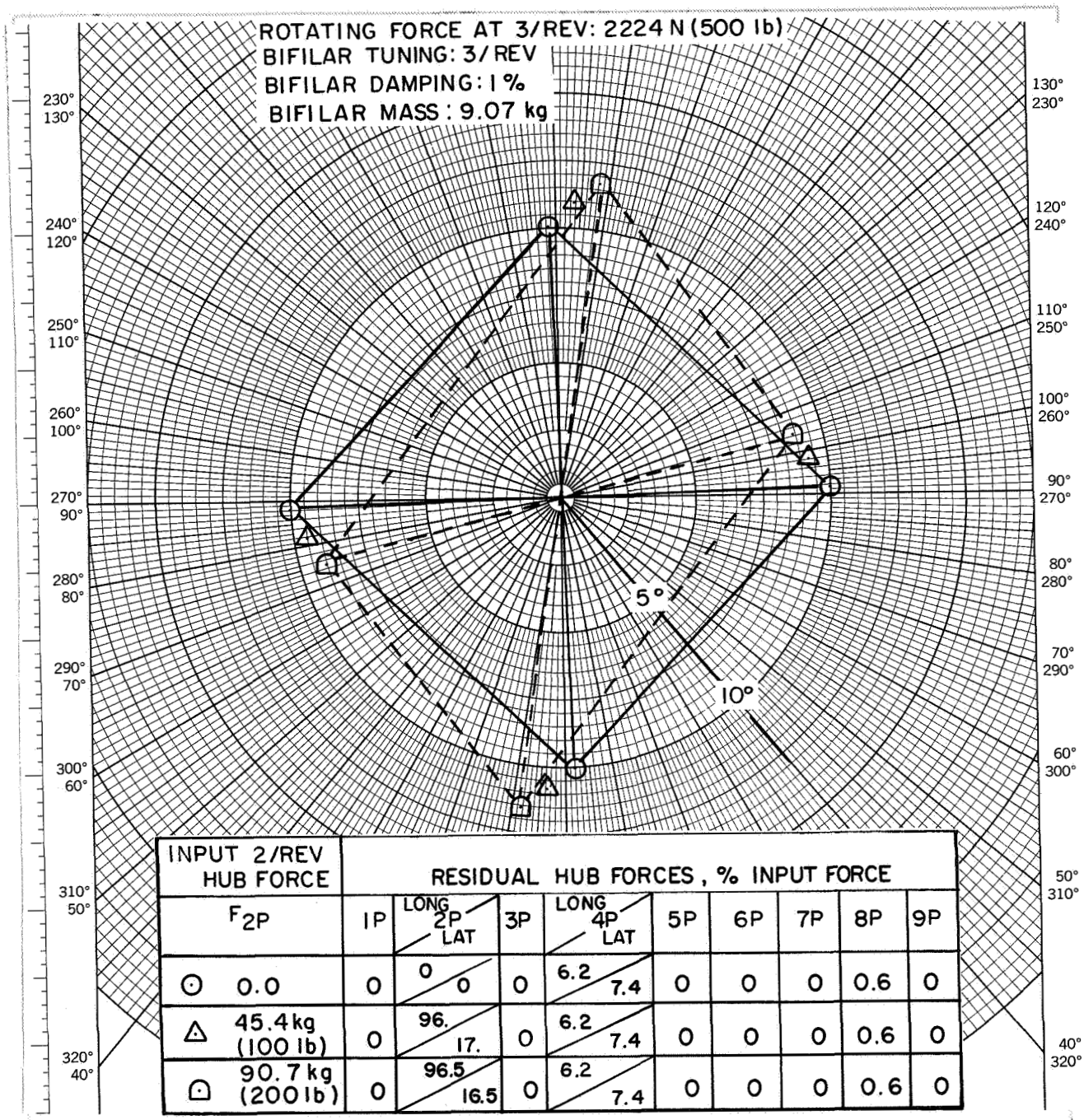

INPUT 2/REV HUB FORCE	RESIDUAL HUB FORCES, % INPUT FORCE								
F_{2P}	1P	LONG 2P / LAT	3P	LONG 4P / LAT	5P	6P	7P	8P	9P
⊙ 0.0	0	0 / 0	0	6.2 / 7.4	0	0	0	0.6	0
△ 45.4 kg (100 lb)	0	96. / 17.	0	6.2 / 7.4	0	0	0	0.6	0
⊡ 90.7 kg (200 lb)	0	96.5 / 16.5	0	6.2 / 7.4	0	0	0	0.6	0

Figure 4.4-6. Bifilar Pattern as Affected by 2/Rev Hub Force

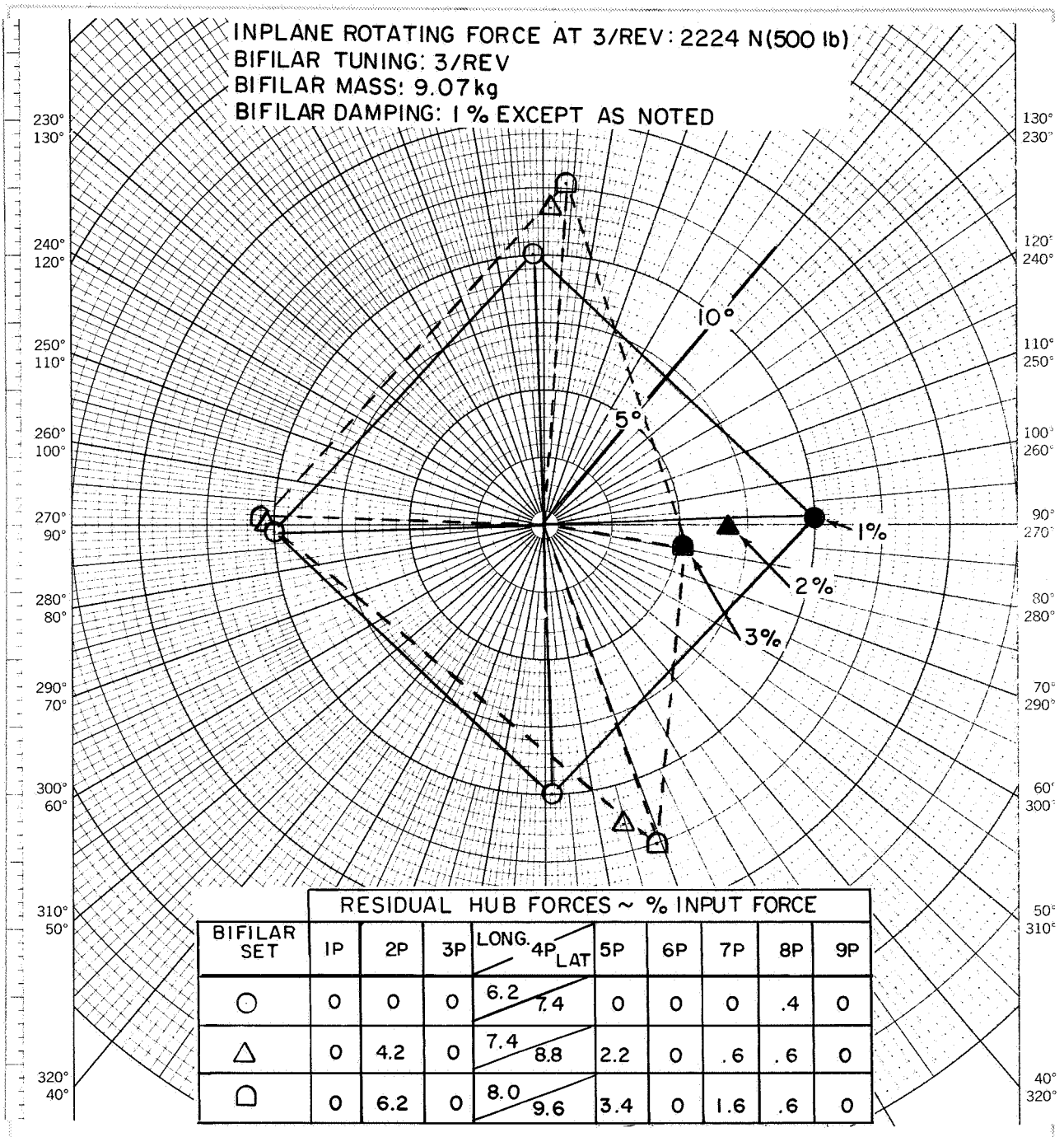

RESIDUAL HUB FORCES ~ % INPUT FORCE

BIFILAR SET	1P	2P	3P	LONG. 4P LAT	5P	6P	7P	8P	9P
○	0	0	0	6.2 / 7.4	0	0	0	.4	0
△	0	4.2	0	7.4 / 8.8	2.2	0	.6	.6	0
∩	0	6.2	0	8.0 / 9.6	3.4	0	1.6	.6	0

Figure 4.4-7. Bifilar Performance as Affected by Tolerance on Damping

9.6%). However, the odd harmonic forces generated are quite substantial: 2/rev being the major odd harmonic force, and 5/rev to a lesser extent.

Tuning - It was briefly discussed earlier with respect to the dynamic mass effect that for large bifilar amplitudes, the bifilar will be detuned due to the fact that small angle assumption, in particular, the sine of the amplitude is equal to the amplitude in radians, is no longer true. Referring again to Figure 4.4-3, for an inplane hub excitation of 4448 N (1000 lb), the linear analysis will calculate a bifilar response amplitude of 22^{o} resulting in hub acceleration of 0.29 g. The non-linear analysis predicts bifilar amplitude at 29.5^{o} and hub acceleration of 0.77 g. In this extreme case, the bifilar masses have more than 30% increase in amplitude as compared to those that are in-tune, and the transmissibility is more than two and one half times higher. Manufacturing tolerances on the tracking hole diameter, contour, diameter of the tuning pin, bifilar arm offset distance from the center-line of rotation and etc, all contribute to the possible small differences in tuning of each bifilar mass. These small differences will be greatly amplified when the response is in the non-linear range. The effect of difference in tuning is explored using the non-linear bifilar analysis with selected bifilar masses set to different frequencies.

Figure 4.4-8 shows the effect of off-tuning on the bifilar response pattern when two opposite bifilar masses are off-tuned. Basically, the bifilar masses form a near rectangular pattern. The transmitted 4/rev residual force is increased by an additional 70%, from 6 - 7% to 11 - 13% when the tuning is off by +.05/rev from 3/rev, the tuned frequency. Of importance is the odd harmonic, namely, the 2/rev, force generated. Besides a hefty twenty percent of the original 3/rev excitation has been transmitted as 2/rev residual hub force, which is nearly twice the 4/rev residual, the transmissibility is degraded at an ever increasing rate with the percent of off-tuning. With only one bifilar mass being off-tuned, the 2/rev is less severe, however, there are additional odd harmonics, 5/rev and 7/rev and a small amount of 1/rev, Figure 4.4-9. Note that the bifilar response pattern varies from the ideal square to an "arrow" shape.

The effect of combined over- and under-tuned bifilar masses on the bifilar performance is shown in Figure 4.4-10. One bifilar set has two adjacent masses tuned +.015/rev and -.015/rev from the baseline 3/rev. The other set has two opposite ones being over- and under-tuned. While both sets generate odd harmonic forces, the set with adjacent discrepant bifilar masses is seen to have higher 2/rev residual force whereas the set with opposite discrepant masses generates higher 5/rev residual force. The response pattern, in general, is of quadrilateral shape, almost indistinguishable from those formed with one bifilar mass having different damping value, Figure 4.4-7.

When two pairs of opposite bifilar masses have different dampings, while their tunings are identical, the response pattern, shown in Figure 4.4-5 previously, is of a near diamond shape. Figure 4.4-11 shows the

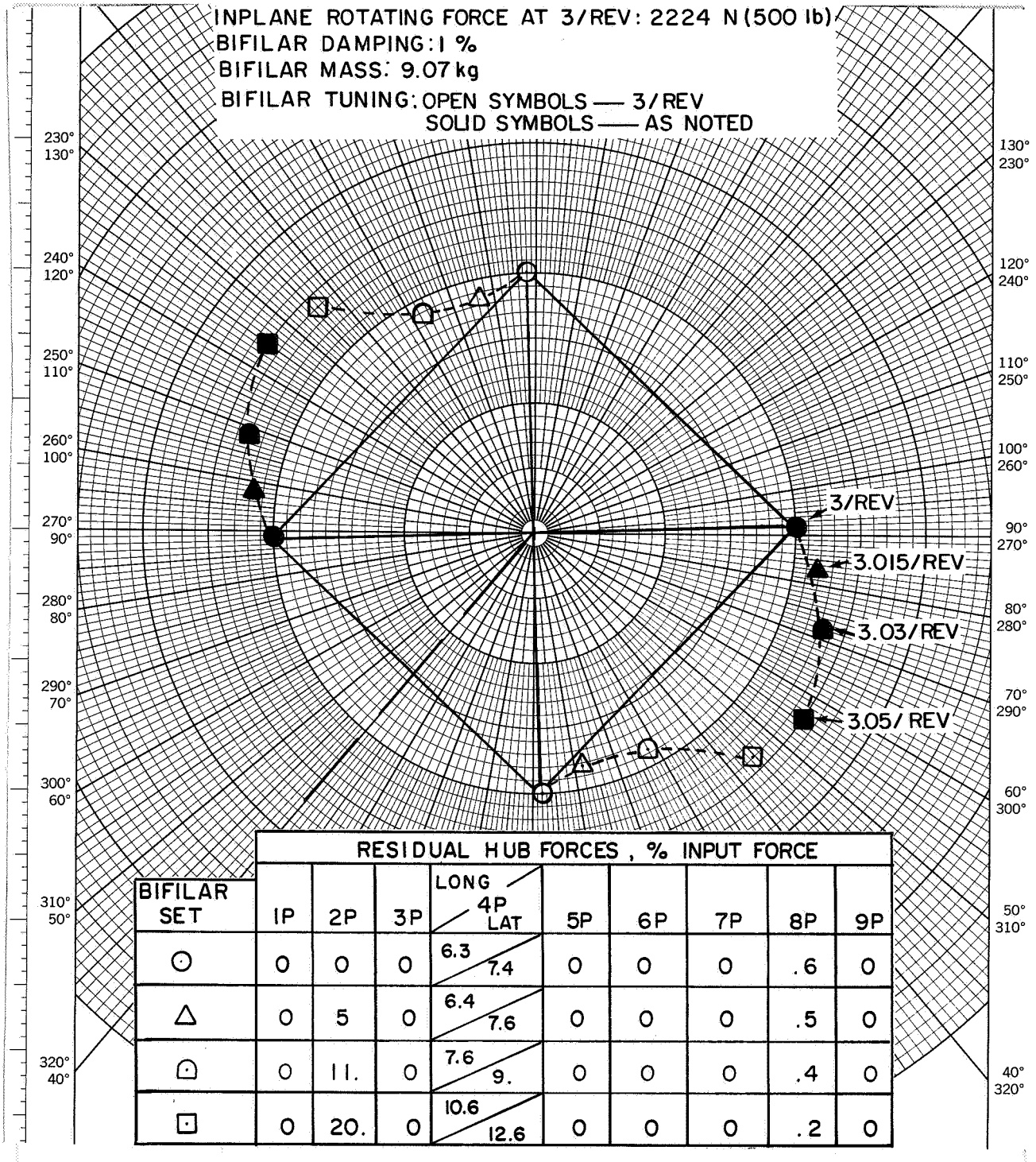

RESIDUAL HUB FORCES, % INPUT FORCE									
BIFILAR SET	1P	2P	3P	LONG 4P / LAT	5P	6P	7P	8P	9P
⊙	0	0	0	6.3 / 7.4	0	0	0	.6	0
△	0	5	0	6.4 / 7.6	0	0	0	.5	0
⊡	0	11.	0	7.6 / 9.	0	0	0	.4	0
□	0	20.	0	10.6 / 12.6	0	0	0	.2	0

Figure 4.4-8. Bifilar Pattern as Affected by Variation in Tuning

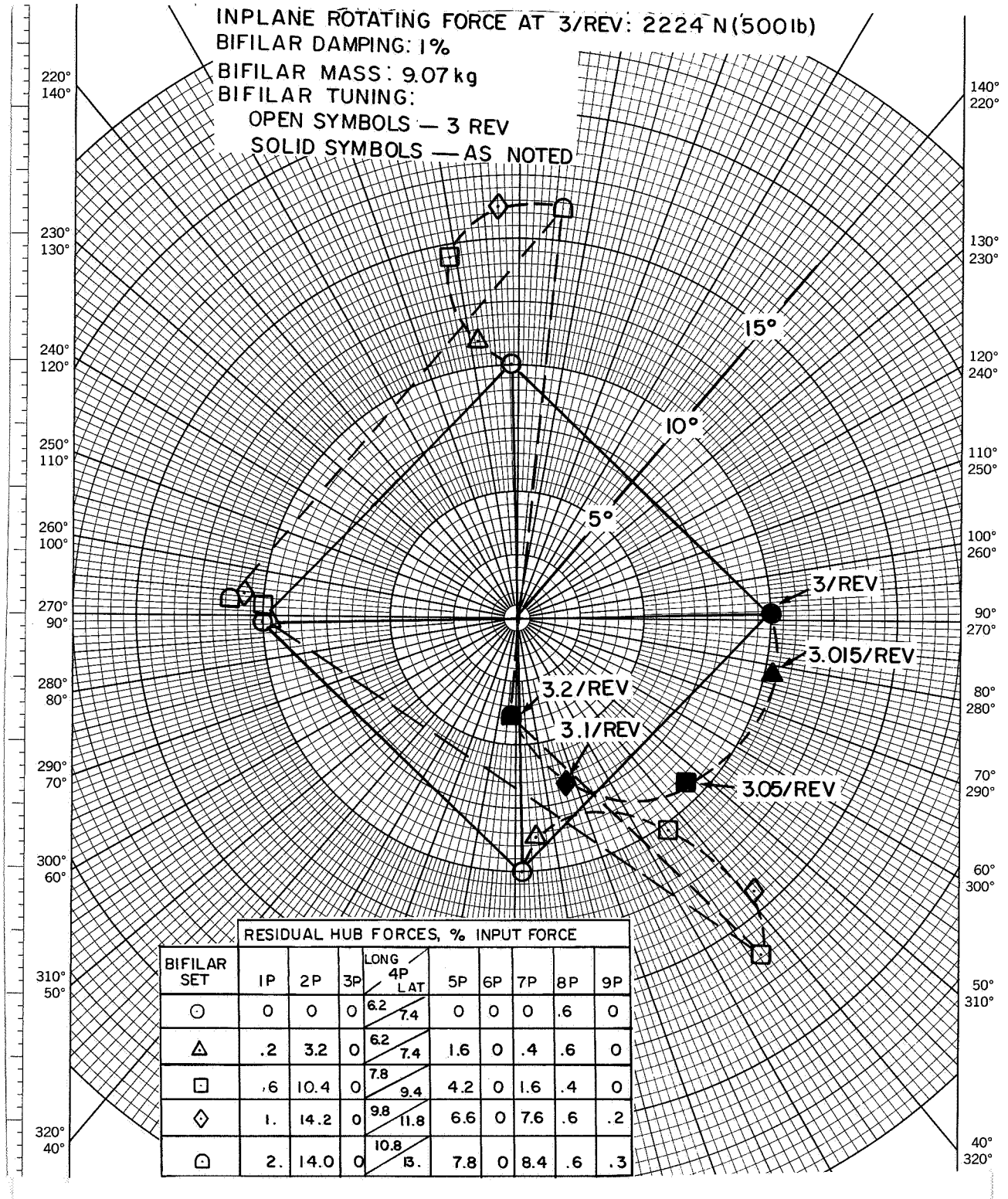

RESIDUAL HUB FORCES, % INPUT FORCE

BIFILAR SET	1P	2P	3P	LONG 4P LAT	5P	6P	7P	8P	9P
⊙	0	0	0	6.2 / 7.4	0	0	0	.6	0
△	.2	3.2	0	6.2 / 7.4	1.6	0	.4	.6	0
⊡	.6	10.4	0	7.8 / 9.4	4.2	0	1.6	.4	0
◇	1.	14.2	0	9.8 / 11.8	6.6	0	7.6	.6	.2
⊙	2.	14.0	0	10.8 / 13.	7.8	0	8.4	.6	.3

Figure 4.4-9. Bifilar Performance as Affected by Tolerance in Tuning

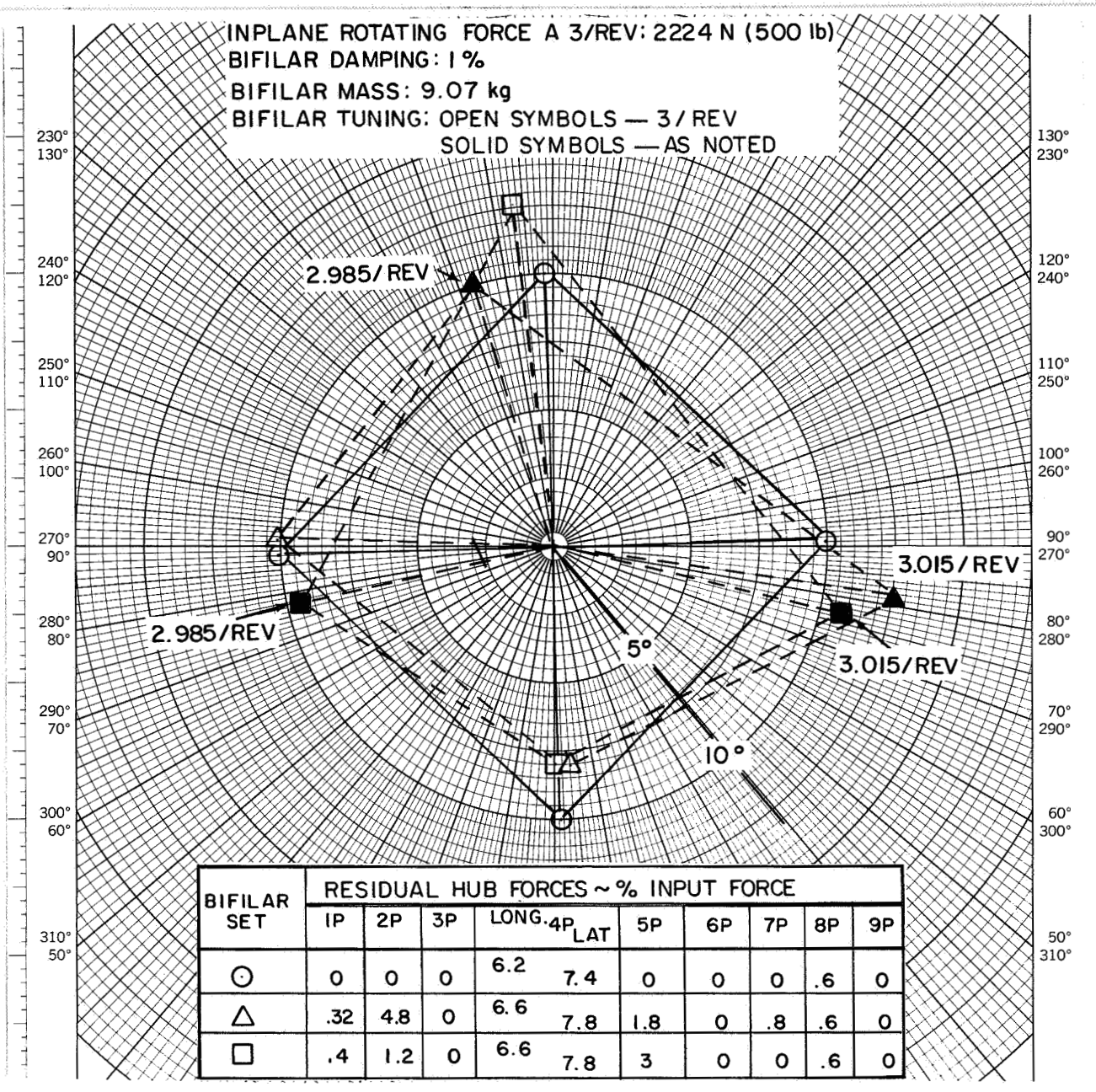

BIFILAR SET	RESIDUAL HUB FORCES ~ % INPUT FORCE								
	1P	2P	3P	LONG. 4P / LAT 4P	5P	6P	7P	8P	9P
⊙	0	0	0	6.2 / 7.4	0	0	0	.6	0
△	.32	4.8	0	6.6 / 7.8	1.8	0	.8	.6	0
□	.4	1.2	0	6.6 / 7.8	3	0	0	.6	0

Figure 4.4-10. Effect of Combined Over- And Under-Tuning on Bifilar Performance

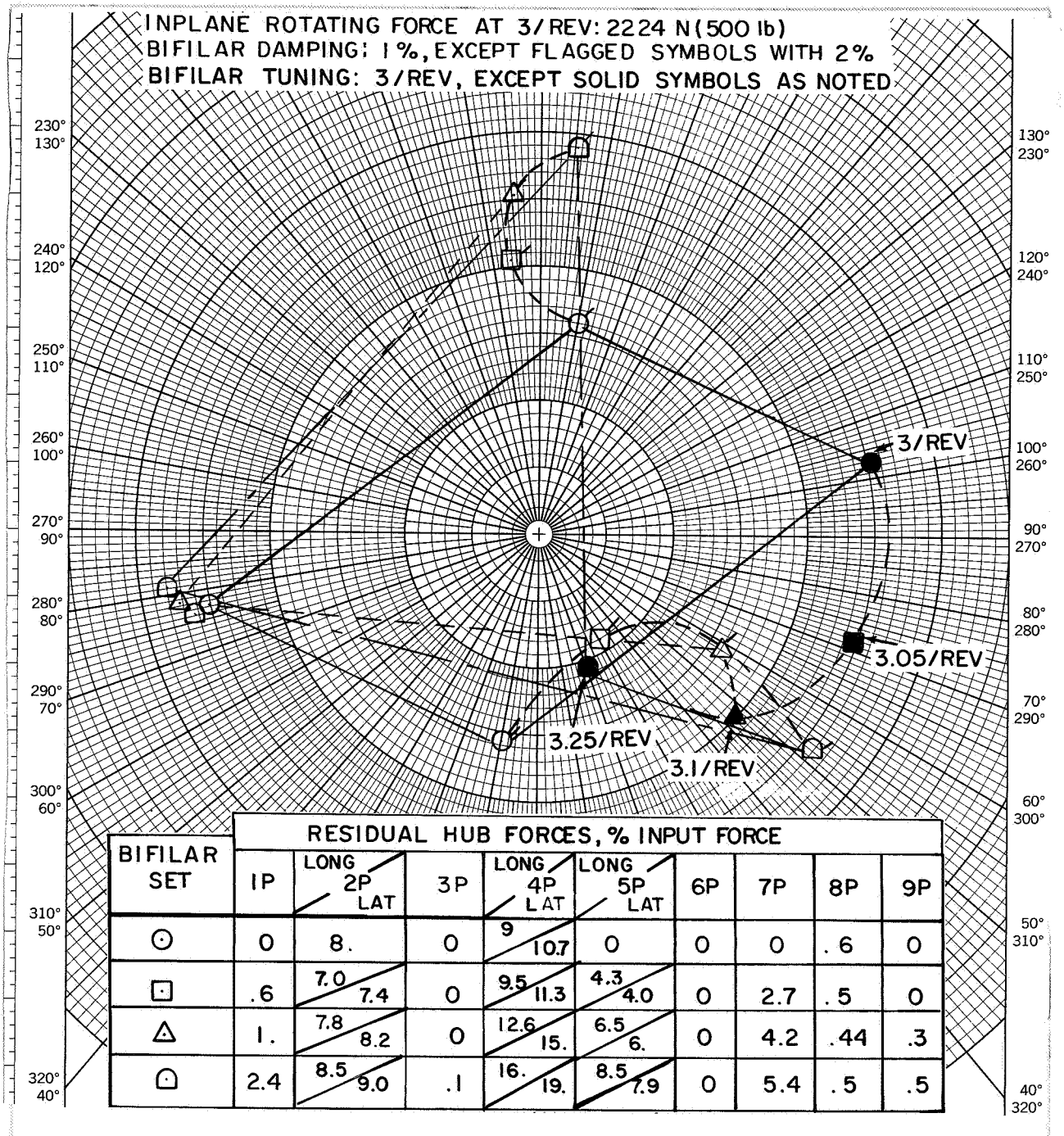

BIFILAR SET	RESIDUAL HUB FORCES, % INPUT FORCE								
	1P	LONG 2P / LAT	3P	LONG 4P / LAT	LONG 5P / LAT	6P	7P	8P	9P
⊙	0	8.	0	9 / 10.7	0	0	0	.6	0
⊡	.6	7.0 / 7.4	0	9.5 / 11.3	4.3 / 4.0	0	2.7	.5	0
△	1.	7.8 / 8.2	0	12.6 / 15.	6.5 / 6.	0	4.2	.44	.3
⌂	2.4	8.5 / 9.0	.1	16. / 19.	8.5 / 7.9	0	5.4	.5	.5

Figure 4.4-11. Bifilar Pattern as Affected by Combined Tolerances in Damping and Tuning

effect on the near diamond pattern when one of the bifilar masses is over-tuned. Evidently, a large phase angle has been created due to the off-tuned bifilar mass. The diamond pattern is changed to patterns range from a quadrilateral to an arrow head, when the tuning changes from +.05/rev to +.25/rev. An intermediate pattern of double triangle serves as a transition from the quadrilateral to the arrow head at an intermediate off-tuned frequency.

4.5 Interaction of 3/rev and 5/rev Bifilars

3/rev bifilars are usually employed to absorb the 4/rev hub motion on the basis that 3/rev forces in the rotating system are greater than the 5/rev forces for a four-bladed rotor. However, although the hub motion may be the result of a pure 3/rev rotating force, unequal longitudinal and lateral hub impedances can cause a resultant elliptic hub response. This will produce 5/rev as well as 3/rev bifilar arm excitations in the rotating system as discussed in Section 4.2 relative to Figure 4.2-4. Therefore 5/rev bifilars may be required. To examine this situation, the baseline case with 3/rev excitation of 2224 N was run with three different 5/rev forces. The results are presented in Figure 4.5-1. As illustrated in Figure 4.5-1, without 5/rev excitation, the 5/rev bifilar masses still respond to the 4/rev hub motion due to the applied 2224 N rotating force at a frequency of 3/rev. With 5/rev rotating force applied at the hub in addition to the 2224 N 3/rev force, the 5/rev bifilar masses respond accordingly while the 3/rev masses show a slight amplitude and phase change. Most important is the residual hub force at 4/rev. Figure 4.5-2 shows the residual 4/rev hub forces for various combinations of 3/rev and 5/rev rotating system excitation.

The longitudinal residual hub force increases monotonically with the increasing 5/rev rotating excitation at various levels of 3/rev force. The lateral residual hub force, on the other hand, decreases with increasing 5/rev excitation until a minimum is reached. After that, it increases rapidly with even greater 5/rev excitation. As shown in Figure 4.5-2, at higher 3/rev force levels, the minimum of the lateral residual is reached at a higher 5/rev excitation. If we fix our frame of reference at 4/rev, then the 3/rev force will cause a clockwise rotating 4/rev response (backward whirl) while the 5/rev will cause a counter clockwise rotating response (forward whirl). Both responses start out at longitudinal direction and therefore add up. When they reach the lateral direction, they are in the opposite directions and consequently subtract from each other. If the 3/rev is greater than the 5/rev, as usually is the case, the difference will diminish when the 5/rev is increased until a minimum is reached and then increases with ever increasing 5/rev force. Of course, the characteristics of the residual forces in two directions are functions of hub impedance as well. For a known combination of 3/rev and 5/rev excitation hub forces, Figure 4.5-2 suggests that there will be a desirable hub impedance combination resulting in the lowest residual forces.

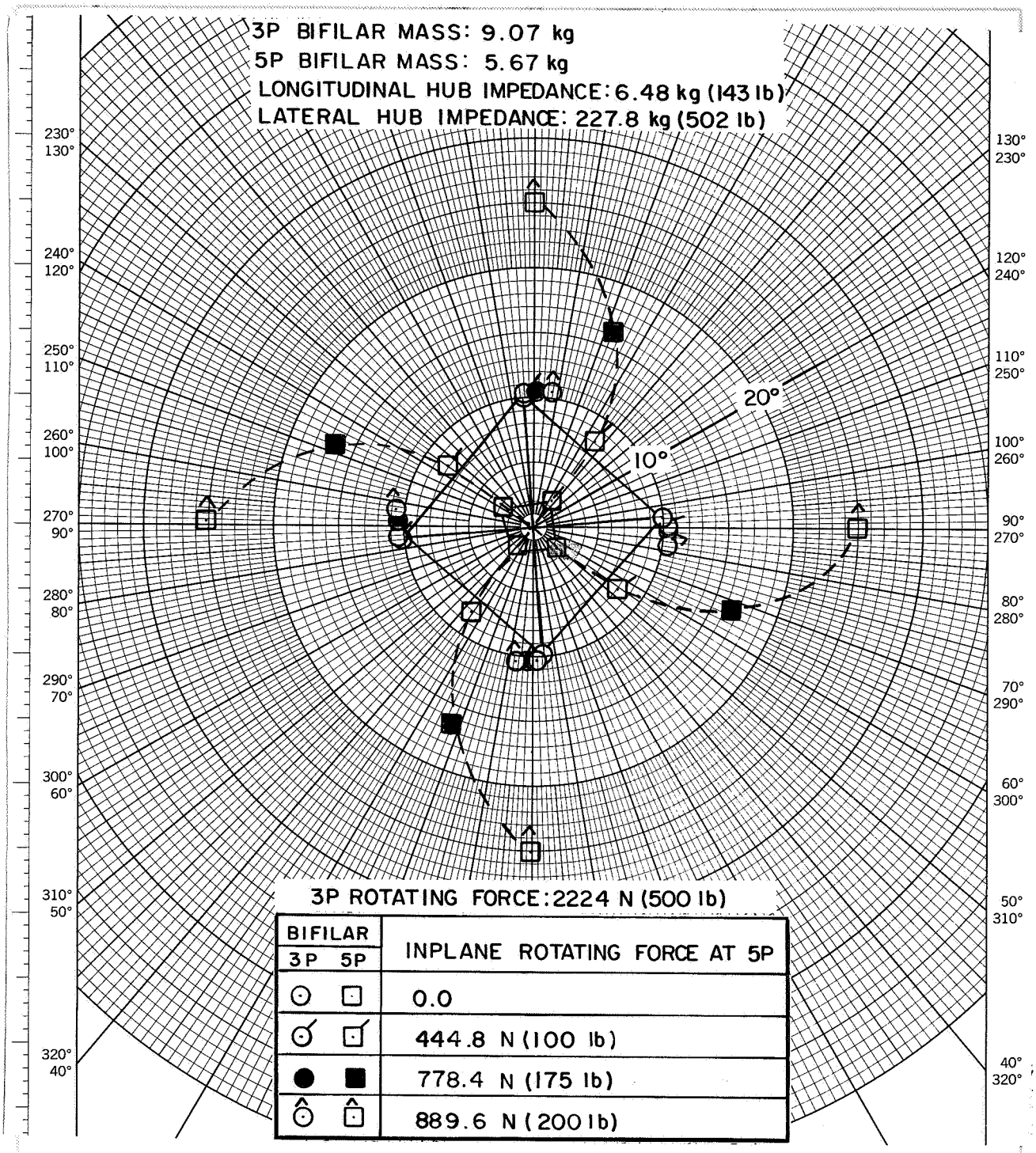

Figure 4.5-1. Interaction of (N-1)/Rev and (N+1)/Rev Bifilars

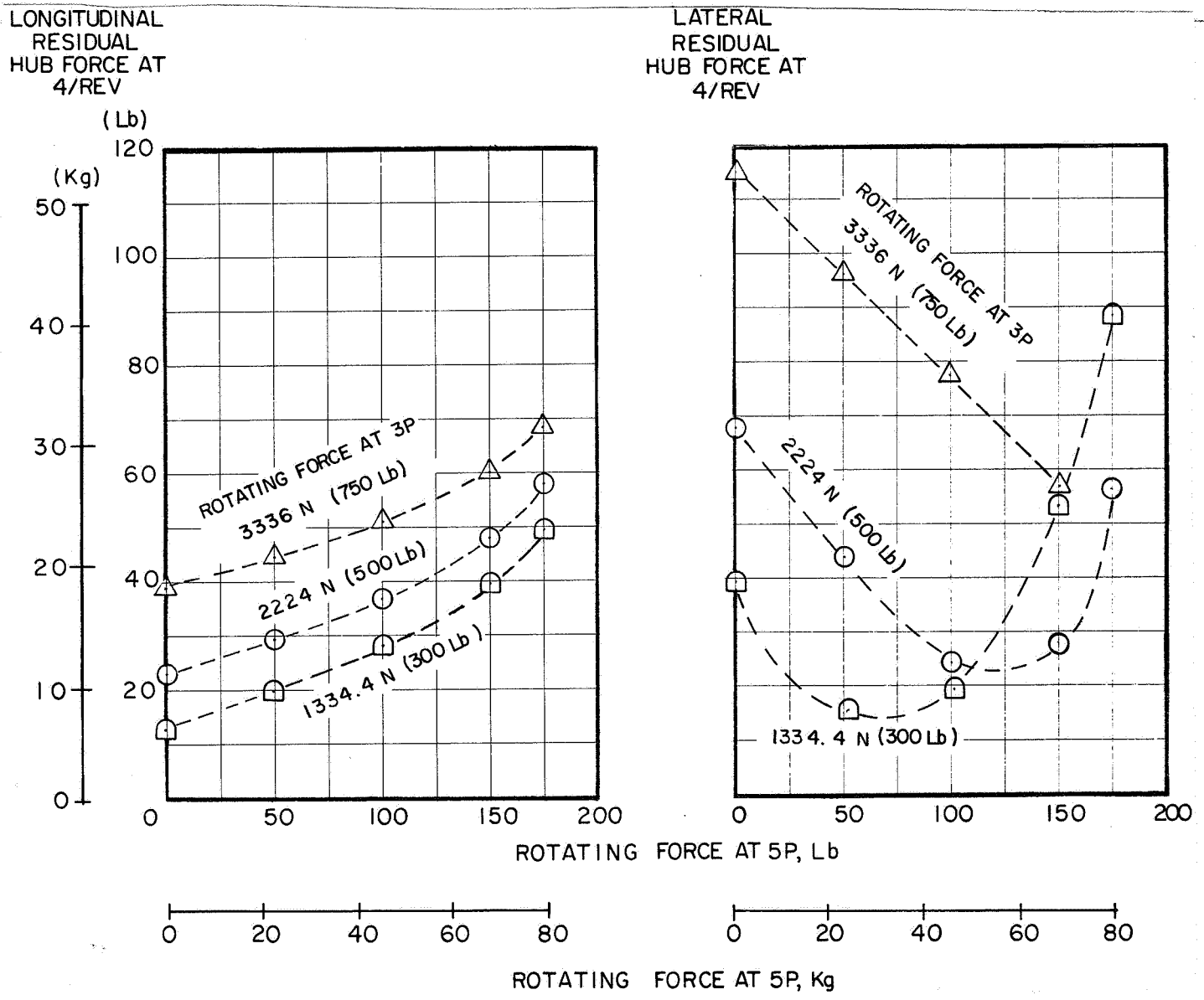

Figure 4.5-2. Residual Hub Force as Affected by Interaction of 3/Rev and 5/Rev Bifilars

SECTION 5

COMPARISON OF ANALYSIS AND FLIGHT TEST DATA

It is apparent from Section 4 that the prediction of bifilar absorber dynamic response is highly dependent on knowledge of bifilar dynamic mass, tuning and damping, rotor hub impedance and differences among the individual bifilar weights due to manufacturing tolerances. In addition, rotor hub vibratory forces must be known since they constitute the excitation of the system. In subsequent sections correlation of bifilar dynamic response with available flight test data is presented. The results are based upon nominal bifilar mass, tuning and damping characteristics for each configuration. Slight differences among the individual bifilar weights tuning and damping due to manufacturing tolerances are not modeled (since they are not defined). Rotor hub vibratory loads are based upon available test data. The nature of the analysis input data necessarily results in something less than a rigorous correlation. An "exact" correlation will require a laboratory test wherein individual bifilar weight mass, tuning and damping characteristics are measured and applied forces are prescribed. Nevertheless, the correlation results presented herein are judged to be sufficient to demonstrate the validity of the analysis.

5.1 Flight Test Configurations

A requirement in the selection of the bifilar absorber flight data for correlation was the availability of recorded motions for all the bifilar masses within the set and hub accelerations. Although many Sikorsky helicopters have employed bifilar vibration absorbers, only a limited number of configurations have had all bifilar masses instrumented. Three configurations were chosen for their availability of the absorber and hub response data and the availability of parameter variations; i.e. bifilar tuning, dynamic mass, and combination of 3P and 5P bifilar absorbers.

Configuration	Aircraft	Bifilar Configuration
1	Prototype BLACK HAWK	3P inplane with circular bushing. Tuning 3.03/rev, mass 13.6 Kg.
2	Prototype S-76	3P and 5P inplane with circular bushing. Tuning and mass were respectively: 3.045/rev/9.07 Kg and 5.05/rev/6.08 Kg.
3	Prototype S-76	3P inplane with circular bushing. Tuning 3.045/rev, mass 9.07 Kg.

For configuration 1, the prototype BLACK HAWK, data available consist of a level flight forward speed sweep at 100% N_R and a rotor speed sweep at 140 kn. Data for configurations 2 and 3 consist of a level flight forward speed sweep at 100% N_R and a rotor speed sweep at 145 kn. For configuration 2, additional data are available for variations in bifilar dynamic mass and 3P bifilar tuning.

5.2 Comparison and Discussion of Flight Test Data

Configuration 1 - The response patterns of the prototype BLACK HAWK 3P inplane bifilar absorber with dynamic mass of 13.6 kg tuned to 3.03/rev as affected by airspeed at 100% N_R are shown in Figure 5.2-1. Note that there is a scale difference between the top figure which shows airspeeds from 40 kn to 100 kn, and the bottom figure, which shows airspeeds from 120 kn to 165 kn. In general, bifilar mass amplitude increases with increasing airspeed. This is to be expected, since vibratory loads at the main rotor hub are approximately proportional to the square of airspeed, resulting in higher bifilar response with increased airspeed. An exception is at 40 kn, which is at the end of the transition airspeed region where vibratory excitation is higher than speeds immediately above. The bifilar mass response amplitudes, as a result, are also higher.

One observation can be made immediately looking at Figure 5.2-1. The bifilars are far from being ideal because none of the patterns is of a ideal square. The pattern is of general quadrilateral shape at low airspeed, turns into "arrow" shape at 120 kn, then becomes a double triangle at 140 kn, and finally returns to quadrilateral or near square at higher speed. As previously discussed in Section 4.4 with respect to Figure 4.4-11, when one bifilar mass is off-tuned, the bifilar response pattern is of a quadrilateral nature. It turns into a double triangle and then an arrow as the bifilar becomes more and more off-tuned. Since the circular bifilar tuning will decrease with increasing mass amplitude, as demonstrated in Figure 4.4-3, the bifilar on the prototype BLACK HAWK is purposely over-tuned to 3.045/rev at small swing angle such that at cruise speed it is ideally tuned and best utilized. The arrow and the double triangle shapes, at 120 and 140 kn respectively, signify the fact that the bifilar masses are approaching ideal tuning at different rates with increasing forward speed. This is illustrated conceptually in Figure 5.2-2.

As shown in Figure 5.2-2, the ideal tune point is identified at a bifilar tuning ratio of 1.00 and is the point of peak amplification for the device. These amplification curves are dependent upon damping and bifilar tuning. Three levels of damping are illustrated: low (curve I), medium (curve II) and high (curve III). The implication is that if the damping of each individual bifilar mass is different, for the same input of g level motion to each bifilar arm, the resulting motion will be different as shown previously in Section 4.4. When the bifilar is off the ideal tune point, either above or below, the potential for differences in mass motion are far less than when at the "ideal" point even if the individual mass dampings are different. Therefore at these conditions the mass motions tend to be more similar. The curve labeled A in Figure 5.2-2 illustrates the non-linear tuning aspects of the circular bushing bifilar absorber. The reduction of bifilar tuned frequency with increased angle is accounted for by having overtuned (e.g. @ 1.02 or 1.03) bifilars and

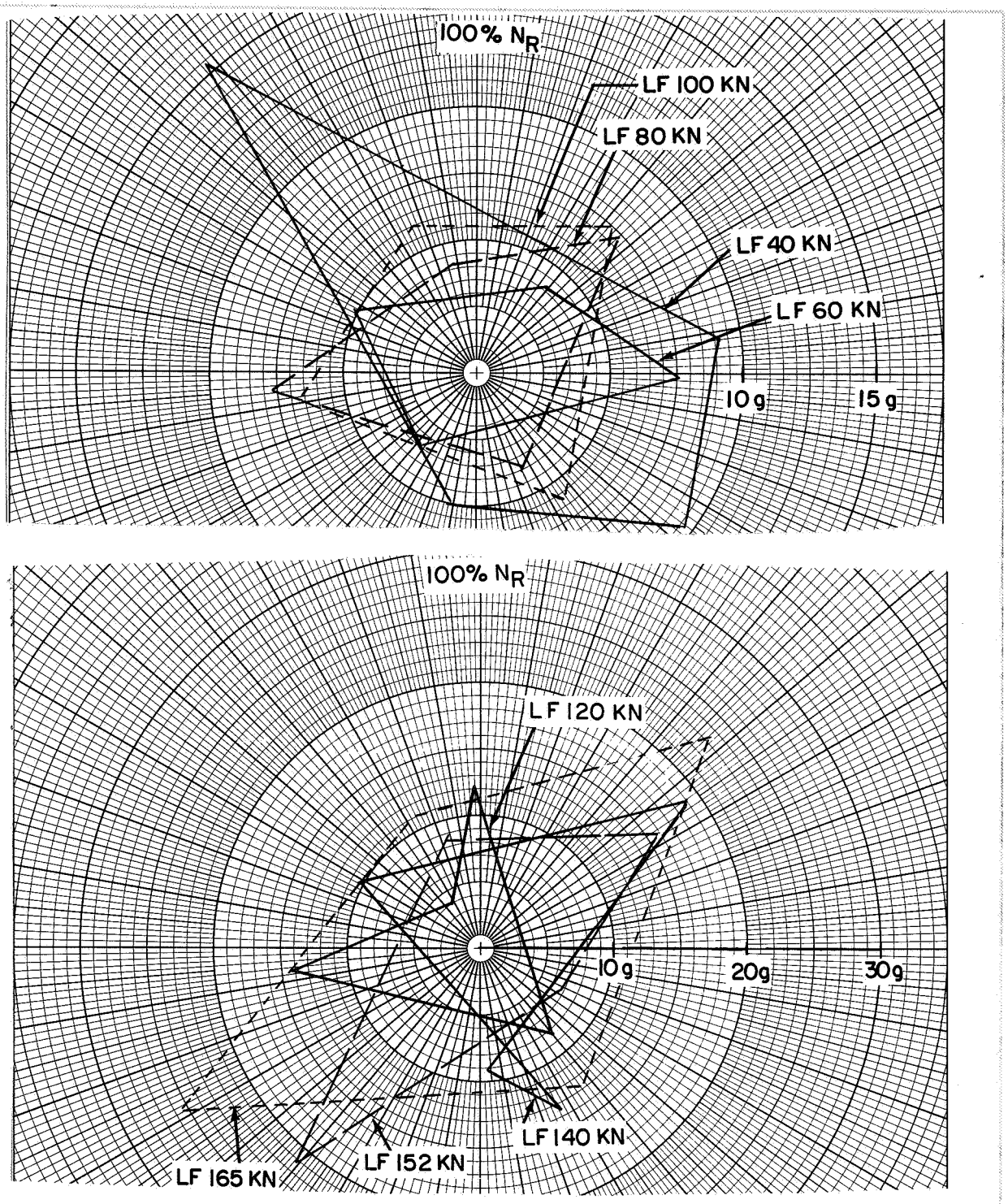

Figure 5.2-1. Prototype BLACK HAWK 3/Rev Bifilar Response Pattern as Affected by Airspeed

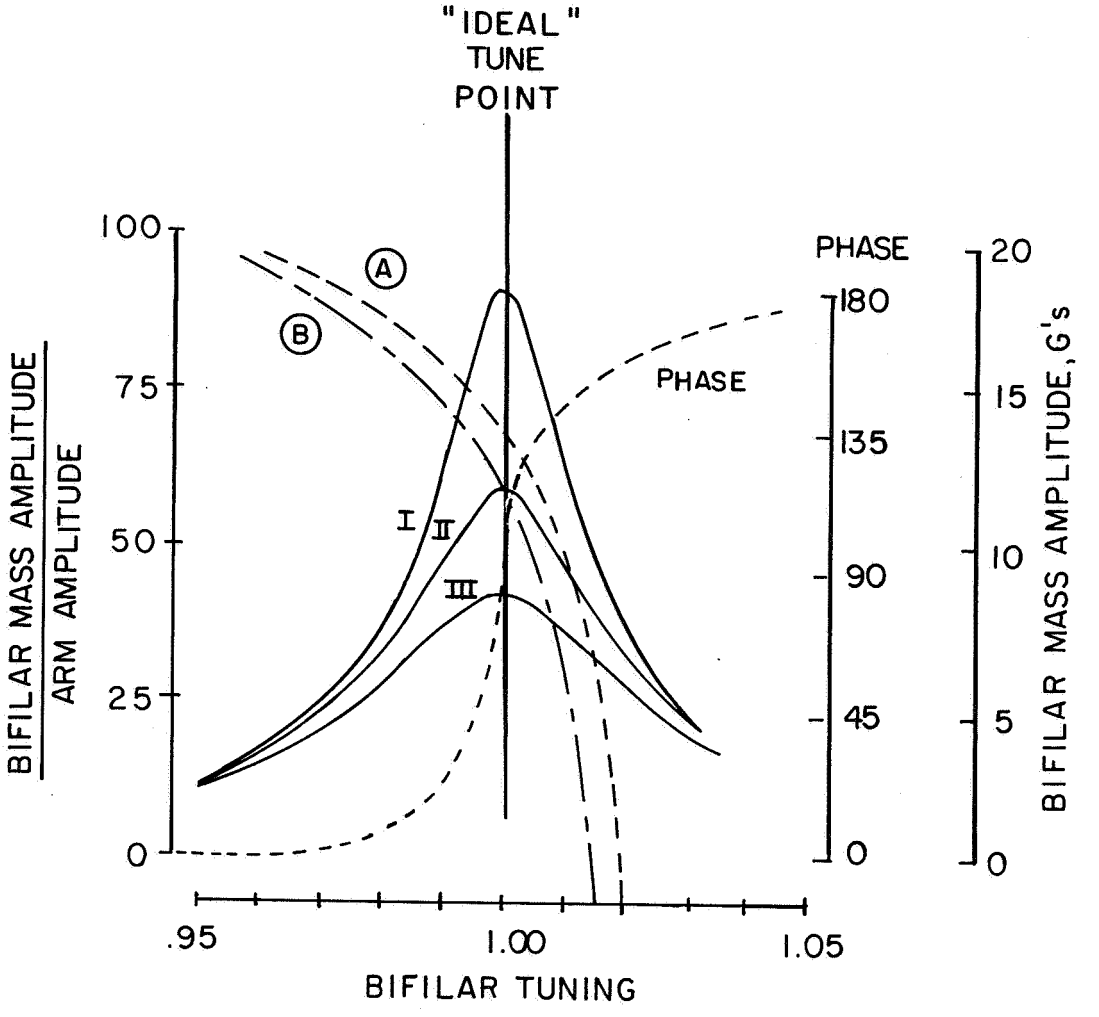

Figure 5.2-2. Difference in Tuning and Damping Affects Bifilar Response

as the airspeed is increased and the rotor forces build up, the absorber amplitudes increase and the bifilar moves toward the "ideal" tune point. This is desirable because the bifilars tend to be "in tune" (best amplification therefore best vibration absorption performance) at the high airspeeds where the N/rev is generally the highest. Curve B of the figure illustrates the situation where 3 bifilar masses are following curve A and the other, the off-tuned bifilar mass, Curve B. At each bifilar mass motion, even if the damping/amplification curve were the same the resulting motions of the Curve B mass would be different than Curve A. The situation becomes worse near the "ideal" tune point where even the relative phase of the mass motion of the bifilar on Curve B could be 180° from where it should be. The resulting response pattern would look like those shown at 120 and 140 kn in Figure 5.2-1.

The bifilar response patterns for the variation of rotor speed at 140 kn level flight condition are shown in Figure 5.2-3. Again, as in the case of forward speed variation, the patterns are not the ideal square. They vary from the quadrilateral, 98 and 99% N_R, to double triangle, 100 and 101% N_R, and to arrow head, 102 to 104% N_R; the similar sequence of response pattern variation as in the case of forward speed variation from high airspeed to low airspeed, Figure 5.2-1. This suggests that the bifilars have seen a tuning frequency ratio variation with varying rotor speed.

This characteristic requires comment since the bifilar absorber is a device which relies on the centrifugal force field to provide the restoring spring therefore, it has nominally been considered a self-tuning device. In other words, the tuning frequency, expressed as the ratio of bifilar frequency to the rotor speed, is independent of the rotor speed. The incorporation of the amplitude dependent non-linearity into the equation affects the tuning frequency ratio at high bifilar swing angle. In addition, examination of the coupled non-linear inplane bifilar equation, Reference 2, reveals that the bifilar is also coupled with the longitudinal and lateral hub accelerations through the non-linear term of the bifilar amplitude, in addition to the linear coupling terms which depend on the sine and cosine of the azimuth angle. The restoring spring for the bifilar is proportional to the rotor speed squared, therefore the uncoupled tuning frequency ratio remains constant as the rotor speed is varied for small bifilar swing angle. However, the coupling with the hub impedance is not proportional to rotor speed squared. As a consequence, the coupled tuning frequency ratio will vary with the rotor speed.

The effect of rotor speed can be seen more readily when the bifilar responses are plotted versus rotor speed as shown in Figure 5.2-4. These curves, faired through the data with a reasonable amount of scatter, show that all bifilar responses increased when the rotor speed was increased from 98% to 101% N_R, evidently due to an increasing hub excitation with rotor speed. The cause for the increased excitation are many, e.g., the coupled rotor/airframe impedance variation with rotor speed or the blade aerodynamic excitation. Further increase in rotor speed see the responses of No. 1, 3 and 4 bifilar masses dropping off and that of No. 2 still climbing and then leveling off at 104% N_R. Apparently, the No. 2 bifilar mass was tuned higher than the rest while both Nos. 2 and 4 masses had less damping than the other two.

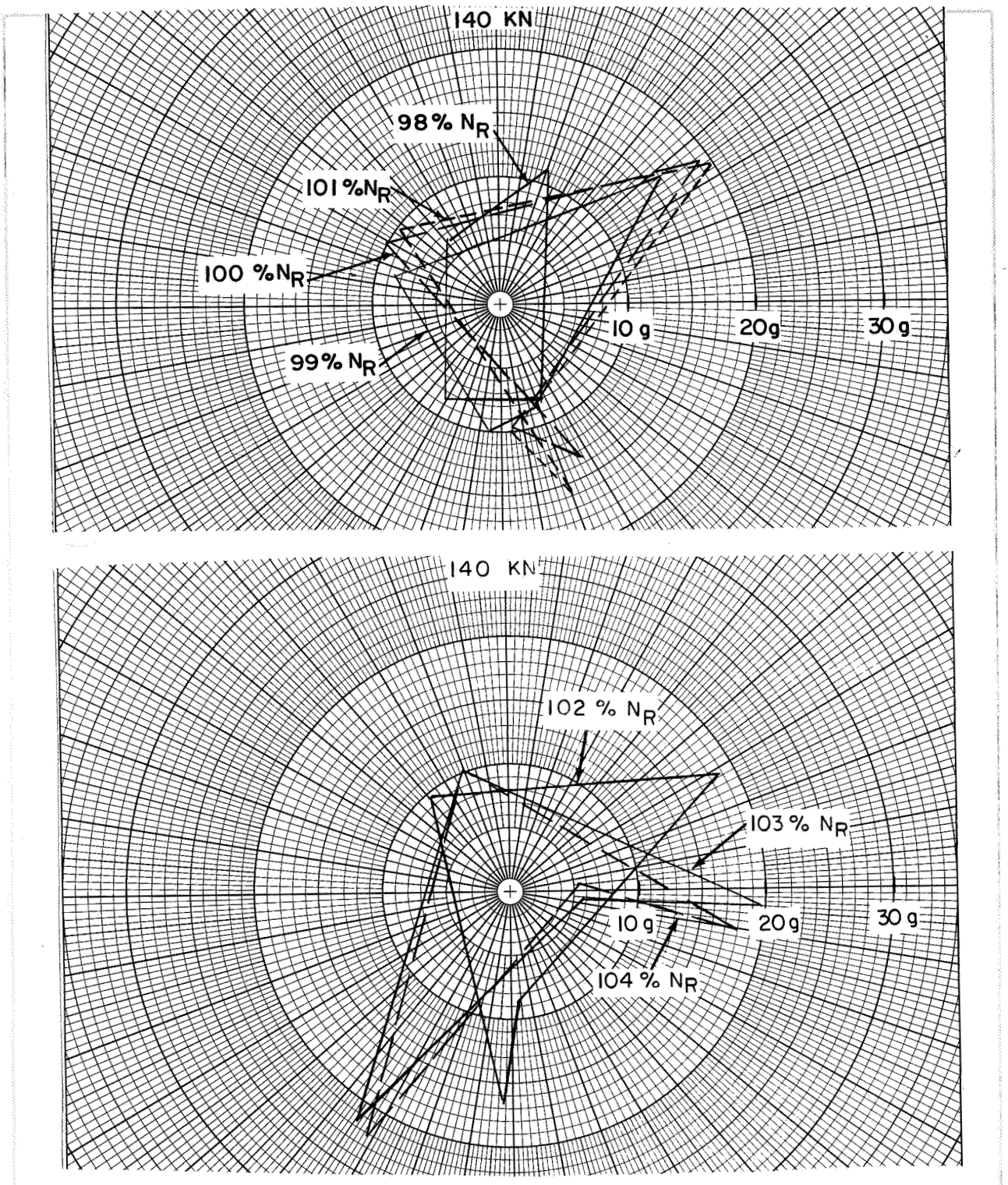

Figure 5.2-3. Prototype BLACK HAWK 3/Rev Bifilar Response Pattern as Affected by Rotor Speed

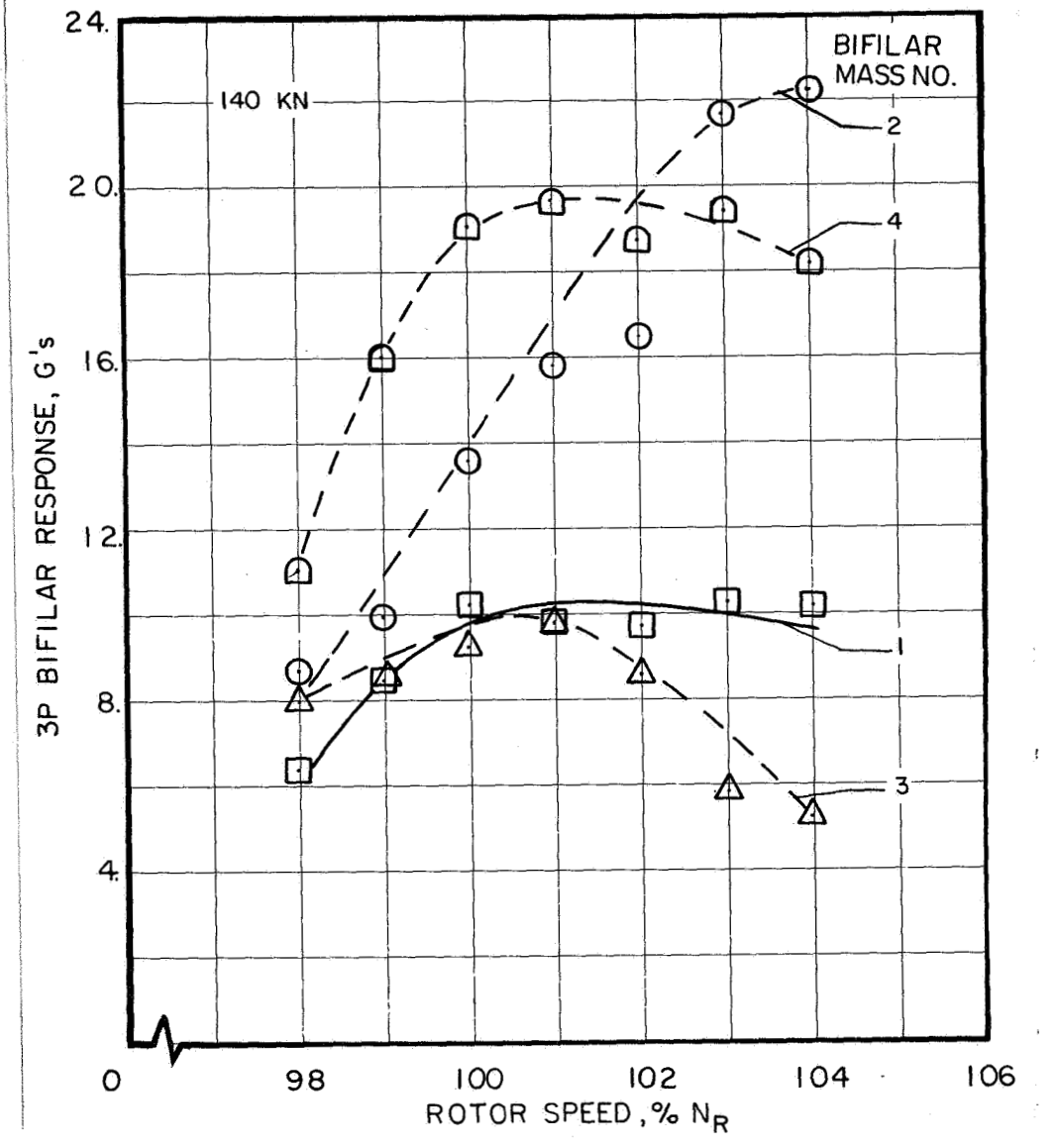

Figure 5.2-4. Rotor Speed Effect on Prototype BLACK HAWK 3/Rev Bifilar Response

Correlation of the analysis with the BLACK HAWK test data depends upon knowledge of hub inplane vibratory loads and hub impednace as well as rotor impedance and bifilar mass, tuning and damping characteristics. The BLACK HAWK hub impedance is available from shake test results and has been previously presented in Section 4.1.

BLACK HAWK rotor hub inplane vibratory loads are estimated in the following way. From the analytical results presented in Section 4.2 we observe that the force produced by the bifilar absorber is of approximately equal magnitude to the hub vibratory force but with a phase shift (which accounts for the residual hub forces observed with the bifilar functioning). This characteristic suggests that the magnitude of the hub vibratory forces can in fact be reasonably estimated from bifilar absorber mass response. Figure 5.2-5 presents BLACK HAWK 3/rev hub inplane vibratory forces estimated from the 3P bifilar mass response. It is noted that later in this section, hub loads for the S-76 helicopter estimated by this procedure are shown to agree well with hub loads determined from full scale wind tunnel test data.

Since the individual mass response is different from each other, the average bifilar mass tangential response is compared with the analysis for the correlation study. The correlation of the analysis of the BLACK HAWK with flight test data are shown in Figures 5.2-6 and 5.2-7. Bifilar absorber mass tangential response and 3/rev hub response for both the airspeed sweep and the rpm sweep are considered. The degree of correlation is considered to be very good. From these results we conclude that the analytical model clearly includes the important mechanisms involved in predicting the dynamic response of rotorhead bifilar absorbers.

Configuration 2 - This configuration is the prototype S-76 with a 9.07 Kg 3P bifilar tuned to 3.045/rev and a 6.08 Kg 5P bifilar tuned to 5.05/rev. Figures 5.2-8 through 5.2-11 present flight measured bifilar mass tangential responses for the baseline Configuration 2 mass and tuning values. Figure 5.2-8 presents the 3P bifilar mass tangential response patterns as a function of airspeed. Similar 5P bifilar response data are shown in Figure 5.2-9. Figures 5.2-10 and 5.2-11 show respectively, the 3P and 5P bifilar absorber responses for rotor speed sweeps at 145 Kn.

From an examination of these response patterns, it is clear that the bifilars do not always respond in the ideal square pattern (i.e. equal amplitudes and 90^{o} relative phase between weights). As discussed previously the causes for this non-ideal response patterns are due to small differences among individual bifilar weights' tuning and damping and as for the correlation study of the BLACK HAWK, the average bifilar mass tangential response is compared with the analysis. For the several test conditions where one of the bifilar mass responses is missing, the remaining three responses were averaged.

Hub vibratory loads for the S-76 were obtained in two ways. Full scale wind tunnel tests of the S-76 main rotor in the NASA-Ames 40 x 80 ft. tunnel produced one set of loads. Hub loads were also estimated from the flight test bifilar mass motions by applying the assumption that bifilar output

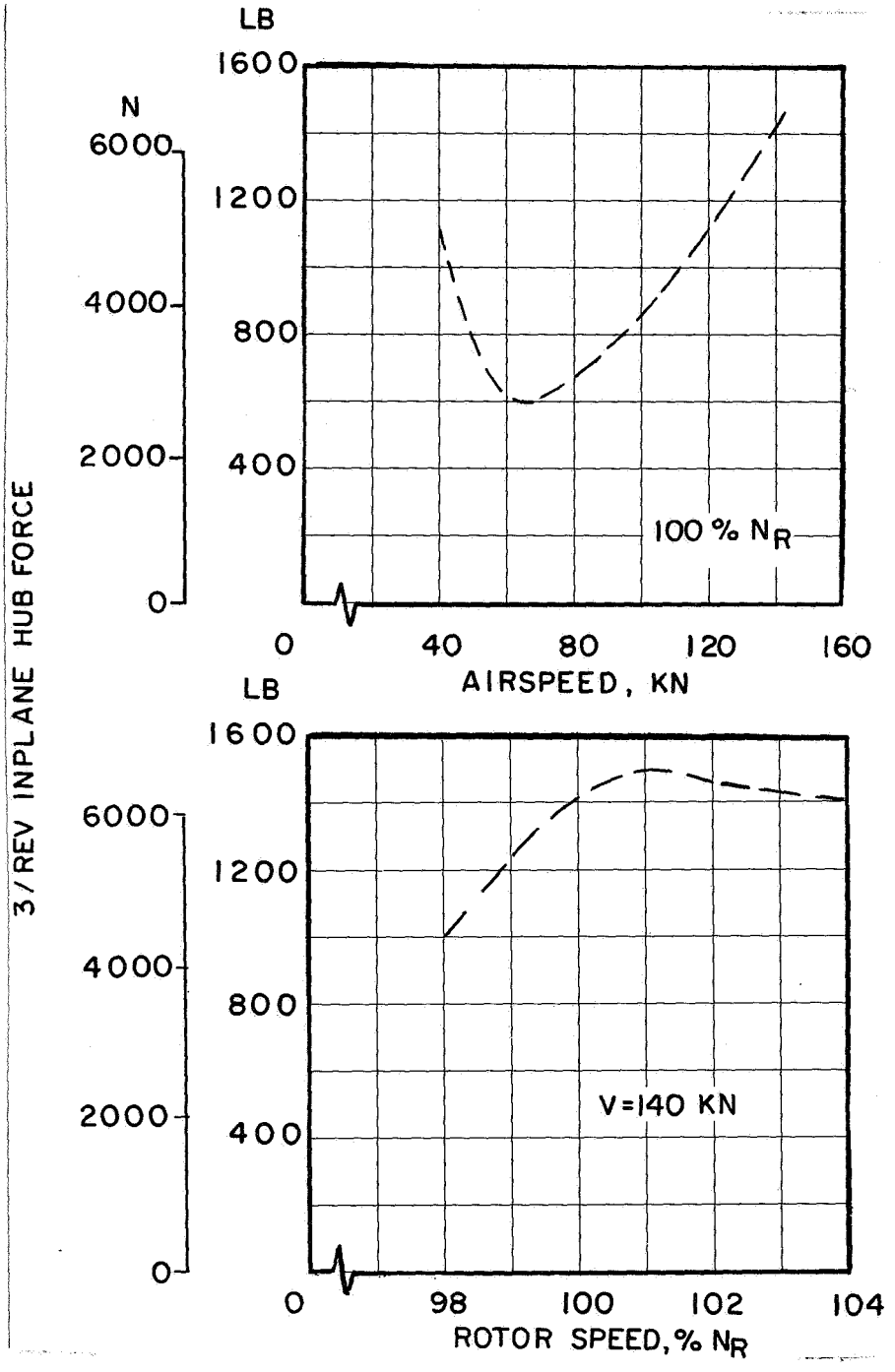

Figure 5.2-5. 3/Rev Inplane Hub Force, Configuration 1

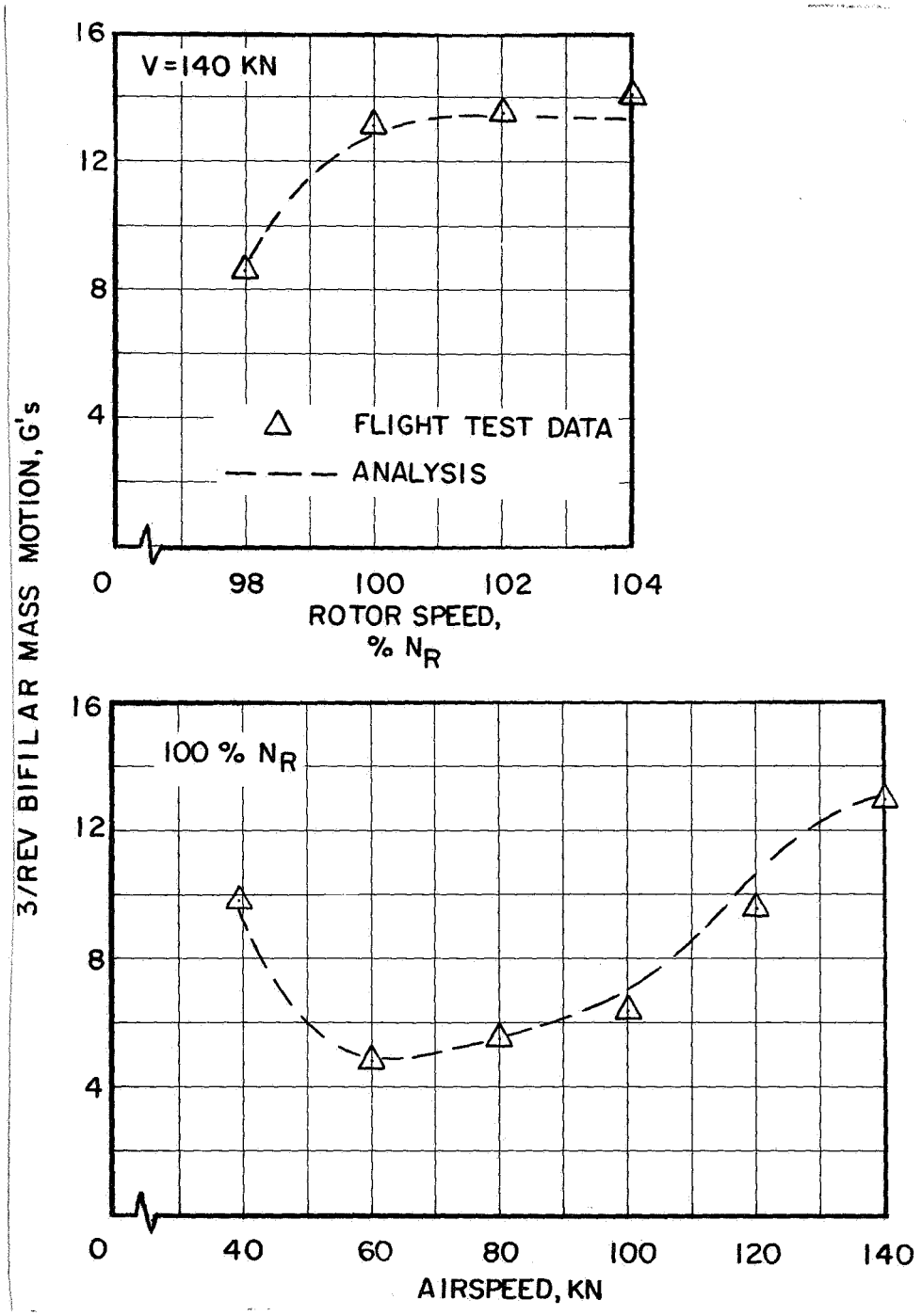

Figure 5.2-6. Correlation of 3/Rev Bifilar Mass Motion, Configuration 1

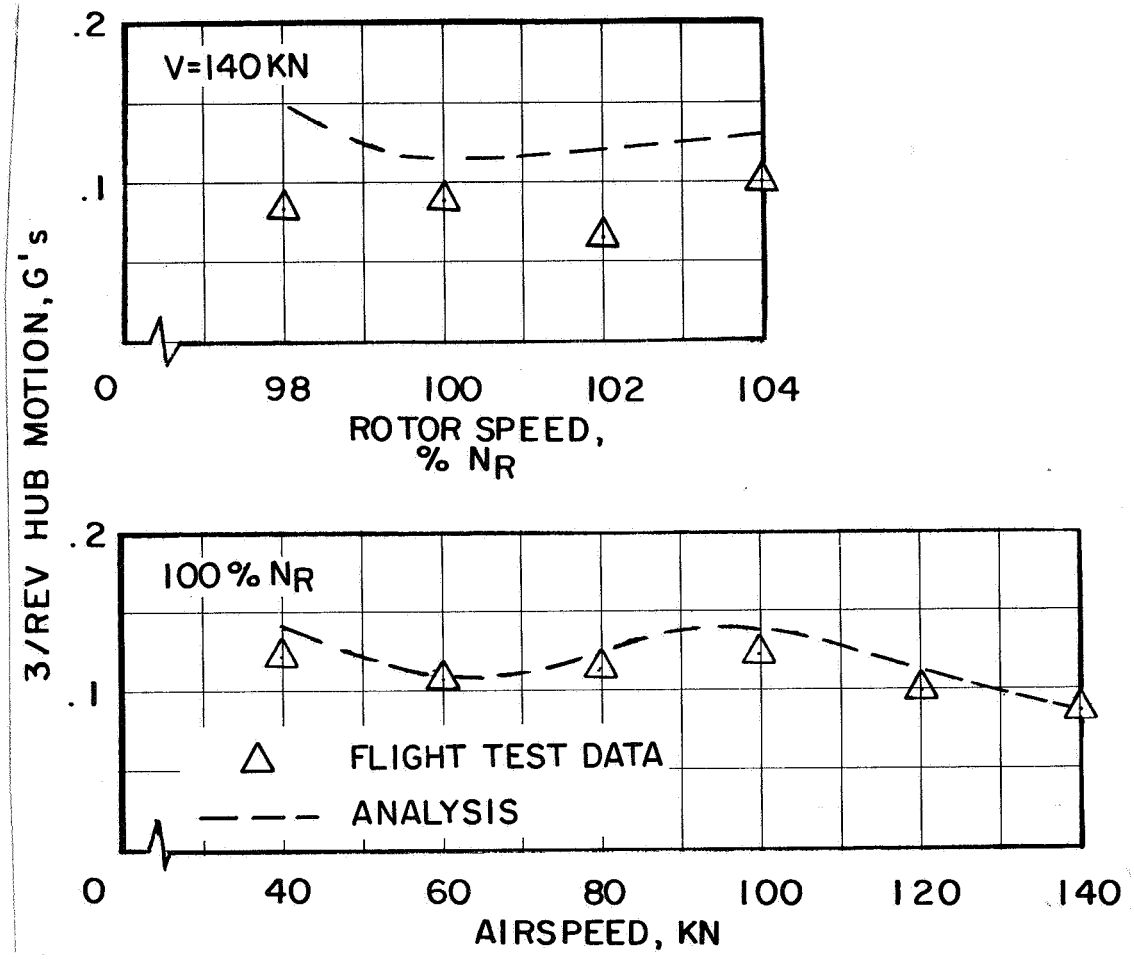

Figure 5.2-7. Correlation of 3/Rev Inplane Hub Motion, Configuration 1

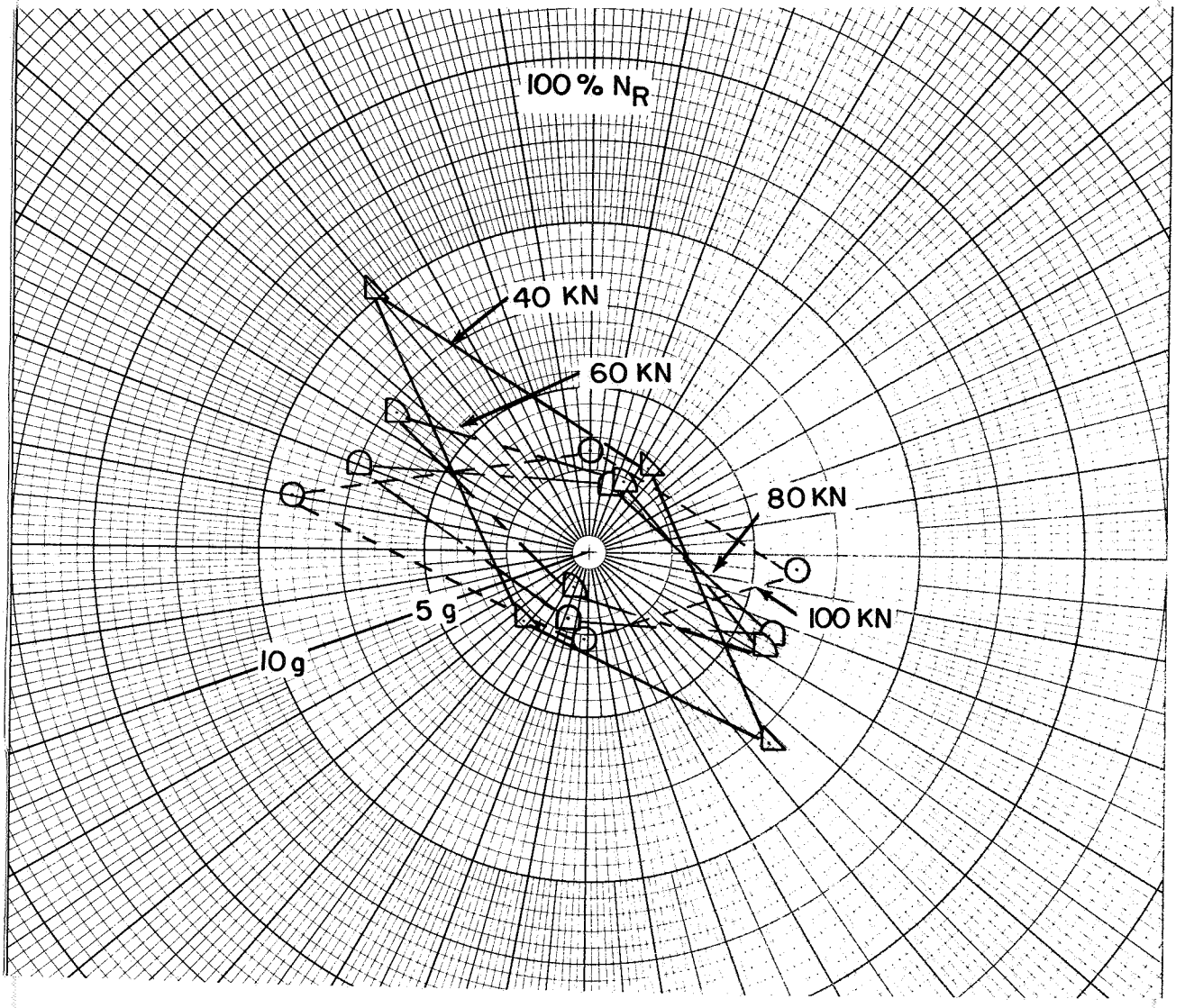

(a)

Figure 5.2-8. Configuration 2, 3/Rev Bifilar Mass Response - Effect of Airspeed

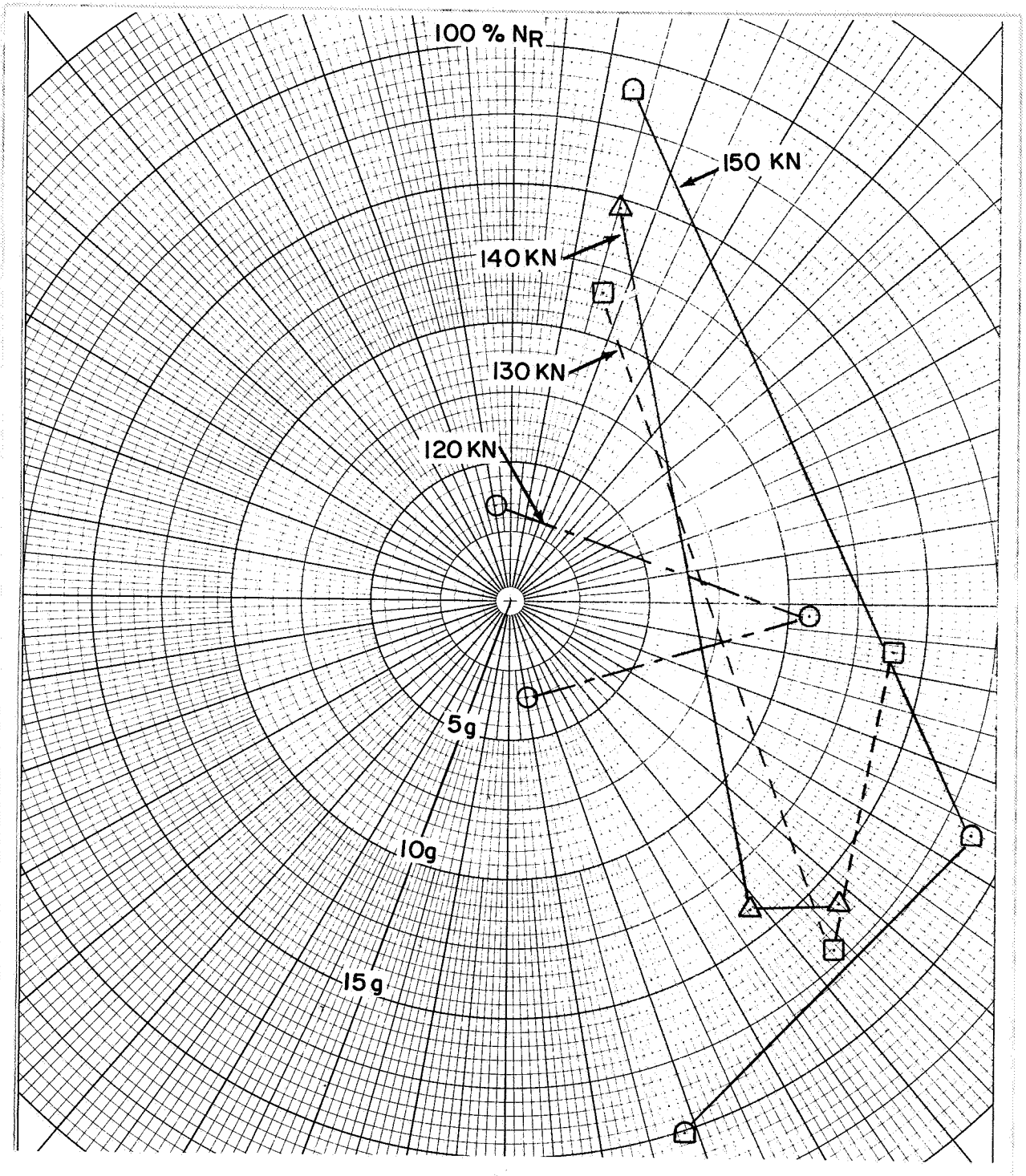

(b)

Figure 5.2-8. Concluded.

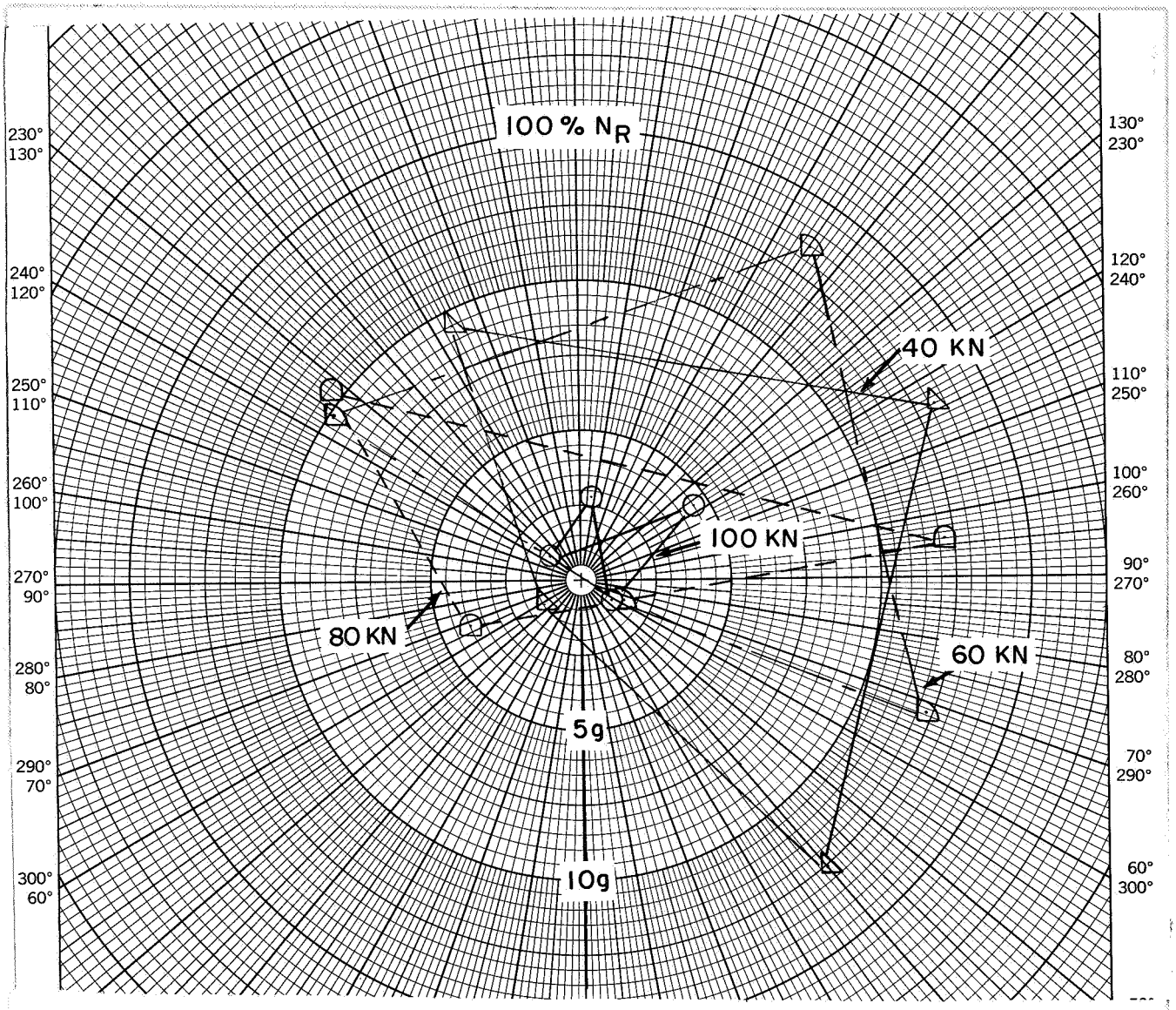

(a)

Figure 5.2-9. Configuration 2, 5/Rev Bifilar Mass Response - Effect of Airspeed

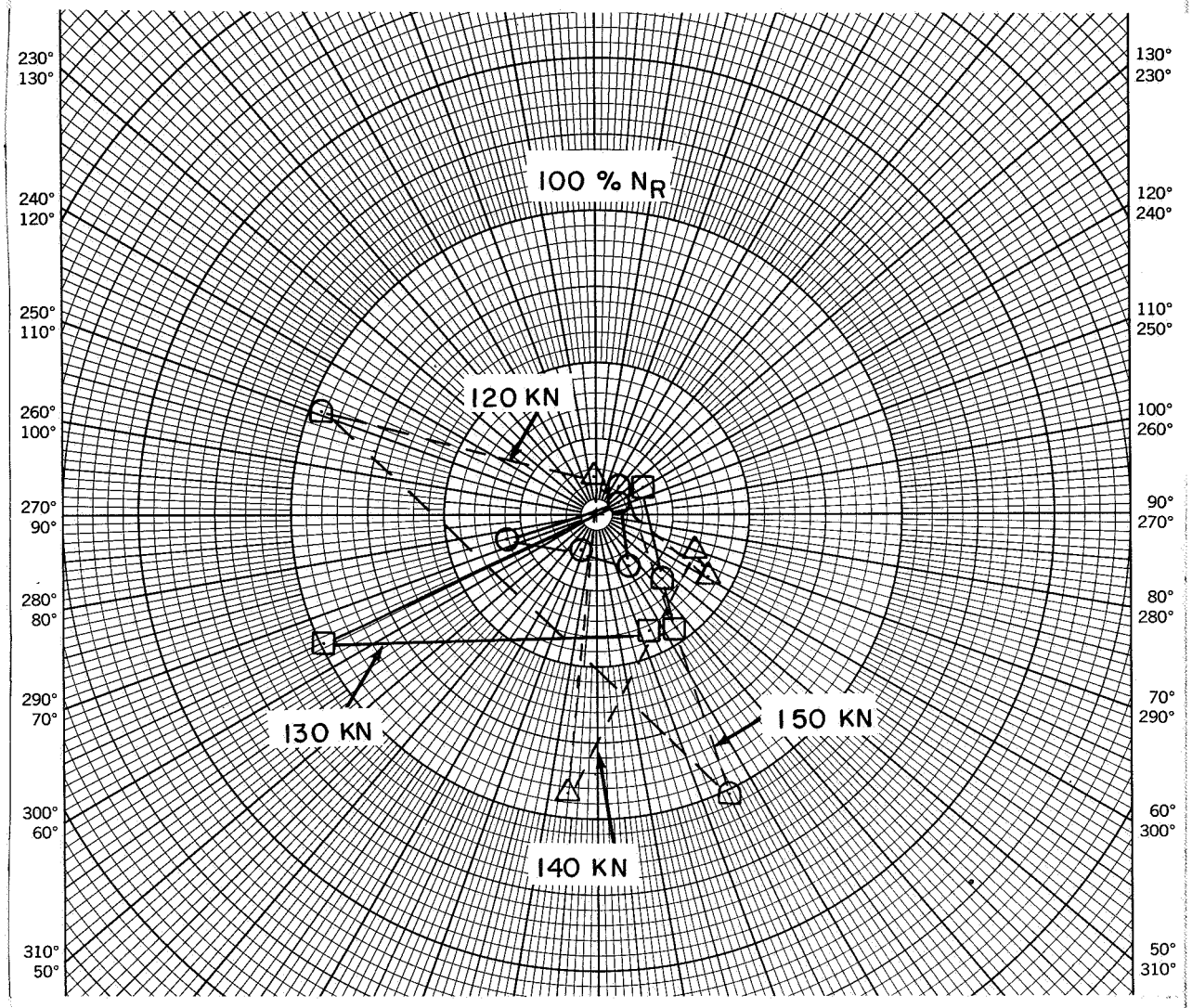

(b)

Figure 5.2-9. Concluded.

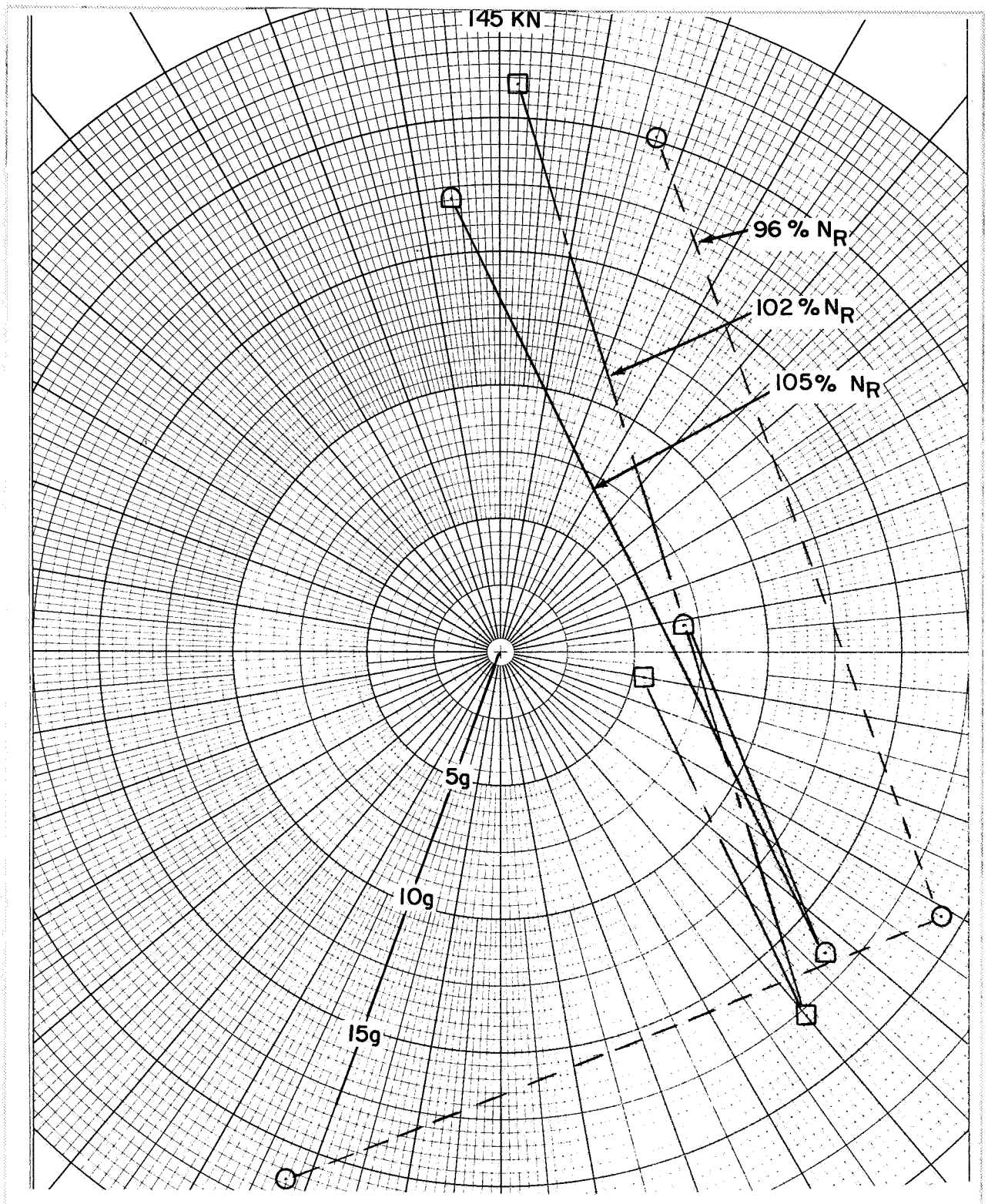

Figure 5.2-10. Configuration 2, 3/Rev Bifilar Mass Response - Effect of Rotor Speed

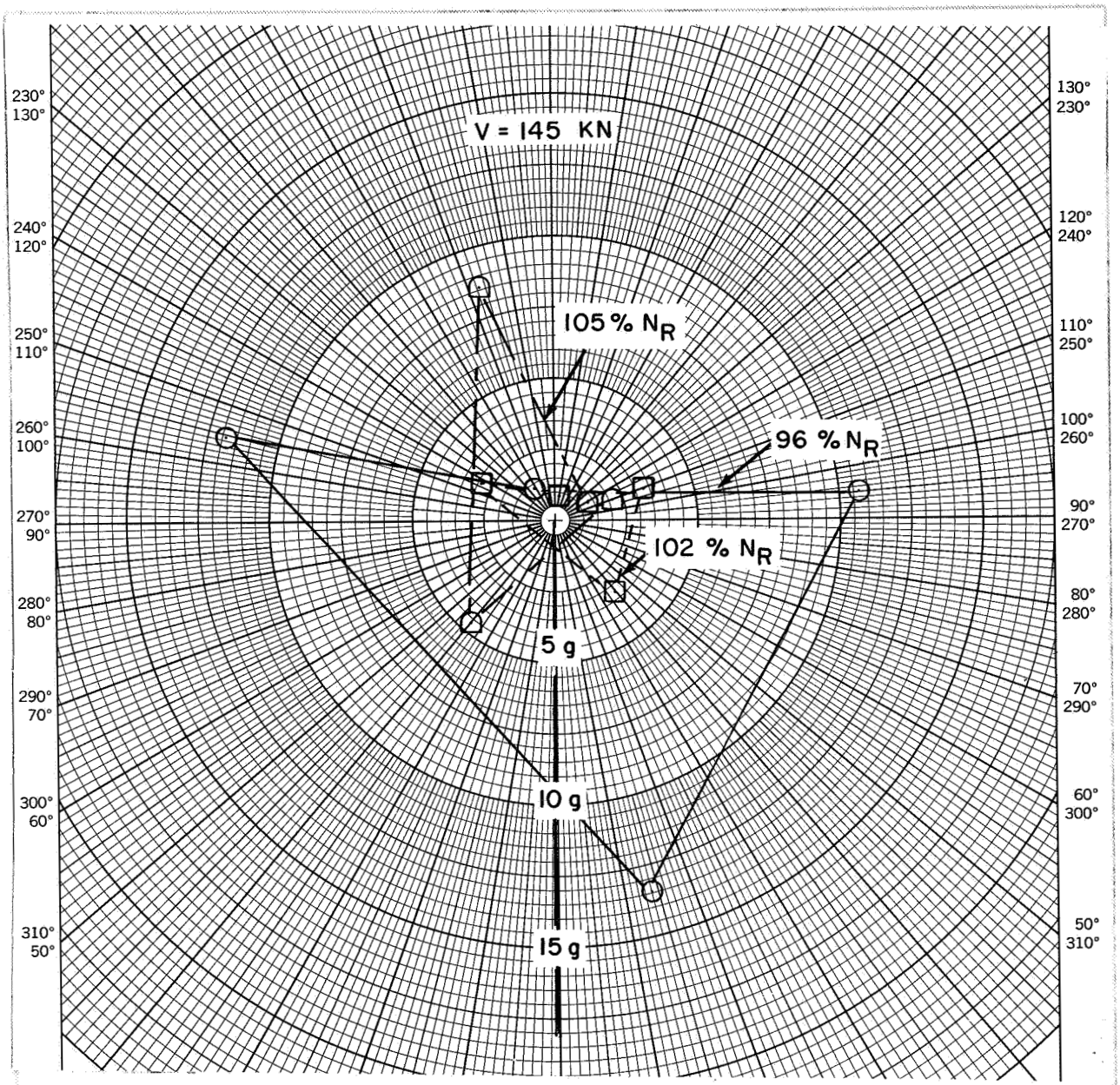

Figure 5.2-11. Configuration 2, 5/Rev Bifilar Mass Response - Effect of Rotor Speed

force is nearly equal in amplitude to hub vibratory force (see Section 4.2, Figure 4.2-2). The bifilar absorbers on the S-76 are configured to react cyclic 3/rev and 5/rev inplane hub shear forces. Therefore 3/rev and 5/rev hub vibratory loads are of interest for the correlation. The hub vibratory loads for the S-76 are presented in Figures 5.2-12 and 5.2-13. The 3/rev hub inplane vibratory loads obtained from wind tunnel tests had been adjusted to account for the rotor/fuselage aerodynamic coupling that was not properly represented by the wind tunnel test article. The closer proximity of the rotor to the fuselage on the flight vehicle has been calculated to produce 20% higher hub loads than the wind tunnel test article. The differences between the calculated hub loads (based on flight test measured bifilar mass motions) and the adjusted wind tunnel measured loads are attributed to the differences in the dynamic characteristics of the fuselage of the flight vehicle and the wind tunnel test stand (Rotor Test Apparatus) because hub loads are affected by coupled rotor/fuselage dynamic response.

Using the hub vibratory loads shown in Figures 5.2-12 and 5.2-13, and hub impedances from shake tests, the 3/rev and 5/rev bifilar tangential responses and residual hub vibration were calculated. The analytic results are compared with similar flight test data in Figures 5.2-14 to 5.2-17. From Figure 5.2-14 it is seen that the 3/rev bifilar mass responses are predicted very well by the analysis. The residual hub responses at 3/rev are also predicted well (Figure 5.2-15) particularly for the airspeed sweep. It is likely that the lack of good correlation of the residual 3P hub response with rotor speed variation is probably due to the accuracy of the hub impedance calculated from the shake test data.

The predicted 5/rev bifilar absorber response and residual 5/rev hub accelerations are compared with test data in Figures 5.2-16 and 5.2-17. The results are considered good for the airspeed sweep but only fair for the rpm sweep. Potential causes for the lack of correlation are inaccurate bifilar mass motions from test or the hub impedance computed from the shake test.

For a series of tests, the dynamic mass of the 3P bifilar was increased from the standard 9.07 kg (20 lb) to 13.61 kg (30 lb) with the tuning frequency reduced slightly, from 3.045/rev to 3.030/rev. The resultant bifilar response patterns for the airspeed sweep at 100% N_R and the rotor speed sweep at 145 kn are shown in Figures 5.2-18 and 5.2-19 respectively. Comparing these patterns to those shown in Figures 5.2-8 and 5.2-10, it is clear that the changes in patterns with airspeed and rotor speed are essentially the same. The more important conclusion is that the effect of increasing the dynamic mass by 50% reduces the bifilar response amplitude by approximately 30%. This is as predicted in Section 4.4. Figures 5.2-20 and 5.2-21 present a comparison of predicted bifilar absorber response and residual hub vibration with flight test data for this configuration. The hub loads used in the analysis were those shown in Figures 5.2-12 and 5.2-13. The good correlation suggests that the hub load estimates are accurate.

Configuration 2 was also flown with the tuning of the 3P bifilar changed from 3.045/rev to 3.00/rev. Comparison of analysis and test results for this

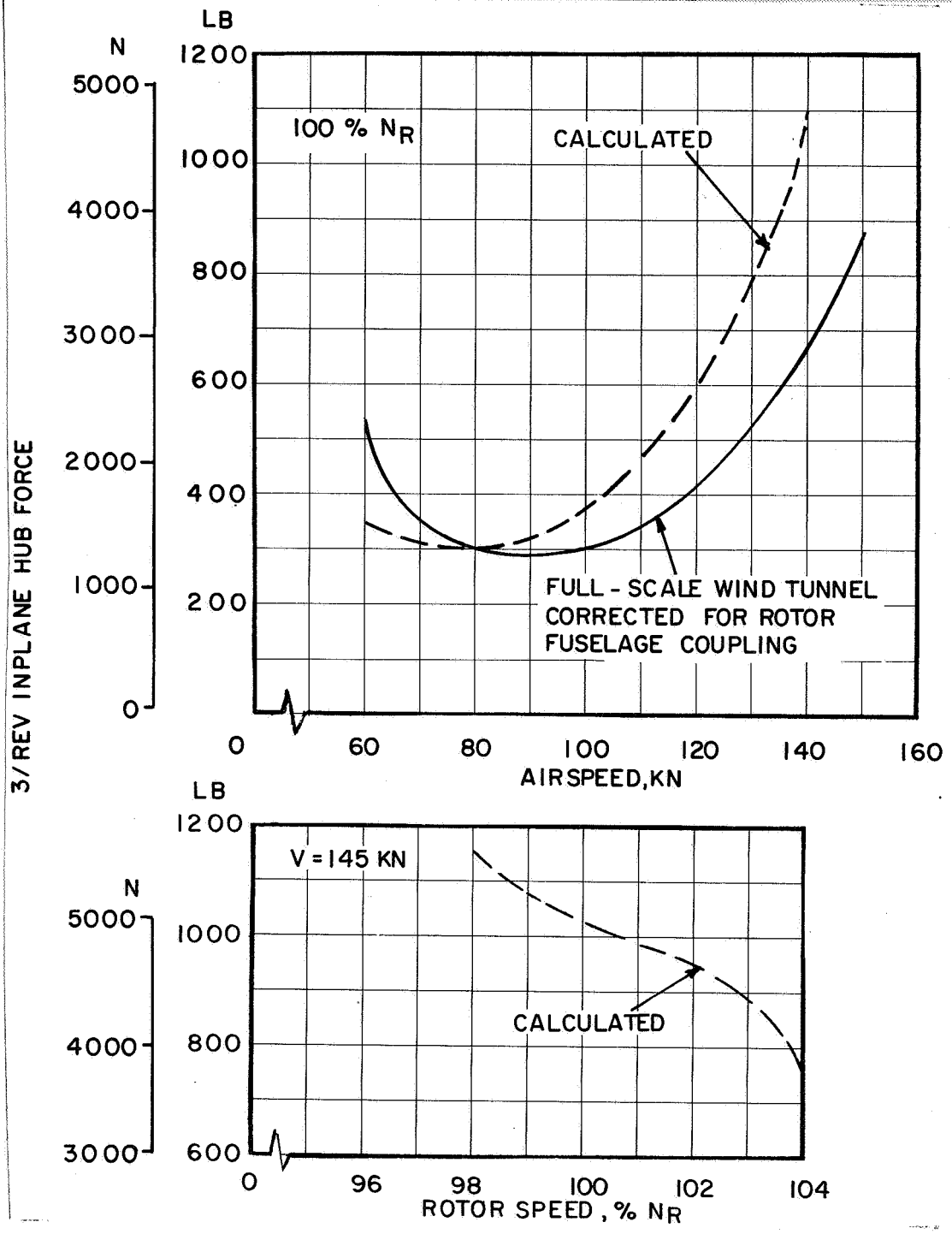

Figure 5.2-12. 3/Rev Inplane Hub Force, Configuration 2

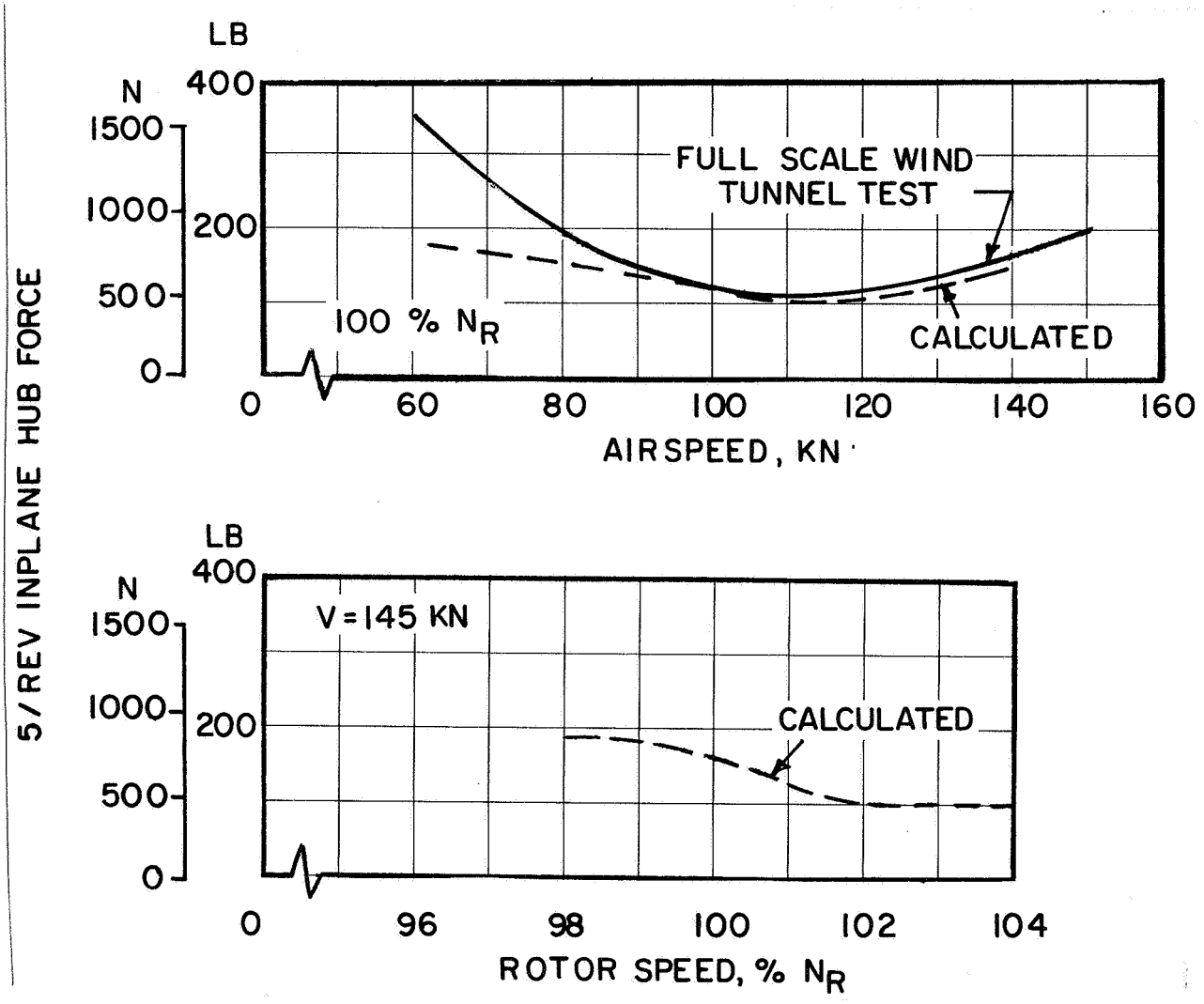

Figure 5.2-13. 5/Rev Inplane Hub Force, Configuration 2

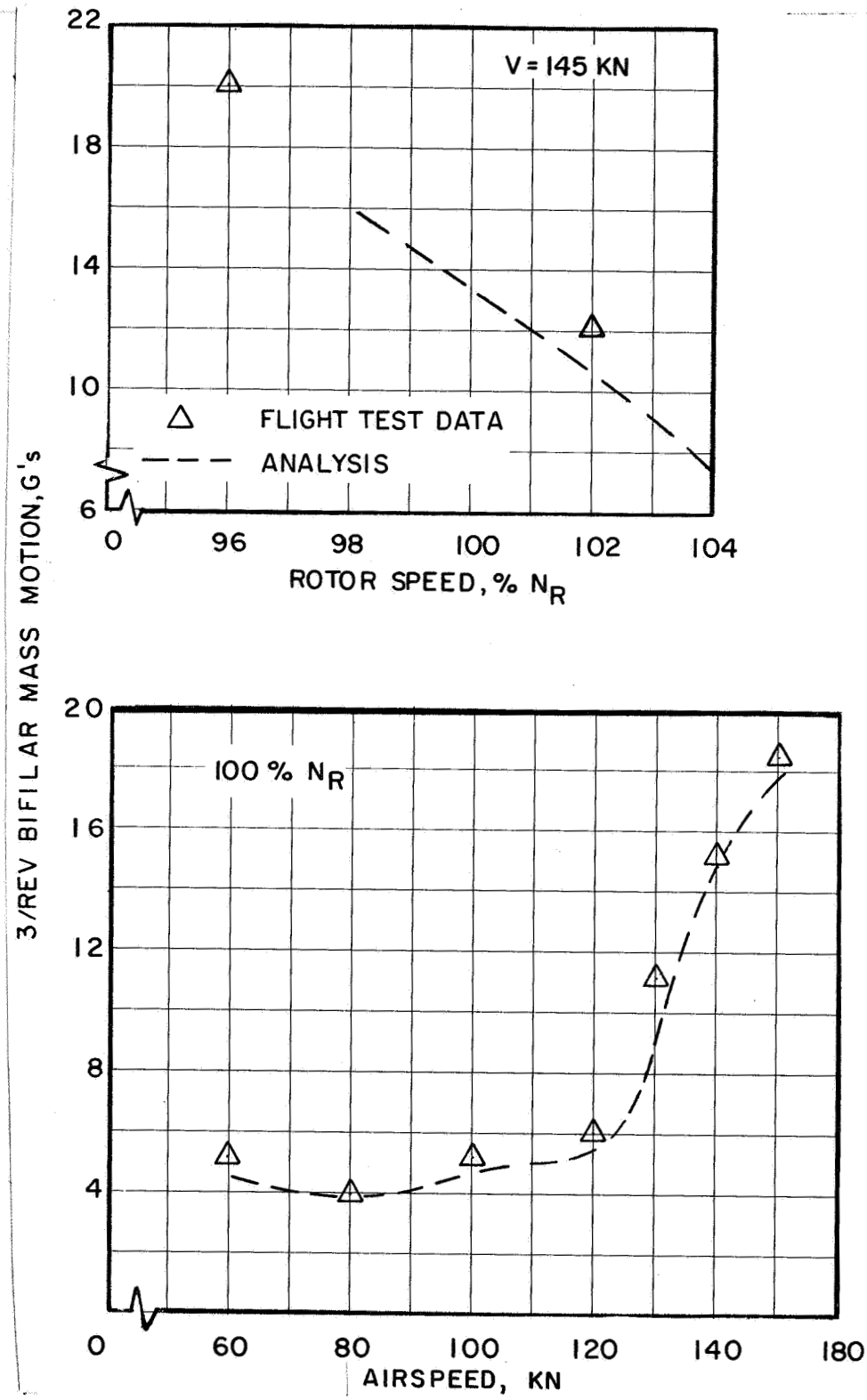

Figure 5.2-14. Correlation of 3/Rev Bifilar Mass Motion, Configuration 2

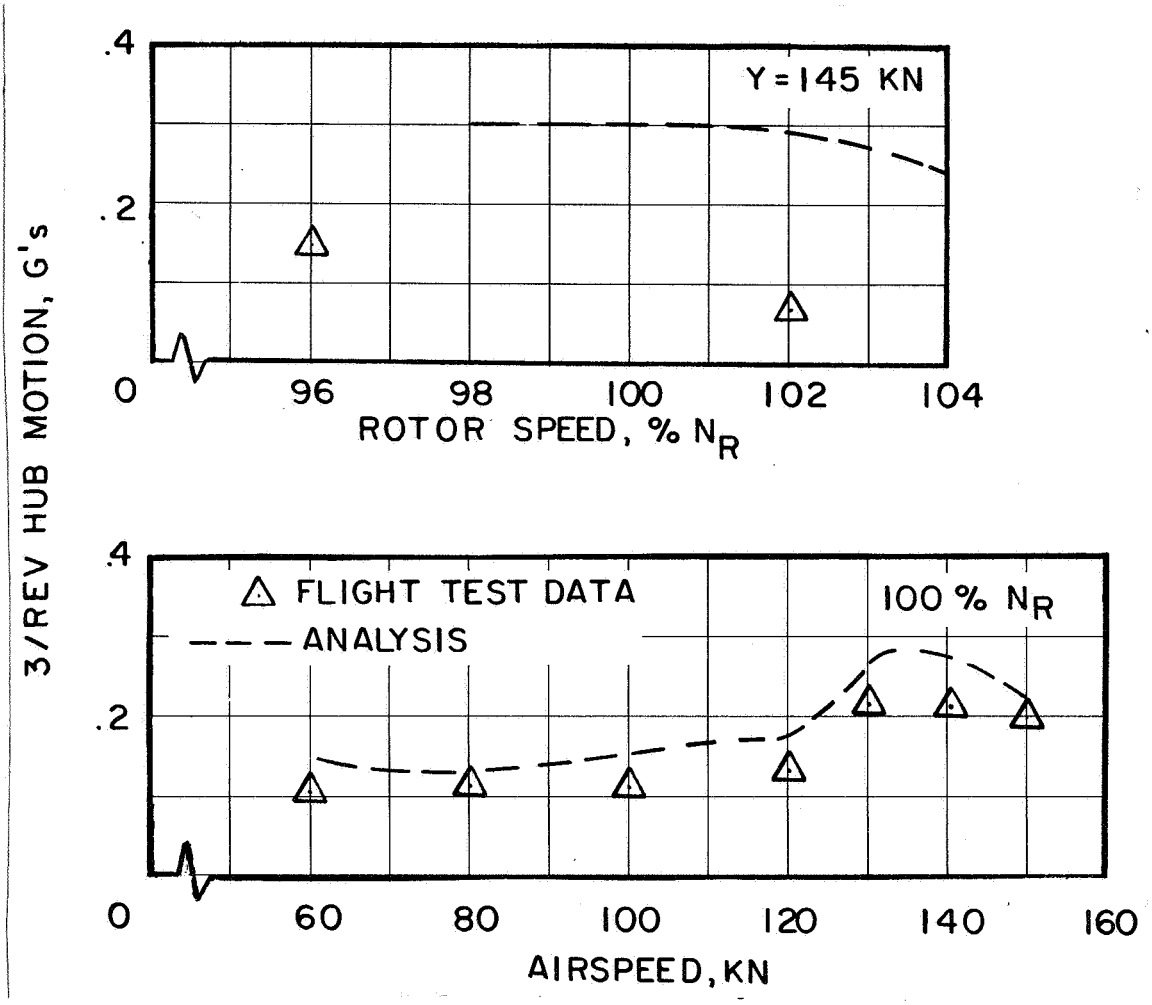

Figure 5.2-15. Correlation of 3/Rev Hub Motion, Configuration 2

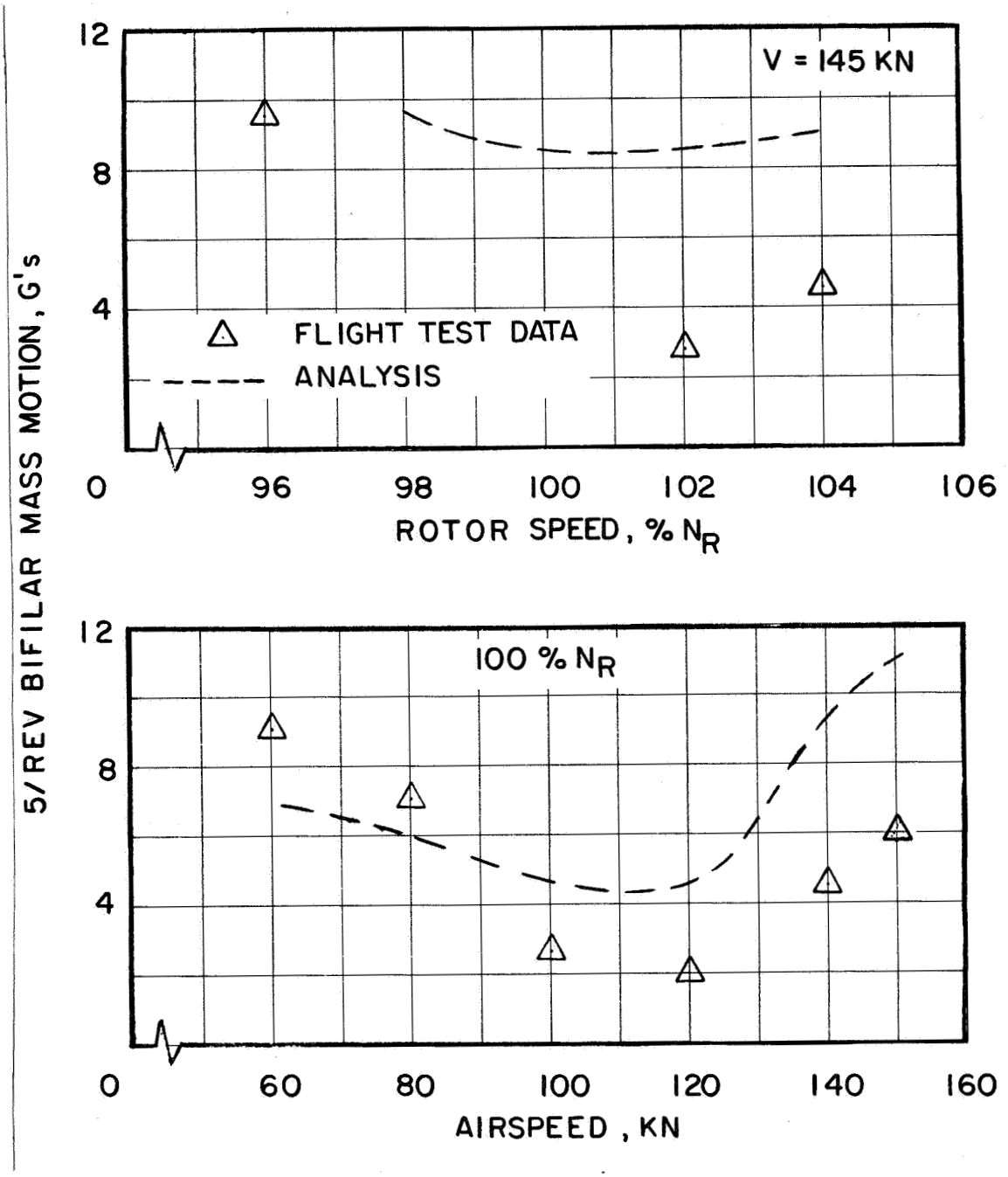

Figure 5.2-16. Correlation of 5/Rev Bifilar Mass Motion, Configuration 2

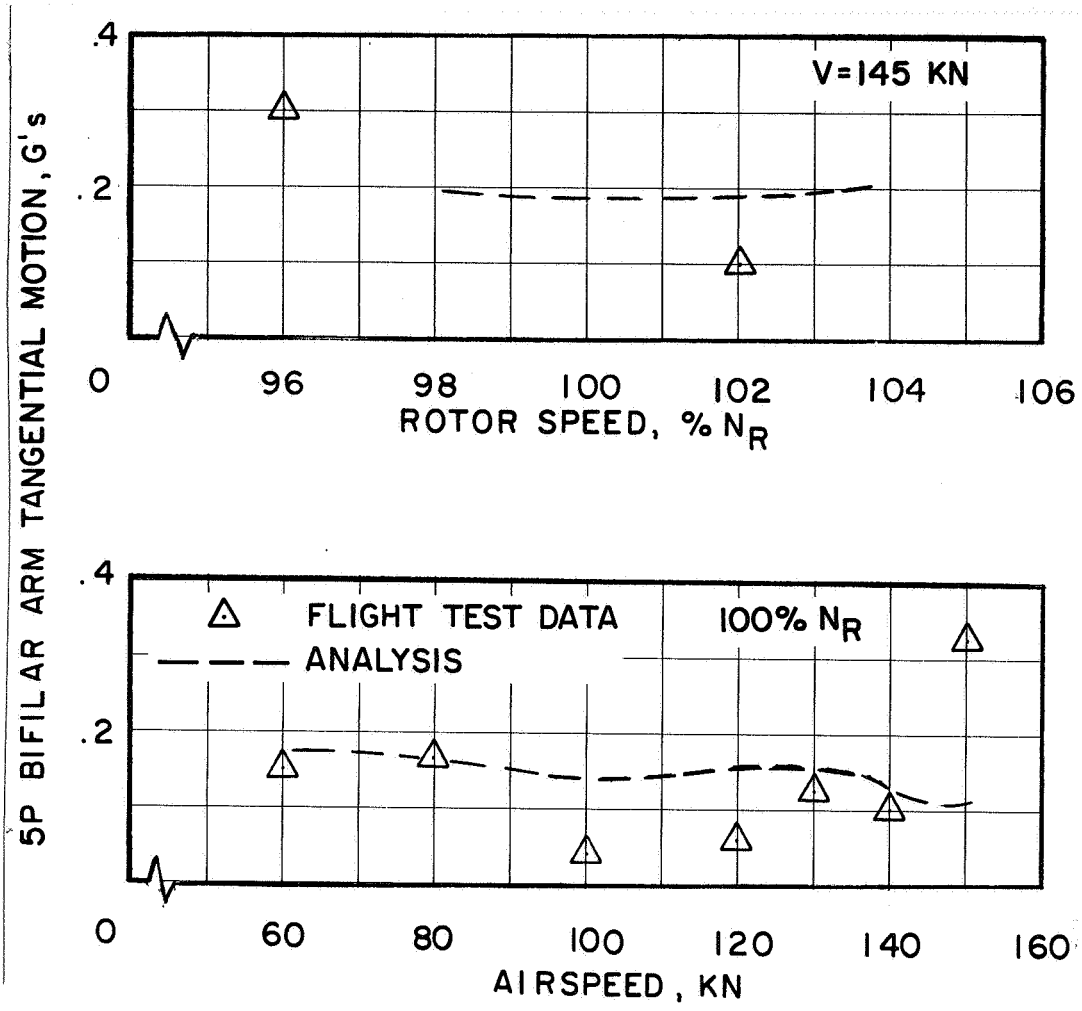

Figure 5.2-17. Correlation of 5/Rev Hub Motion, Configuration 2

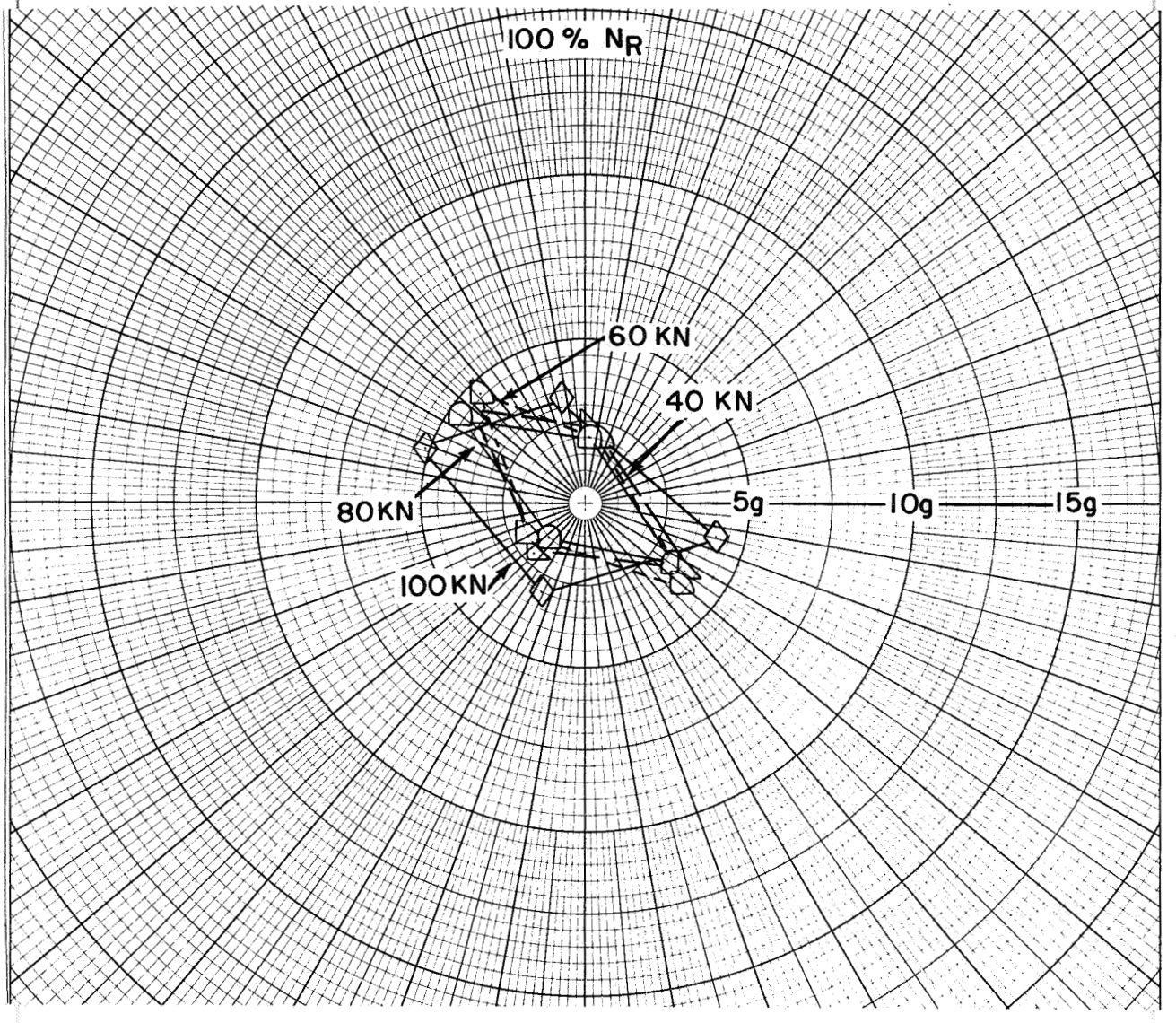

(a)

Figure 5.2-18. Configuration 2, 3/Rev Bifilar Mass Response With Combined Tuning and Mass Variation From Baseline - Effect of Airspeed

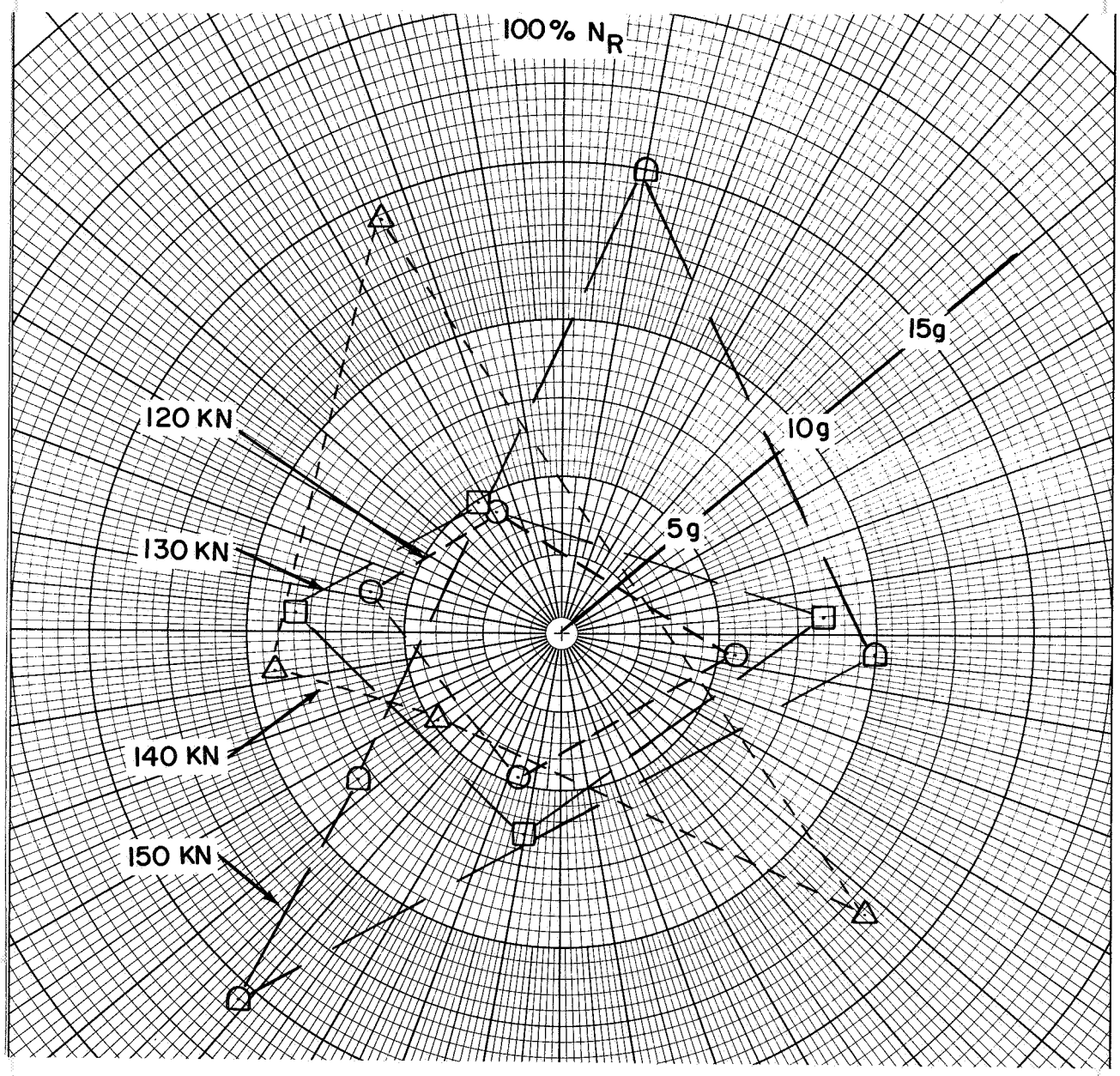

(b)

Figure 5.2-18. Concluded.

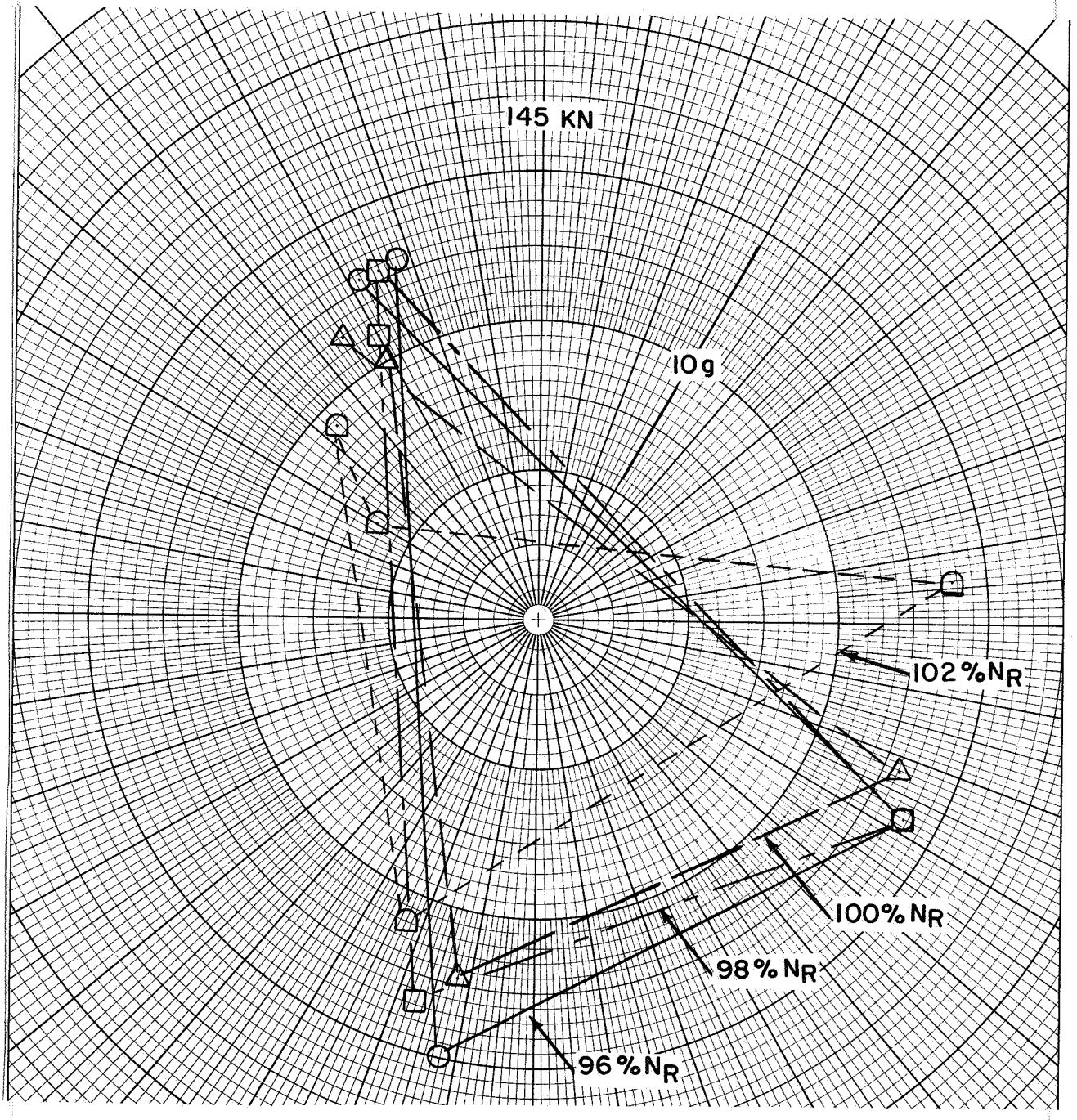

Figure 5.2-19. Configuration 2, 3/Rev Bifilar Mass Response With Combined Tuning and Mass Variation from Baseline - Effect of Rotor Speed

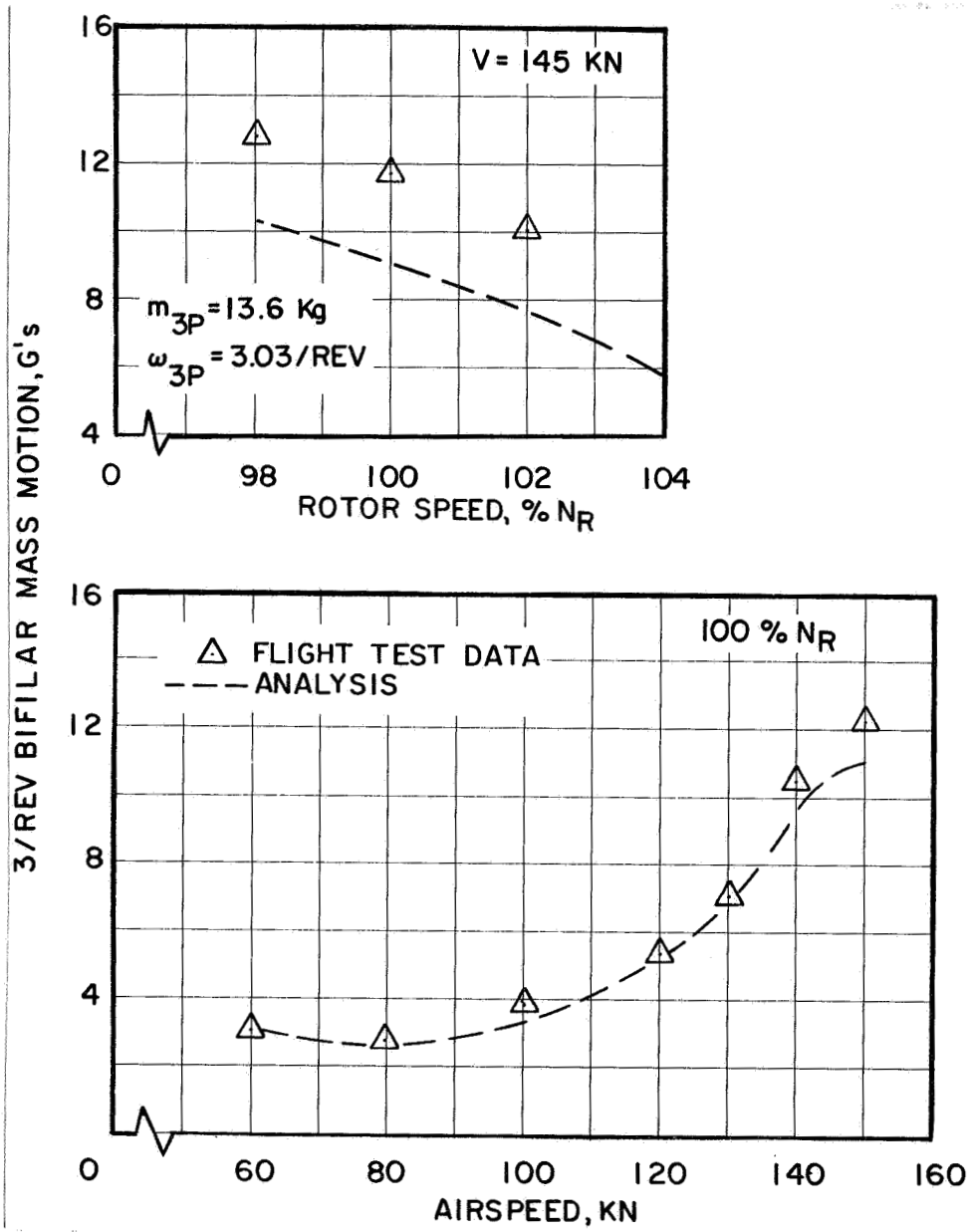

Figure 5.2-20. Correlation of 3/Rev Bifilar Mass Motion With Combined Tuning and Mass Variation From Baseline, Configuration 2

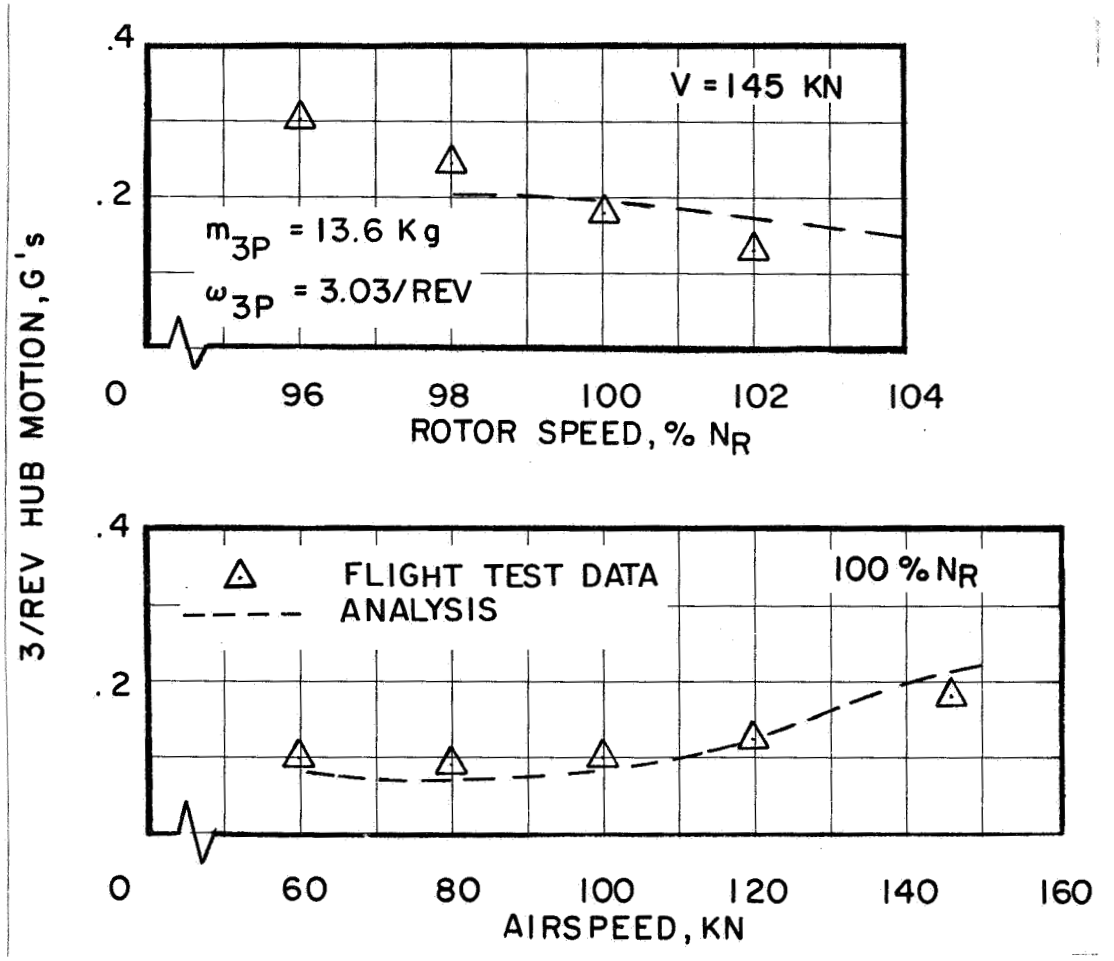

Figure 5.2-21. Correlation of 3/Rev Hub Motion With Combined Tuning and Mass Variation from Baseline, Configuration 2

bifilar configuration is shown in Figure 5.2-22. Hub loads used in the analysis were again those presented in Figures 5.2-12 and 5.2-13, and again the correlation is good.

Configuration 3 - This is the prototype S-76, flown with the circular bushing 3/rev bifilar absorber with dynamic mass of 9.07 kg (20 lb) and tuning of 3.045/rev. Bifilar response patterns are shown in Figures 5.2-23 for an airspeed sweep at 100% N_R. Note that one bifilar mass motion is not available.

The bifilar amplitude of response increases with increasing airspeed, except at 40 kn. This is exactly the same trend as that shown in Figure 5.2-8. Comparing the incomplete patterns of Figure 5.2-23 versus those shown in Figure 5.2-8, it is reasonable to assume that the complete bifilar response patterns would be similar.

Correlation of analytical and test bifilar mass responses are shown in Figure 5.2-24. Residual hub vibration is compared in Figure 5.2-25. Hub loads and hub impedance used for the analysis are the same as those used for Configuration 2. The analysis again predicts the dynamic response of the system well for the airspeed sweep.

Figure 5.2-26 presents the 5/rev hub response for the airspeed and rotor speed sweeps. Recall that this configuration does not include a 5P bifilar. The analysis predicts the response reasonably well. Comparing this figure with Figure 5.2-17 shows that the 5P bifilar absorber on the S-76 reduces hub vibration at 5/rev by 60-70%.

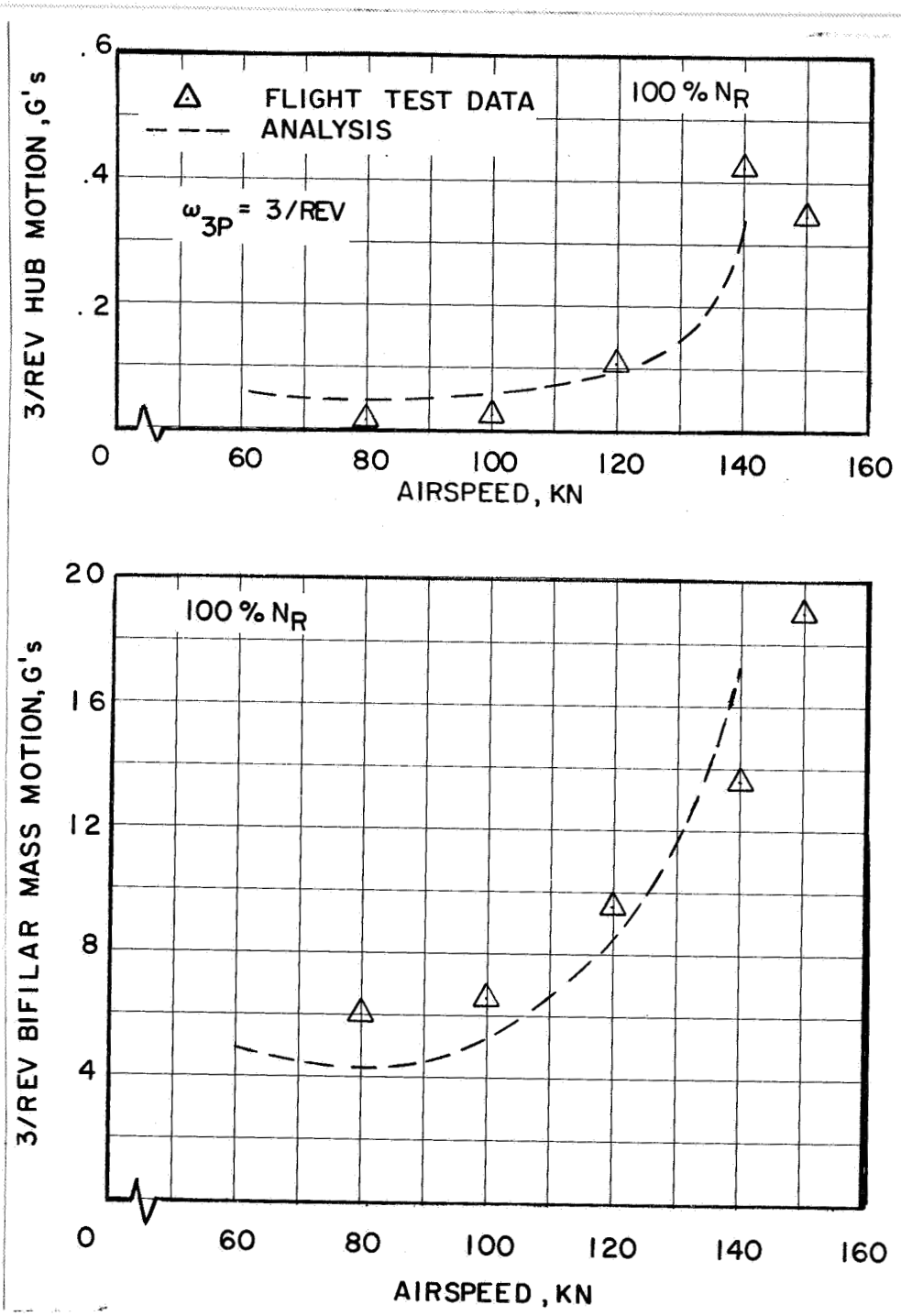

Figure 5.2-22. Correlation of 3/Rev Hub and Bifilar Mass Motion With Tuning Variation from Baseline, Configuration 2

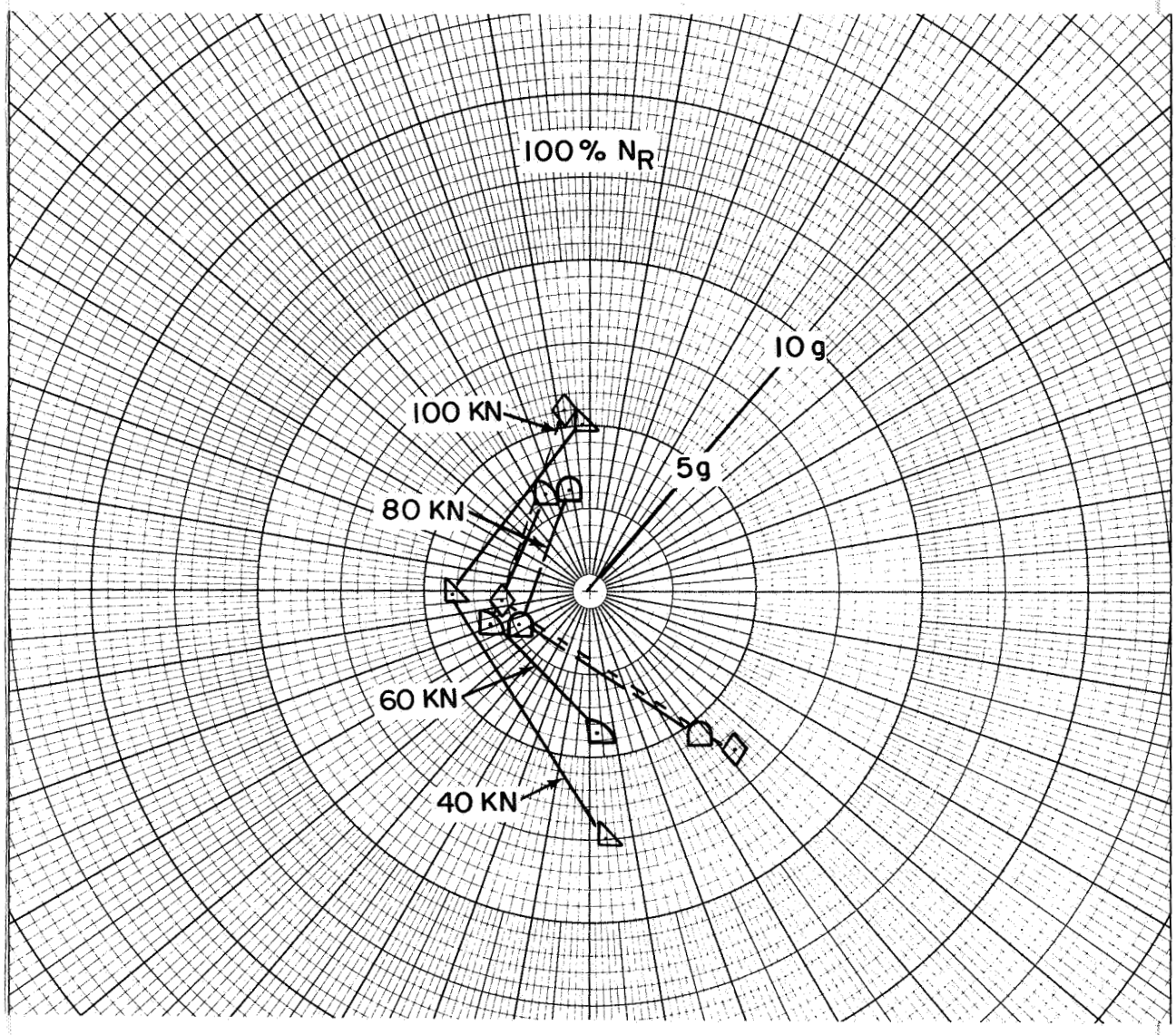

(a)

Figure 5.2-23. Configuration 3, 3/Rev Bifilar Mass Response - Effect of Airspeed

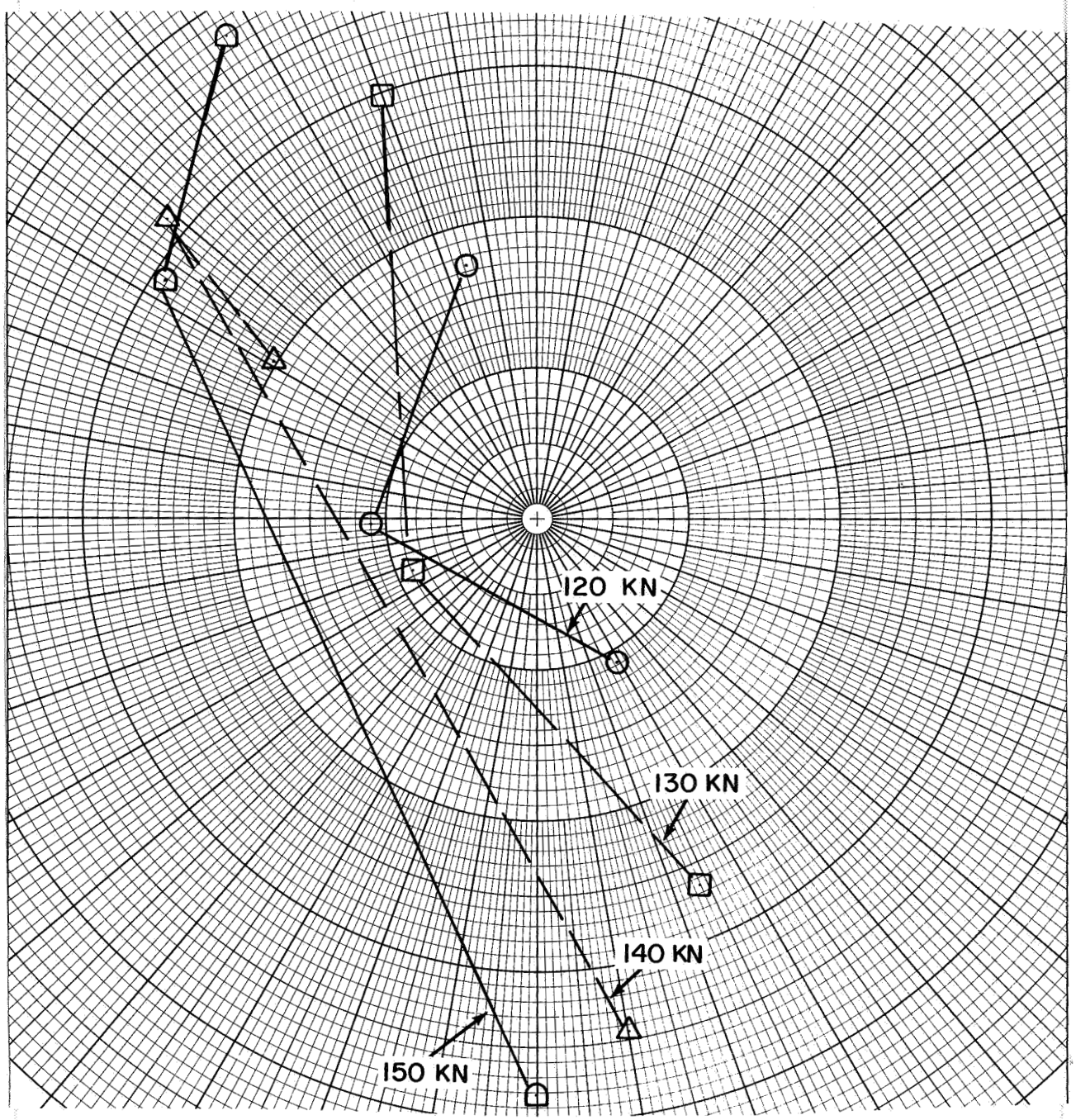

(b)

Figure 5.2-23. Concluded.

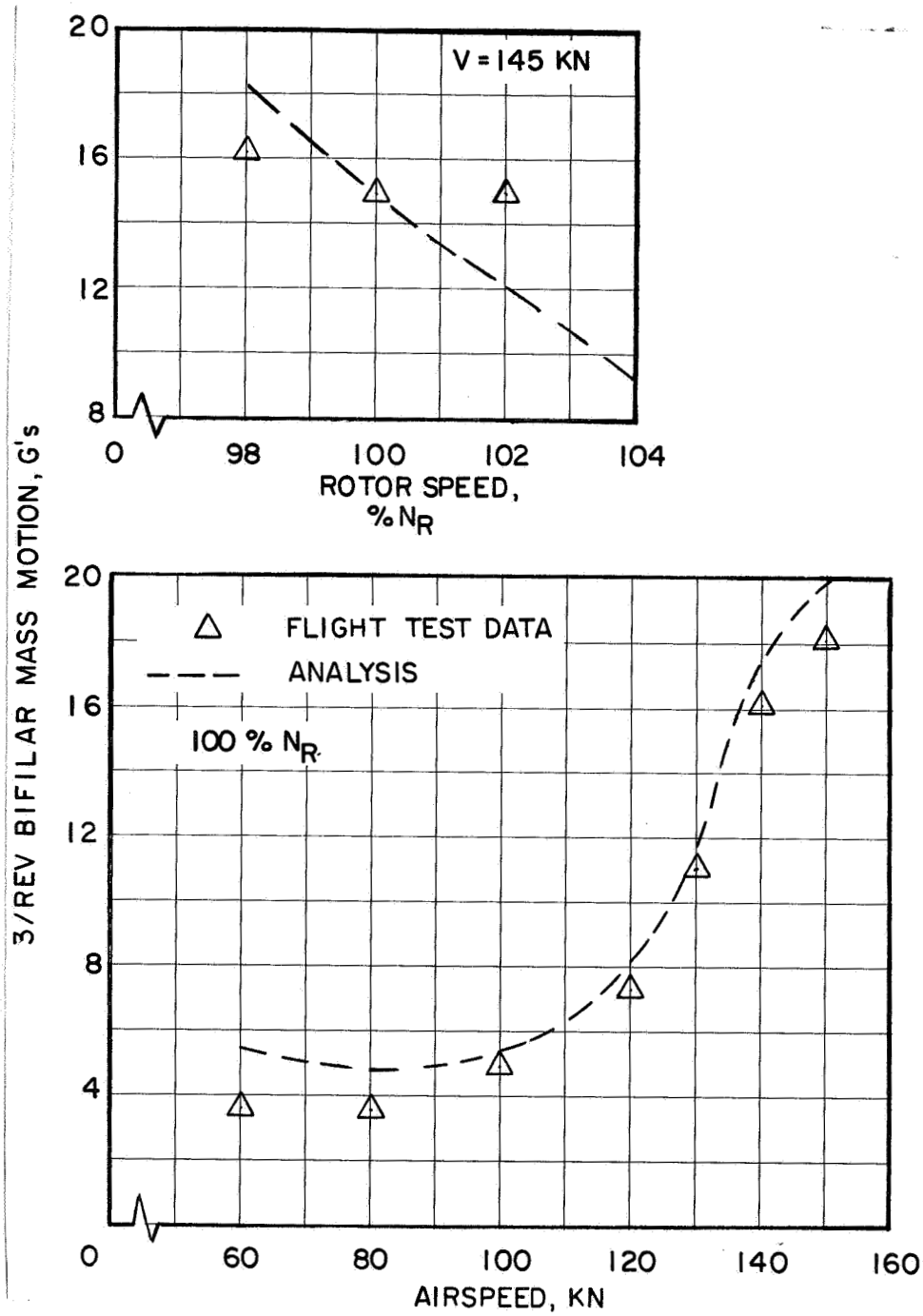

Figure 5.2-24. Correlation of 3/Rev Bifilar Mass Motion, Configuration 3

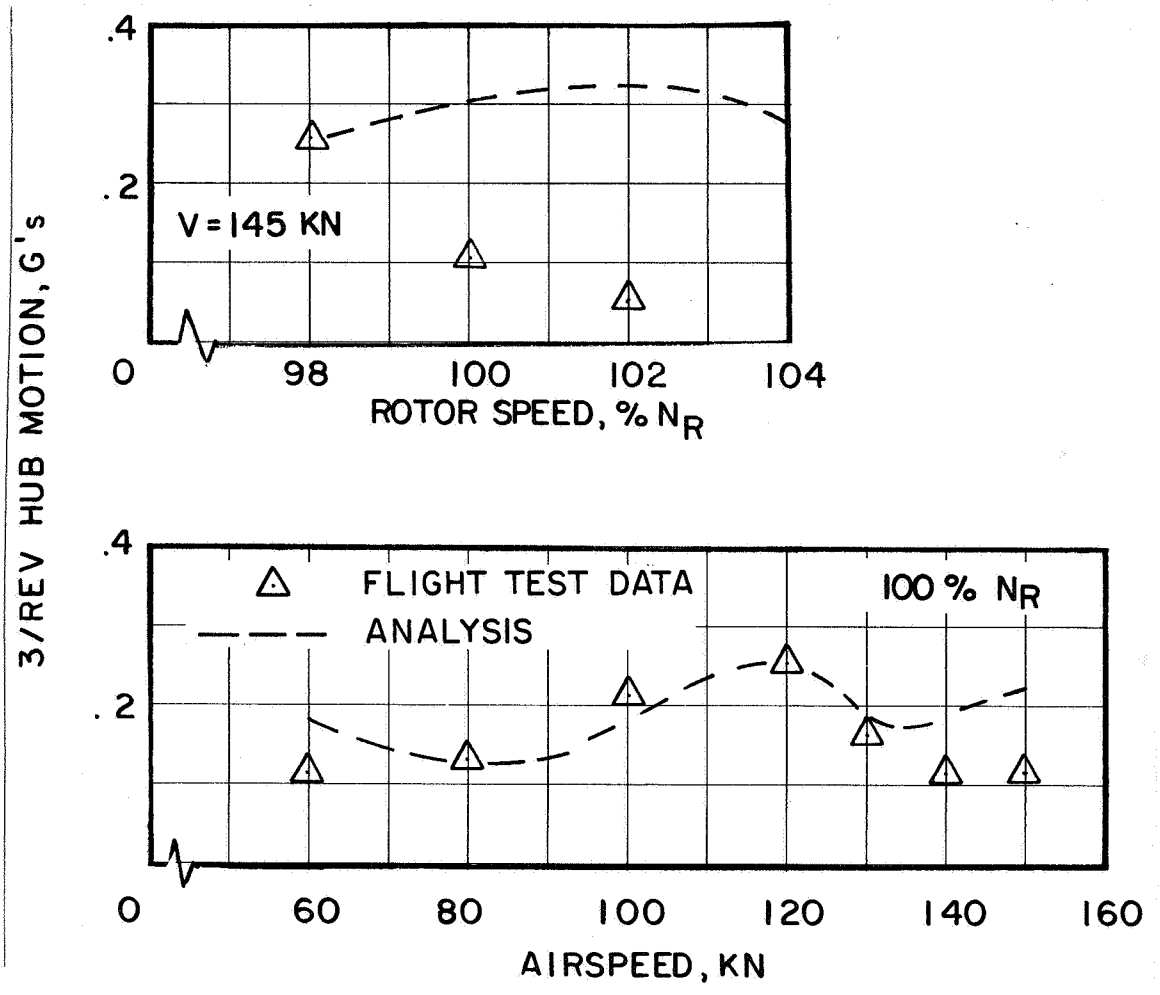

Figure 5.2-25. Correlation of 3/Rev Hub Motion, Configuration 3

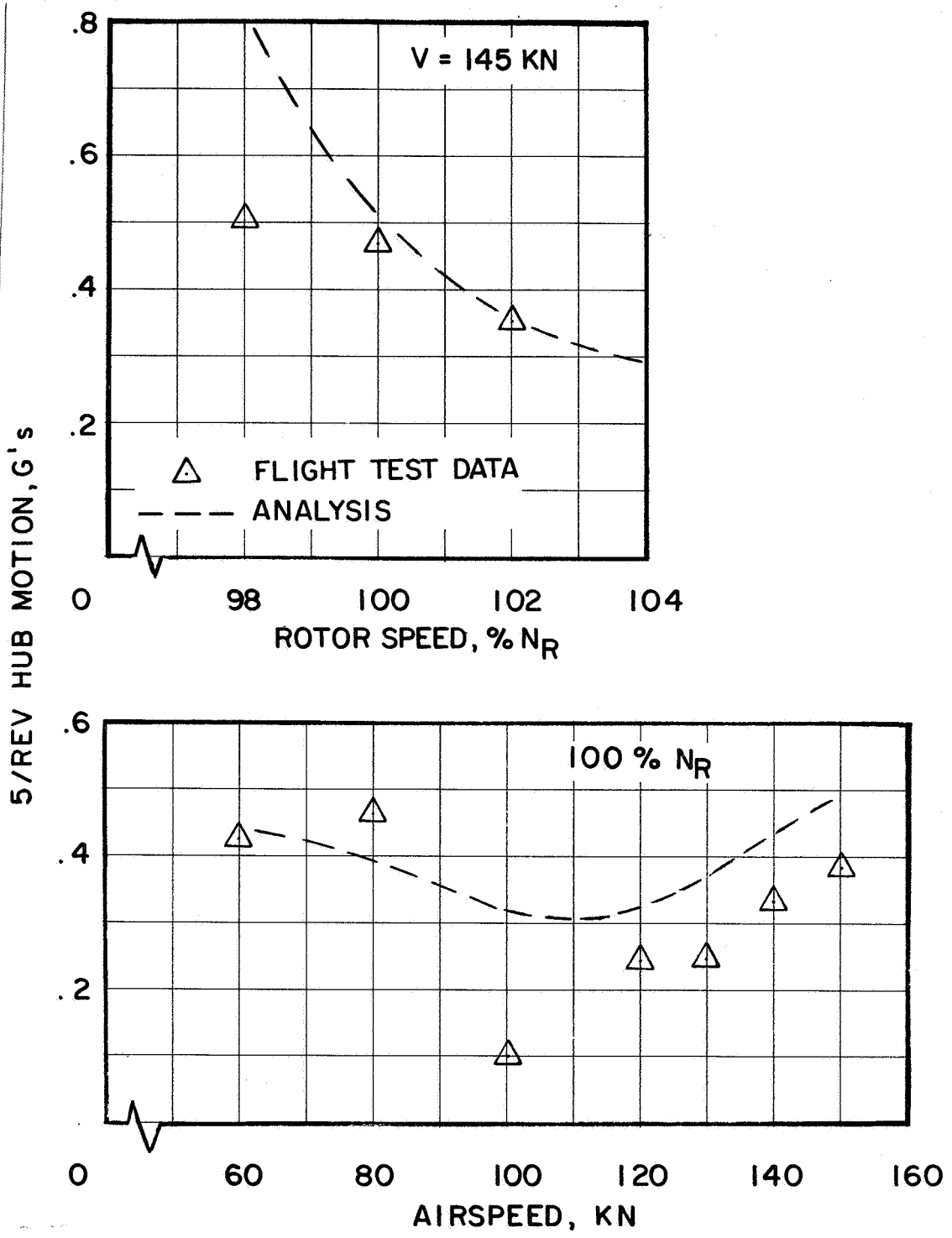

Figure 5.2-26. Correlation of 5/Rev Hub Motion, Configuration 3

SECTION 6

CONCLUSIONS AND RECOMMENDATIONS

Based on the study presented in this report, the following conclusions and recommendations are formulated.

Conclusions:

1. The bifilar absorber is an effective vibration control device which attenuates excitation at its source. The effectiveness of the absorber depends on the basic design parameters of dynamic mass, damping and tuning, as well as the impedance of its attachment point.

2. For an inplane bifilar absorber, hub impedances in two inplane directions influence absorber effectiveness. Equal longitudinal and lateral hub impedances, both magnitude and sign, produce maximum bifilar absorber effectiveness. When the longitudinal and lateral impedances are equal but of the opposite sign, the bifilar absorber will be totally ineffective.

3. There exists an optimum combination of longitudinal and lateral hub impedance for a fixed set of (N-1)/rev and (N+1)/rev excitation forces.

4. It has been demonstrated that the coupled rotor/airframe dynamics must be included in the analysis in order to obtain the correct impedance for evaluation of bifilar performance.

5. The individual bifilar mass motion is very sensitive to and dependent on the tolerances in the bifilar basic design parameters. Not only will the discrepant bifilar mass respond differently than the ideal masses, but it will also cause the ideal masses to respond differently.

6. When the bifilar masses respond in a pattern other than ideal, the performance of the absorber in terms of attenuation of N/rev excitation force deteriorates. In addition, substantial non-N/rev forces at various rotor harmonics (2/rev, 5/rev and 7/rev for a 3/rev bifilar) can be generated depending on the distortion of the ideal response pattern.

7. Precise knowledge of the hub excitation forces in (N-1)/rev frequency as well as (N+1)/rev frequency for a particular flight condition are required, in addition to the knowledge of damping and tuning of individual dynamic masses, in order to calculate the complete dynamic response and effectiveness of the bifilar for correlation with flight data.

8. The trends of bifilar mass response patterns with variation in airspeed and rotor speed from flight test have been compared with the calculated patterns, and a good correlation has been established. In addition, the test data show similar variation of bifilar mass response to changes in dynamic mass, tuning and addition of (N+1)/rev bifilar absorber, as those calculated using the coupled rotor/bifilar/airframe analysis.

Recommendations:

1. A laboratory experiment where the excitation force, hub impedance, dynamic mass, tuning can be controlled and varied should be conducted to provide parametric data for a quantitative verification of the analysis developed under this contract.

2. The analysis should be expanded to include tracking hole contours other than circular to permit indepth study of contour tolerances control requirements as well as contour design for maximum absorber effectiveness.

REFERENCES

1. Paul, W. F., Development and Evaluation of the Main Rotor Bifilar Absorber, Proceedings of the 25th AHS Forum, May 1969.

2. Cassarino, S. J. and Mouzakis, T., Bifilar Analysis User's Manual - Volume II, NASA CR-159228, July, 1980